LOCAL SCOUR IN RIVERS

THE EXTENT OF THE PROBLEM IN SOUTH AFRICA
THE STATE OF THE ART OF NUMERICAL MODELLING

N Armitage • M Cunninghame • A Kabir •
B Abban

WRC Report No. KV 185/07

Water Research Commission

Local Scour in Rivers

The Extent of the Problem in South Africa
The State of the Art of Numerical Modelling

Report to the
Water Research Commission

by

Neil Armitage, Margaret Cunninghame, Alamgir Kabir & Benjamin Abban

Department of Civil Engineering
University of Cape Town
Private Bag Rondebosch 7701
SOUTH AFRICA

WRC Report No KV 185/07
ISBN 978-1-77005-552-0

April 2007

Obtainable from:

Water Research Commission
Private Bag X03
Gezina
0031

The publication of this report emanates from a project entitled *The prediction of, and protection against, local scour in rivers* (WRC Project No. K8/565).

Table of Contents

List of Figures

List of Tables

Notation

Symbol	Description	Normal units
a	Reference depth for sediment concentration set equal to the roughness height	m
a_r	Sediment concentration reference depth	m
A	Cross-sectional area of stream	m^2
A_X	Area of province X	km^2
b_p	Pier breadth	m
B_X	Number of bridges in province X	No.
c	Specific heat of fluid	J/kgK
c_{bed}	Bed sediment concentration	
$C_{1\varepsilon}$	Constant in transport equations for k-ε turbulence model	-
$C_{2\varepsilon}$	Constant in transport equations for k-ε turbulence model	-
$C_{3\varepsilon}$	Constant in transport equations for k-ε turbulence model	-
C_p	Pressure coefficient	-
C_μ	Constant in transport equations for k-ε turbulence model	-
d	Sediment particle diameter	m
d_{50}	Median sediment particle diameter (= $(d_{15.9} + d_{84.1}) / 2$)	m
d_X	Sieve size passed by X% of sediment by mass	m
D_*	Dimensionless sediment particle diameter	-
E	Specific energy	J/kg
f	Frequency of vortex shedding	Hz
g	Gravitational acceleration (≈ 9.81)	m/s^2
$\boldsymbol{g}$	Gravity vector	m/s^2
G_k	Generation of k due to mean velocity gradients	
G_b	Generation of k due to buoyancy	
i	Internal (thermal) energy	J/kg
k	Turbulent kinetic energy	m^2/s^2
k_s	Effective channel bed roughness	m
$k_{s+\Delta}$	Effective channel bed roughness with for bed forms	m
k_T	Coefficient of thermal conductivity	W/mK
L	Bed form length	m
L_a	Abutment length normal to direction of flow	m
Mn	Movability number	-
Mn_c	Critical Movability Number for incipient sediment motion	-

$Mn_{c(\beta,\gamma)}$	Critical Movability Number on a sloped channel bed	-
p	Pressure	N/m^2
p_x	Static pressure at position x along flow direction	N/m^2
p_0	Upstream undisturbed static pressure	N/m^2
P_t	Applied unit stream power	W/m^3
P_X	Population of province X	No.
q_b	Volumetric bedload transport per unit width	m^2/s
q_s	Volumetric sediment transport rate per unit width	m^2/s
Q	Flow	m^3/s
$\mathbf{Q}$	Heat flux vector	J/s
Re	Flow Reynolds Number	-
Re_*	Particle Reynolds Number (= $u_* d/\nu$)	-
RI	Flood flow recurrence interval	years
S_E	Source of energy per unit volume per unit time	J/m^3s
S_k	Source term in transport equation for k	
S_{Mi}	Body force per unit volume in the i-direction	N/m^3
S_s	Relative density (= ρ_s/ρ)	-
S_s'	Relative density (= ρ_s/ρ - 1)	-
St	Strouhal number	-
S_ε	Source term in transport equation for ε	-
S_ϕ	Source term in transport equation for ϕ	-
t	Time	s
T	Temperature	K
T_*	Dimensionless excess bed shear stress parameter	-
u	Component of velocity in x-direction	m/s
$\mathbf{u}$	Velocity vector	m/s
u_i	Velocity component in the i-direction	m/s
$\overline{u}_i$	Time-averaged velocity component in i-direction	m/s
u_*	Shear velocity (= $(\tau_0 / \rho)^{0.5}$)	m/s
U	Mean approach velocity (= Q/A)	m/s
v	Component of velocity in y-direction	m/s
v_{ss}	Sediment particle settling velocity	m/s
w	Component of velocity in z-direction	m/s
x	Horizontal distance from the origin in the direction of flow	m
x_i	Co-ordinate direction i	m
y	Vertical height above the origin	m
y^+	Wall unit distance	-
Y_M	Source term in transport equations of k-ε turbulence model	

z	Horizontal distance from the origin normal to the direction of flow (transverse direction)	m
Δ	Bed form height	m
ε	Turbulence dissipation rate	m^2/s^3
Γ	Diffusion coefficient	m^2/s
ϕ	Arbitrary scalar quantity	-
ϕ_r	Angle of repose of sediment	Degrees
Φ	Dissipation function (= P_t)	W/m^3
μ	Total fluid viscosity (= $\mu_l + \mu_t$)	Ns/m^2
μ_l	Dynamic molecular fluid viscosity	Ns/m^2
μ_t	Turbulent fluid viscosity	Ns/m^2
ν	Kinematic viscosity of water (= μ/ρ)	m^2/s
ρ	Density of fluid	kg/m^3
ρ_s	Sediment particle density	kg/m^3
ρ_w	Density of water (≈ 1000)	kg/m^3
σ	Standard deviation	
σ_k	Turbulent Prandtl Number for k	-
σ_ε	Turbulent Prandtl Number for ε	-
τ	Shear stress	N/m^2
τ_c	Critical bed shear stress for incipient motion	N/m^2
τ_0	Shear stress at the channel bed	N/m^2
τ_{ij}	Shear stress acting in the j-direction on a plane normal to the i-direction	N/m^2
Ω	Scour potential	-
ψ	Slope correction factor for Mn_c	-

Abbreviations

Abbreviation	Description
1D	One-dimensional
2D	Two-dimensional
3D	Three-dimensional
ASM	Average Stress Model
CFD	Computational Fluid Dynamics
DNS	Direct Numerical Simulation
k-ε	A two-equation turbulence model
k-ω	A two-equation turbulence model
LES	Large Eddy Simulation turbulence model
MAC	Marker-and-Cell method
PC	Personal Computer
RAM	Random Access Memory
RANS	Reynolds averaged Navier-Stokes equations
RNG	Re-normalised Group turbulence model
RSM	Reynolds Stress Model
VLES	Very Large Eddy Simulation turbulence model
VOF	Volume of Fluid method

Acknowledgements

I am particularly indebted to my three post-graduate students, Ms Margie Cunninghame, Mr Alamgir Kabir and Mr Benjamin Abban for the tremendous amount of work that they put into their sections of this report (Chapters 3 and 4) which constitute the overwhelming bulk of text. They also helped with the editing – Margie and Benjamin in particular. Thank you very much. The project was facilitated by the financial support of the Water Research Commission – represented by Drs Kevin Pietersen and Renias Dube – for which I am also extremely grateful.

A number of individuals assisted Ms Margie Cunninghame in her collection of data on the extent of local scour around river bridges in South Africa. They included:

- Mr Harry Viljoen and Mr Anton Nell of the Western Cape Department of Transport
- Mr Michel Slabbert and Mr Kobus Oosthuizen of the Free State Department of Transport
- Mr Johan Janse van Rensburg of Leporogo Specialist Engineers and Mr Jerome Mayimele of Limpopo Province
- Mr Rob Lindsay and Mr Mike Wiles from the KwaZulu-Natal Department of Transport
- Mr James Rautenbach of Africon Consulting Engineers
- Mr Graham Simpson of VelaVKE

Margie received additional funding from the Harry Crossley Foundation.

Neil Armitage, PrEng, PhD
Project Leader and Editor
January 2007

Executive Summary

Rationale for the study

The ability to predict local scour and its opposite, local deposition, is of critical importance to South Africa. Local scour can undermine bridge foundations (not just road/rail, but also pipe bridges) and riverbanks. Local deposition can clog river abstraction works used in the provision of water to rural communities and agriculture. Together, they impact aquatic environments and change the courses of rivers. Any structure placed in a river, whether of natural or of human origin, will tend to promote scour and deposition.

The failure of river crossings and engineering structures in rivers in South Africa due to scour damage can result in substantial financial and economic losses in flood-affected regions. For example, the well-known failure of the John Ross Bridge over the Tugela River during 1987 floods in Natal was caused by scour which undermined the bridge pier foundations (Van Bladeren & Burger, 1989). Vehicles which normally used the bridge had to travel significant additional distances. Such failures do not, however, occur in isolation as during these floods a total of 120 bridges in Natal were destroyed or severely damaged. As a consequence, substantial losses were felt by the local economy. Designing for scour is not, however, a mature science. There have been many developments since the publications of the South African National Roads Agency Ltd. *Road Drainage Manual* and the Committee of State Road Authorities (1986) and *Guidelines for the Hydraulic Design and Maintenance of River Crossings*, TRH 25 (1994). Furthermore, the mounting evidence for global climate change suggests that southern Africa must start preparing itself for the likely consequences of even more severe flood events and consequential damage to structures. There is also an increasing problem associated with scour and deposition around urban culverts / bridges – particularly as the modern tendency is to move away from concrete-lined channel sections towards more natural looking waterways.

The recently completed WRC study entitled *A unit stream power model for the prediction of local scour* (Armitage & McGahey, 2003) showed that there is still no universally agreed design procedure that can cope with all the observed scour and deposition phenomena. Most methodologies place considerable reliance on the use of dimensional analysis and empirical formulae and are extremely inaccurate. Physical models are more reliable, but are expensive. The road ahead ultimately lies with the use of computational fluid dynamics (CFD). A crude numerical model for the prediction of scour and deposition with the aid of CFD was developed in the course of the aforementioned WRC study.

The role of the engineering departments in many government institutions is changing from design to regulatory, and thus they are employing fewer and possibly less experienced engineers, and years of accumulated wisdom in design is gradually being

lost. They have extremely limited funds for research. There is a pressing need for the development of appropriate tools to enable the designers of the future to make the optimal use of limited resources. These tools should include design guides for local conditions and the development of suitable software.

Objectives

The main objectives of this consultancy were as follows:

- Report on the extent to which local scour and deposition around culverts and bridges is a problem in South Africa.
- Conduct a literature review of the current state of the art regarding the CFD modelling of scour and deposition around manmade structures in the fluvial environment.
- Report on research needs with respect to the development of appropriate CFD tools for the prediction of scour and deposition around engineering structures.

Layout of this report

Chapter 2 offers a brief introduction to river scour in general, and local scour in particular. The mechanisms causing local scour around two simple structures – cylindrical piers and vertical plate abutments are also described.

Chapter 3 commences with a historical overview of scour damage to major river crossings in South Africa, and particularly Natal, over the past five decades. This is followed by a description of a field and desk study of 121 bridges currently experiencing scour problems. Analyses of the nature of the damage were conducted and estimates of the associated repair costs made. The study focused on scour at South African provincially maintained road bridges although pipe and rail bridges and other hydraulic structures were included to a lesser degree. Emphasis was placed on the assessment of scouring mechanisms such as general, local and constriction scour which attack bridge foundations directly. Erosion of earth embankment dams and berms was not considered.

Chapter 4 looks at numerical modelling of local scour in rivers through Computational Fluid Dynamics (CFD). CFD is the numerical modelling of fluid flow and associated phenomena (Versteeg & Malalasekera, 1995; Olsen, 1999). The fundamental equations and methods used by CFD are briefly described. Although there are many commercial and general-purpose CFD codes available, local scour is difficult to model owing to the three-dimensional nature of the vortices that are set up in the vicinity of hydraulic structures. This chapter describes previous work in the modelling of scour, and then illustrates the current capability of two well-known codes, FLUENT Version 6.2 (a general CFD code) and TELEMAC Version 5.4 (a specialised river modelling code).

Chapter 5 contains some general conclusions as well as providing recommendations for future research. It is followed by **References** and **Appendices**. The Appendices include cost estimates of current scour damage in South Africa, as well as giving details of commercial CFD codes (general and specialised river modelling codes) currently on the market.

Limitations of the study

It is important that the reader appreciates that local scour is but one type of scour. Scour, whether it be in the form of long-term bed degradation, constriction scour, bend scour, confluence scour or local scour, is a major engineering problem as all forms of scour have the potential to undermine hydraulic structures and potentially cause their collapse. This report focuses only on local scour; for the reason that it is one of the greatest threats to hydraulic structures whilst simultaneously being one of the most difficult to analyse as a result of the three-dimensional aspect of vortex formation and dissipation around these structures. Even in the context of a discussion of local scour, this report is still constrained. It deals only with two aspects: the extent of the problem in South Africa, and the state of the art of numerical modelling.

When dealing with the extent of the problem in South Africa, the focus is on provincially maintained road-over-river bridges. Other types of structure; e.g. pipe bridges, weirs, spillways, dikes, intake structures, canoe chutes, etc. are largely ignored. Even road bridges, bridges along National roads and roads maintained by local authorities are effectively ignored. Furthermore, estimates of local scour damage are restricted to repair costs with no attempt made to determine consequential costs e.g. delays or the additional maintenance and running costs associated with the temporary deviation of traffic.

In the discussion on the state of the art of numerical modelling, the report assumes the use of commercially available software running on desktop personal computers. Clearly a lot more can be done if the modelling is carried out on supercomputers or high-speed clusters of machines, but this option is not generally available for routine engineering work.

Ultimately the report is designed to give a snap-shot of the situation as it currently stands at the present from the perspective of technology that is readily available to all consulting engineers. It is clear, however, that the rapid improvements in the speed of personal computing and the associated rapid development of software will render this document dated within a relatively short period of time.

The extent of the problem in South Africa

Scour damage is generally associated with extreme flood events. A study of current scour damage at road bridges in South Africa has indicated that severe scour damage is seldom evident at bridges under “normal” flow conditions. Evidence of severe

scouring during past floods was, however, seen at several sites. An estimate of the direct cost of repair of scour-related damage on provincially maintained bridges is approximately R22 million per annum. About 42% of this cost is on bridges in KwaZulu-Natal. This cost excludes the damage incurred in extreme flood events and the economic costs associated with the disruption caused by the failure of major transport links. Inclusion of scour damage during extreme floods events may increase the estimate to between R25 million and R30 million per annum.

The severity of the constriction scour observed in the field study was generally greater than the local scour. It might thus be said that excessive constriction of the flow poses a greater threat to South African river bridges. It must, however, be remembered that local scour cannot be readily observed or measured, particularly during extreme flood events, and the holes are rapidly filled by sediment after the peak flow has passed, which might lead to an underestimate of the impact of local scour. Furthermore, the two types of scour usually act in conjunction so one cannot be studied in the absence of the other.

Local and constriction scour are the two mechanisms occurring most frequently at bridge sites. Local scour was observed at 60% of the 105 bridges investigated whilst constriction scour was observed at 44% of them. The local and constriction scouring were combined at 37% of the sites investigated. The prediction and mitigation of local scour is thus an important area for research.

The state of the art of numerical modelling

The complex nature of real flow phenomena has historically made physical modelling attractive. However, the construction, modification, and operation of physical models can make them extremely expensive which is encouraging engineers to look toward numerical simulation using CFD either as an adjunct to, or as a replacement for, physical models. The main problems associated with CFD relate to the transfer of the underlying physics to the numerical solvers. This is made difficult because of complex interaction of many different factors coupled with the severe limitations in the computational power of the current generation of desk-top machines.

The first step in numerical analysis involves the identification and description of a suitable flow domain. The domain is then divided into finite volumes or finite elements by means of two or three-dimensional meshes. The choice of domain is extremely important. An adequate length of channel upstream and downstream of the structure must be modelled to ensure that any inadequacies in the boundary conditions have been smoothed out in the region of interest in the vicinity of the structure. In the case of relatively symmetrical flows around structures such as circular piers, the computational time can be greatly reduced by defining the line of symmetry and modelling only half the channel width – although this will obscure such physical phenomena such as the von Kárman vortex street. This analytical trick cannot, however, be applied to models around asymmetrical structures such as a spur dike. Finer meshes generally give a more accurate

solution compared with coarser meshes, but they are computationally time intensive. Considerable skill is required to determine the optimum mesh size taking into account the computational time and model accuracy. At present, there are no generally agreed guidelines for mesh refinement – especially close to the structure, the river bed and the air-water (free-surface) interface.

The selection of the turbulence model is a key factor in numerical modelling. Each turbulence model has its advantages and disadvantages depending on the type and nature of the flow field to be modelled. The more accurate turbulence models such as Direct Numerical Simulation (DNS), Large Eddy Simulation (LES), Very Large Eddy Simulation (VLES), or Reynolds Averaged Navier-Stokes (RANS) improve accuracy (in decreasing order), but at an extremely high computational cost associated with the finer meshes and additional time steps required. As a consequence, the k-ε family of turbulence models are by far the most popular and extensively used for predicting the local scouring problems in spite of their well-documented limitations particularly in the separated zones.

Some commercially available CFD codes that could be used to solve scour problems are listed in Appendices B (General codes) and C (Specialised river codes). Trials using one example of each type of code; FLUENT – a general code – and TELEMAC – a specialized river code – quickly revealed major limitations with both. These were chosen on the basis of relatively low cost, good software support, and flexibility (they both allow for user-defined routines). FLUENT had an excellent user interface and great flexibility, but was not originally designed for open channel work, so features such as sediment transport and boundary adjustment had to be specially programmed into the code. The Volume of Fluid method was used to determine the position of the free surface, which was reasonably accurate, but computationally intensive. TELEMAC was designed for open channel work so there were already modules for sediment transport / boundary adjustment, but the three-dimensional module was effectively a multiple two-layer model which was too coarse to pick up some of the small scale vortices that are set up in the vicinity of structures. The default free surface routine assumed hydrostatic pressure variation – which is not the case in the vicinity of a structure. A major shortcoming of TELEMAC was that it had a poor user interface, whilst the documentation was out of date – or in French. Both models demonstrated limitations in the modelling of the velocity gradients (and hence all other parameters such as shear stress that are dependent on the velocity gradient) in the boundary layer near the water / solid interface – unfortunately the most critical area for scour modelling.

Recommendations for future research

The following recommendations are intended to guide further investigations into scour damage in South Africa and research into numerical scour prediction methods:

- Further investigation needs to be made into the extent of the scour damage around bridges resulting from major historical flood events with particular

emphasis on the causes of failure, and the associated economic costs. These costs need to include consequential damages such as the cost of providing temporary services or the additional fuel, maintenance and time cost of travelling additional distances over detours. The investigation should focus particularly on KwaZulu-Natal as the costs associated with scour damage in this province are estimated to account for 42% of the total value of scour damage in South Africa. This is a consequence of KwaZulu-Natal having the highest average rainfall and largest number of bridges of the nine provinces.

- A more extensive review of the causes of failure of other hydraulic structures, e.g. intake structures, weirs and dikes, is necessary to give a better indication of the extent to which scour damage is a contributory factor.
- Local scour is a priority for further research as the severity of scour resulting from this mechanism under flood conditions is difficult to predict – or measure. Local scour was identified as the most prevalent form of scour damage observed at provincial road bridges during this study. More research into the combined effects of local and other forms of scouring should however be undertaken.
- A review of appropriate scour protection measures needs to be undertaken. This would have to be linked to the types of structures and environments found in South Africa.
- More research could also be undertaken into the impacts of deposition – particularly with regard to potential blocking of intake structures.
- Computing power is increasing very rapidly. This is leading in turn to a rapid improvement in the available software. Ongoing research is thus required to ensure that South African engineers keep pace with the development of suitable codes for the prediction of local scour and deposition that will, *inter alia*, enhance their capacity to design safe and durable hydraulic structures. Some aspects that require further attention include:
    - the optimum choice of incipient motion / sediment transport model in association with the appropriate numerical wall model for boundary adjustment
    - the impact of non-cohesive and/or non-uniform bed material
    - the impact of sediment load on flow properties (density, viscosity etc.)
    - live bed scour
    - rate of scour development
    - deposition
    - the potential use of discrete granular phase modelling as an alternative to empirical formulae (such as Van Rijn, 1987 etc.) to make the CFD

model more closely related to the physical processes and thus more generally applicable

- The possible linkages between high definition 3D hydrodynamic models and other types of models e.g. 2D river models, river ecology models etc. need to be explored. For example, 2D river models are ideally suited for the modelling of long river reaches where the flow is predominantly two dimensional. If these 2D models could be linked to a suitable 3D model, they would help to better describe the boundary conditions of the latter model – and thus its ability to predict scour and/or deposition. Meanwhile, ecologists have expressed great interest in modelling the hydraulic habitat of various organisms in an attempt to better understand how these affect the viability of these creatures.

Chapter 1
Introduction

1.1 Rationale

The ability to predict local scour and its opposite, local deposition, is of critical importance to South Africa. Local scour can undermine bridge foundations (not just road/rail, but also pipe bridges) and riverbanks. Local deposition can clog river abstraction works used in the provision of water to rural communities and agriculture. Together, they impact aquatic environments and change the courses of rivers. Any structure placed in a river, whether of natural or of human origin, will tend to promote scour and deposition.

The failure of river crossings and engineering structures in rivers in South Africa due to scour damage can result in substantial financial and economic losses in flood-affected regions. For example, the well-known failure of the John Ross Bridge over the Tugela River during 1987 floods in Natal was caused by scour which undermined the bridge pier foundations (Van Bladeren & Burger, 1989). Vehicles which normally used the bridge had to travel significant additional distances. Such failures do not, however, occur in isolation as during these floods a total of 120 bridges in Natal were destroyed or severely damaged. As a consequence, substantial losses were felt by the local economy. Designing for scour is not, however, a mature science. There have been many developments since the publications of the South African National Roads Agency Ltd. (1986) *Road Drainage Manual* and the Committee of State Road Authorities (1994) *Guidelines for the Hydraulic Design and Maintenance of River Crossings*, TRH 25. Furthermore, the mounting evidence for global climate change suggests that southern Africa must start preparing itself for the likely consequences of even more severe flood events and consequential damage to structures. There is also an increasing problem associated with scour and deposition around urban culverts / bridges – particularly as the modern tendency is to move away from concrete-lined channel sections towards more natural looking waterways.

The recently completed WRC study entitled *A unit stream power model for the prediction of local scour* (Armitage & McGahey, 2003) showed that there is still no universally agreed design procedure that can cope with all the observed scour and deposition phenomena. Most methodologies place considerable reliance on the use of dimensional analysis and empirical formulae and are extremely inaccurate. Physical models are more reliable, but are expensive. The road ahead ultimately lies with the use of computational fluid dynamics (CFD). A crude numerical model for the prediction of scour and deposition with the aid of CFD was developed in the course of the aforementioned WRC study.

The role of the engineering departments in many government institutions is changing from design to regulatory, and thus they are employing fewer and possibly less

experienced engineers, and years of accumulated wisdom in design is gradually being lost. They have extremely limited funds for research. There is a pressing need for the development of appropriate tools to enable the designers of the future to make the optimal use of limited resources. These tools should include design guides for local conditions, and the development of suitable software.

1.2 Objectives

The main objectives of this consultancy were as follows:

- Report on the extent to which local scour and deposition around culverts and bridges are a problem in South Africa.
- Conduct a literature review of the current state of the art regarding the CFD modelling of scour and deposition around manmade structures in the fluvial environment.
- Report on research needs with respect to the development of appropriate CFD tools for the prediction of scour and deposition around engineering structures.

1.3 Layout of this report

Chapter 2 offers a brief introduction to river scour in general, and local scour in particular. The mechanisms causing local scour around two simple structures – cylindrical piers and vertical plate abutments – are also described.

Chapter 3 commences with a historical overview of scour damage to major river crossings in South Africa, and particularly Natal, over the past five decades. This is followed by a description of a field and desk study of 121 bridges currently experiencing scour problems. Analyses of the nature of the damage were conducted and estimates of the associated repair costs made. The study focused on scour at provincially maintained road bridges although pipe and rail bridges and other hydraulic structures were included to a lesser degree. Emphasis was placed on the assessment of scouring mechanisms such as general, local and constriction scour which attack bridge foundations directly. Erosion of earth embankment dams and berms was not considered.

Chapter 4 looks at numerical modelling of local scour in rivers through Computational Fluid Dynamics (CFD). CFD is the numerical modelling of fluid flow and associated phenomena (Versteeg & Malalasekera, 1995; Olsen, 1999). The fundamental equations and methods used by CFD are briefly described. Although there a many commercial and general-purpose CFD codes available, local scour is difficult to model owing to the three-dimensional nature of the vortices that are set up in the vicinity of hydraulic structures. This chapter describes previous work in the modelling of scour, and then illustrates the current capability of two well-known codes, FLUENT Version 6.2 (a general CFD code) and TELEMAC Version 5.4 (a specialised river modelling code).

Chapter 5 contains some general conclusions as well as providing recommendations for future research. It is followed by **References** and **Appendices**. The

Appendices include cost estimates of current scour damage in South Africa, as well as giving details of commercial CFD codes (general and specialised river modelling codes) currently on the market.

Chapter 2
Local scour in rivers

2.1 Introduction

Prior to any discussion regarding the numerical prediction of local scour, it is important that there is a clear understanding of what it entails. Local scour, in the context of this report, refers to the hydraulic erosion of river bed material in the vicinity of, and as a consequence of, an obstruction, e.g. bridge pier or abutment. It is one of several recognised types of river scour.

River scour is generally categorised into three main types (e.g. Breusers & Raudkivi, 1991; HEC-18, 1995; Raudkivi, 1998):

i) General scour

ii) Constriction scour

iii) Local scour

Hoffmans & Verheij (1997), however, only identify two main categories: general scour and local scour, although general scour is further broken down into; overall degradation, constriction scour, bend scour and confluence scour. The fundamental difference between general scour and local scour is that whilst general scour is caused by long-term unidirectional velocity gradients in the vicinity of the bed, local scour is largely a consequence of vortex formation and dissipation. Under this definition, the scour due to bends and confluences may be classified under both categories.

It is the three-dimensional aspect of vortex formation and dissipation that makes local scour particularly hard to model – and thus predict. The vortices are particularly noticeable around hydraulic structures whose intrusion into the river channel generally results in the creation of steep local velocity gradients. This in turn results in extremely erosive conditions in the vicinity of the structures which may, in certain circumstances, may lead to their eventual undermining and collapse. Forewarning of these hazardous conditions is clearly of immense importance to the hydraulics engineer.

It is clear there are an infinite number of hydraulic structure designs. Furthermore, each river is unique. It therefore follows that each combination of structure and fluvial environment will produce a unique scour (and deposition) pattern that will furthermore vary dynamically as the conditions (flow rate, sediment transport, river morphology, vegetation growth, interaction with other structures etc.) change. Since the scour pattern has implications for foundation design, it is important that the engineer be able to model it.

This chapter describes some of the general characteristics of local scour, and then describes the formation of local scour around two simple structures; the circular pier and the right-angled vertical plate abutment.

2.2 The characteristics of local scour

Local scour results from the effect of a structure on local flow patterns and is superimposed on the other types of scour (e.g. general scour, constriction scour, bend scour etc.). It is normal to differentiate between two types of local scour: clear-water scour and live-bed scour (Armitage & McGahey, 2003).

"Clear-water scour" occurs in the absence of general scour. In other words, the flow conditions upstream of the structure are below the critical conditions for incipient motion. All sediment movement thus occurs directly as a result of the altered flow conditions caused by the presence of the structure. An exception is made in the case of wash-load that might have been transported over considerable distances (Raudkivi, 1998).

"Live-bed scour" occurs in the presence of general scour and is superimposed on it. In this case, the flow conditions upstream of the structure are above the critical conditions for incipient motion. Whilst clear-water scour can theoretically reach static equilibrium, live-bed scour can only reach dynamic equilibrium when the rate of sediment entering the scour hole equals the rate of sediment leaving it. A further complication is that river beds are not generally flat but usually consist of bed-forms, such as ripples or dunes, that migrate downstream as sediment is eroded from the upstream face and deposited on the downstream face.

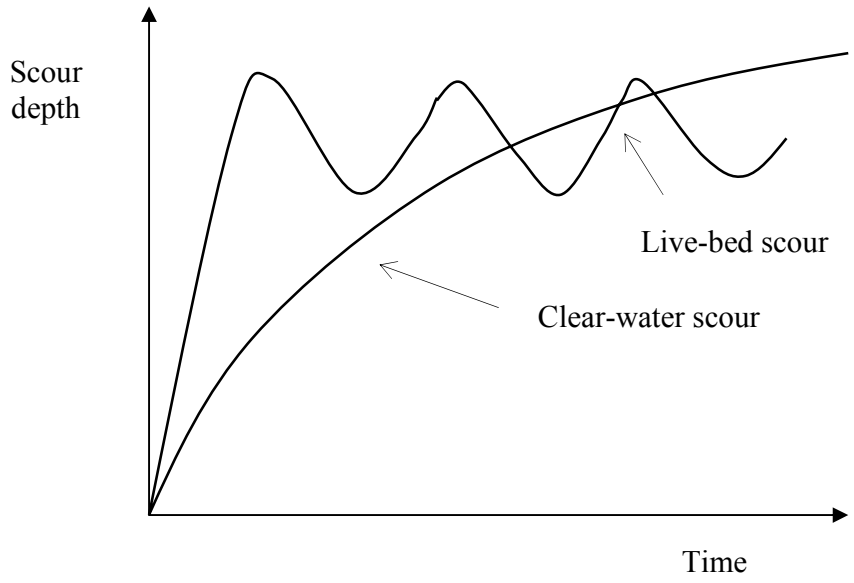

Figure 2-1: Scour depth as a function of time (After Armitage and McGahey, 2003)

A typical plot showing the scour depth versus time for the two types of scour is given in Figure 2-1. It is evident that the scour hole develops much more rapidly in the case of

live-bed scour, but the gross dimensions of the scour hole never reach equilibrium as they are affected by the passage of bed-forms.

Most work in local scour has focused on clear-water scour. Not only is it easier to analyse than live-bed scour, it also results in the larger scour hole, which is particularly important from the perspective of engineering design.

2.3 Local scour around a cylindrical pier

It is normal for the scour around piers and caissons (hereinafter called simply "piers") to be described in terms of the deviation from that for cylindrical piers (e.g. Breusers & Raudkivi, 1991; HEC 18, 1995; Hoffmans & Verheij, 1997; Raudkivi, 1998; Graf, 1998). The maximum scour depth is generally achieved with clear-water scour in uniform sediment (Figure 2-1). Non-uniform sediments tend to limit scour depths as a consequence of armouring.

The flow field around a cylindrical pier is extremely complex. Figure 2-2 shows a schematic diagram of the typical flow patterns around a cylindrical pier with a fully developed scour hole. Four distinct flow patterns can be identified (Armitage & McGahey, 2003):

i) The "bow wave" is caused by the sudden deceleration of the oncoming flow. The rise in the water surface at the leading face of the pier corresponds with the velocity head of the oncoming flow that generally reaches a maximum at, or near, the surface. The flow is forced up and back onto itself to form a bow wave or "roller".

ii) The rise in pressure on the leading face of the pier (termed the "stagnation pressure") decreases with the square of the velocity of the oncoming flow i.e. it generally decreases from top to bottom. This results in a partial reversal of the normal pressure gradient that provides the driving mechanism for a vertical "downflow". The maximum velocity of the downflow in vertical section, according to experimental data by Ettema (1980) and Raudkivi (1986), is situated between 0.05 and 0.02 times the pier breadth, b_p, upstream of the pier, getting closer to the pier as the flow descends towards the bed. The velocity of the downflow also increases in magnitude towards the bed in the vertical section. If no scour is present, the maximum velocity is approximately 40% of the average oncoming velocity, U. This velocity increases to approximately $0.8U$ as the scour depth increases past $2b_p$ (Breusers & Raudkivi, 1991; Raudkivi, 1998). This relatively high velocity flow directed at the base of the pier acts as a water jet that helps to initiate and maintain the scouring process (Graf, 1998). The increased pressure on the leading face of the pier also helps to provide the necessary force for the acceleration of the flow around the sides.

iii) Once a scour hole begins to form, flow separation at the upstream rim results in the formation of a lee eddy that rotates in the opposite direction to the bow roller. This lee eddy is called the "horseshoe vortex" owing to its distinctive shape – it wraps itself around the front half of the pier and extends a few pier diameters downstream on either side before losing its identity and becoming part of the general turbulence. According to Raudkivi (1998), the vorticity of the horseshoe vortex is quite small and its main role in the scouring process comes about through its interaction with other flow structures. For example, it pushes the maximum downflow velocity within the scour hole closer to the pier.

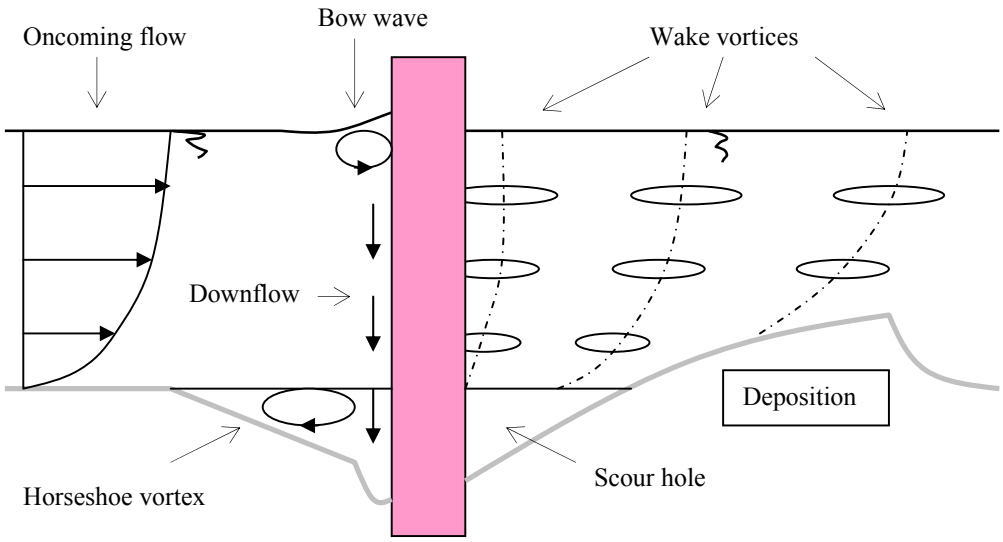

a) Centreline profile

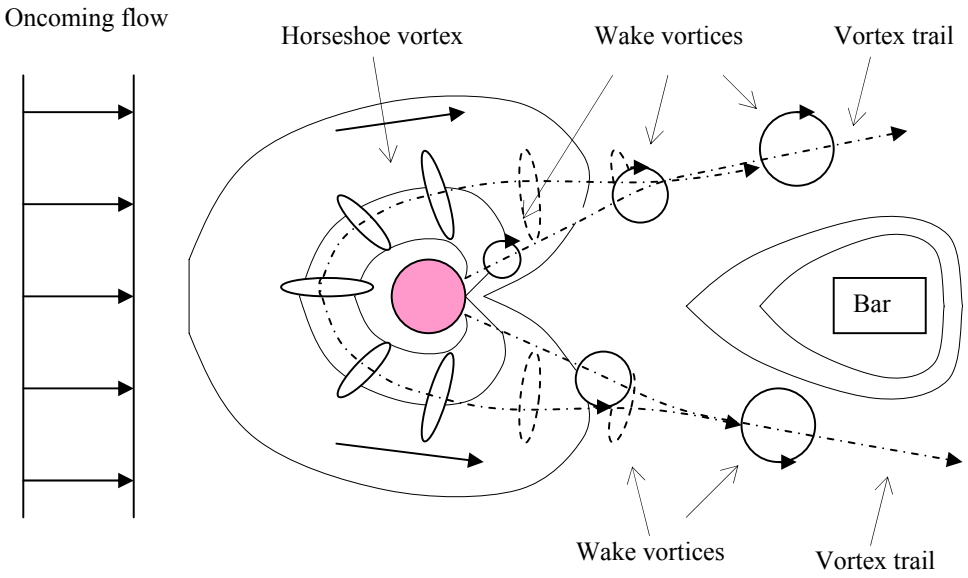

b) Plan

Figure 2-2: Flow patterns around a cylindrical pier
(After Breusers & Raudkivi, 1991; Hoffmans & Verheij, 1997; Raudkivi, 1998)

iv) Flow separation around the sides of the pier results in the formation of "wake vortices" that alternately separate from the two sides to form a Von Kármán vortex street. Near the bed, these vortices interact with the horseshoe vortex and, with their vertical low-pressure centres, lift sediment from the bed like miniature tornadoes (Raudkivi, 1998). The frequency, f, of the vortex shedding is indicated by the Strouhal Number, $St = \left(fb_p / U\right) \approx 0.2$

According to Breusers & Raudkivi (1991), scour hole development commences at the sides of the cylinder with the two holes rapidly propagating upstream around the perimeter of the cylinder to meet on the centreline. The eroded material is transported downstream by the flow. Soon after the commencement of scouring, a shallow groove, concentric with the front portion of the cylinder, is formed by the downflow. This groove often has near-vertical faces with a sharp upper edge. The downflow is turned 180^o in the groove, and the resulting upward flow is deflected by the horseshoe vortex up the scour hole slope. The sand in the region around the rim collapses into the groove from time to time in order to return the slope angle to the angle of repose of the bed material. Sand particles in the groove are lifted by the upflow into the region of the horseshoe vortex where they are either deposited on the slope or transported into and through the wake region. They tend to deposit in the region between the two vortex trails to form a bar. As the scour approaches its equilibrium depth, the groove becomes shallower and can disappear altogether.

Zanke (1978) has distinguished four phases in the evolution of a scour hole: an initial phase, a development phase, a stabilisation phase, and an equilibrium phase (Hoffmans & Verheij, 1997). It sometimes takes several days for clear-water scour to reach equilibrium. If the sand is fine, ripple formation tends to reduce the maximum scour depth (Raudkivi, 1998).

Live-bed scour is complicated by the passage of bed forms past the pier. The equilibrium depth is thus generally defined as the time-averaged scour depth. It is generally less for live-bed scour than clear-water scour (Raudkivi, 1998). Live-bed scour also tends to reach equilibrium much faster than clear-water scour – commensurate with the higher sediment transportation capacity of the flow. The shape of the scour hole around a single cylindrical pier in a uniform flow with its foundation in a uniform bed material has been studied by a number of researchers including Dargahi (1987), Olsen & Melaaen (1993), and, indirectly, by Dey et al. (1995). A typical scour hole profile is shown in Figure 2-2. Dargahi (1987) schematised the plan section of a fully developed cylindrical pier scour hole into a semi-circle on the upstream side and half of an ellipse (cut along the minor axis) on the downstream side. The semi-circle has a radius of about $2b_p$ measured from the centre of the pier, provided that the flow depth is at least $3b_p$. The length of the scour in the downstream direction is in the order of $5b_p$. According to Hoffmans & Verheij (1997), the average upstream slope is approximately equal to the angle of repose, ϕ_r, being a little steeper in the groove close to the pier and a little flatter

outside of this. The average downstream slope is about $\phi_r/2$. The deepest point of the scour hole is usually in the vicinity of the leading face of the pier, but at times it can be found at an angle of up to 60^o to the centreline on either side of the front face (Chiew, 1995).

2.4 Local scour around a vertical plate abutment

There is a large number of different structures that encroach into the channel flow from one or both sides. Spur dikes are built out from the bank of a river to deflect the main river current away from an erodible bank. Guide banks are built around structures such as road embankments to protect them from erosion (Breusers & Raudkivi, 1991). Bridge crossings are often made shorter by locally reducing the width of the river with the aid of approach embankments and abutments that extend across the floodplain into the main channel. In all cases, groynes, dikes, guide banks and abutments (hereinafter called simply "abutments") are horizontal constrictions in the flow that promote three-dimensional flow patterns in a similar manner to piers (Hoffmans & Verheij, 1997). There are many different abutment shapes. To simplify analysis, however, it is usual to describe the scour around each abutment shape in terms of the deviation from that measured for a vertical, sharp-edged, "plate" abutment (e.g. Breusers & Raudkivi, 1991; Hoffmans & Verheij, 1997; Raudkivi, 1998). All abutments, of course, have a finite thickness, but a vertical-wall abutment can be regarded as equivalent to a "plate" abutment if the length of the abutment normal to the dominant flow direction, L_a, is at least five times the width of the abutment (Hoffmans & Verheij, 1997).

The general flow patterns around a vertical plate abutment are depicted in Figure 2-3. To a degree, the flow pattern around an abutment is similar to the flow around one half of a pier. In both cases there is a bow wave (or roller), an associated downflow, a horizontal vortex near the base, and wake vortices that are shed rhythmically from the side of the structure (c.f. Section 2.3). There are, however, important differences. Piers do not generally reduce the channel flow section to any great degree. Abutments, on the other hand, frequently restrict the horizontal width of the channel by a substantial amount. This results in an increased average flow velocity through the remaining open section, and consequential increase in the possibility of scour in that region. Scour resulting from the reduced width of the flow-section is generally termed "constriction scour", but it can be readily seen that it is a special case of general scour (Armitage & McGahey, 2003). Another difference is the "principal" vortex that is the equivalent of the horseshoe vortex in piers. Except in the case of very short abutments, the principal vortex does not generally remain closely attached to the structure, but usually commences from a point somewhat upstream. It lies along the boundary between the fast-moving upstream flow section and the "dead" water trapped in the corner between the abutment and the sidewalls or banks of the channel. Often a secondary, counter-rotating vortex is induced by the principal vortex immediately upstream of it. The flow acceleration into the funnel marked by the principal vortex helps to make this vortex extremely strong and, as a consequence, the maximum scour depth usually occurs immediately upstream of the end of the structure (Hoffmans & Verheij, 1997). Downstream of the structure, wake vortices,

shed from the end of the abutment, travel along the boundary between the main flow channel and a second “dead” water region before dying out into general turbulence. The flow eventually re-attaches itself to the banks of the channel some way downstream of the structure.

Although the two “dead” water regions are hydraulically separated from the main channel by the principal vortex and the vortex trail respectively, very strong eddies can be induced in them through the shearing along the boundary. Under certain circumstances, these eddies can cause the formation of local scour holes. In general, the scour hole around the abutment develops in a similar manner to that around a pier (c.f. Section 2.3), except that there is no sharp-edged groove in the vicinity of the structure.

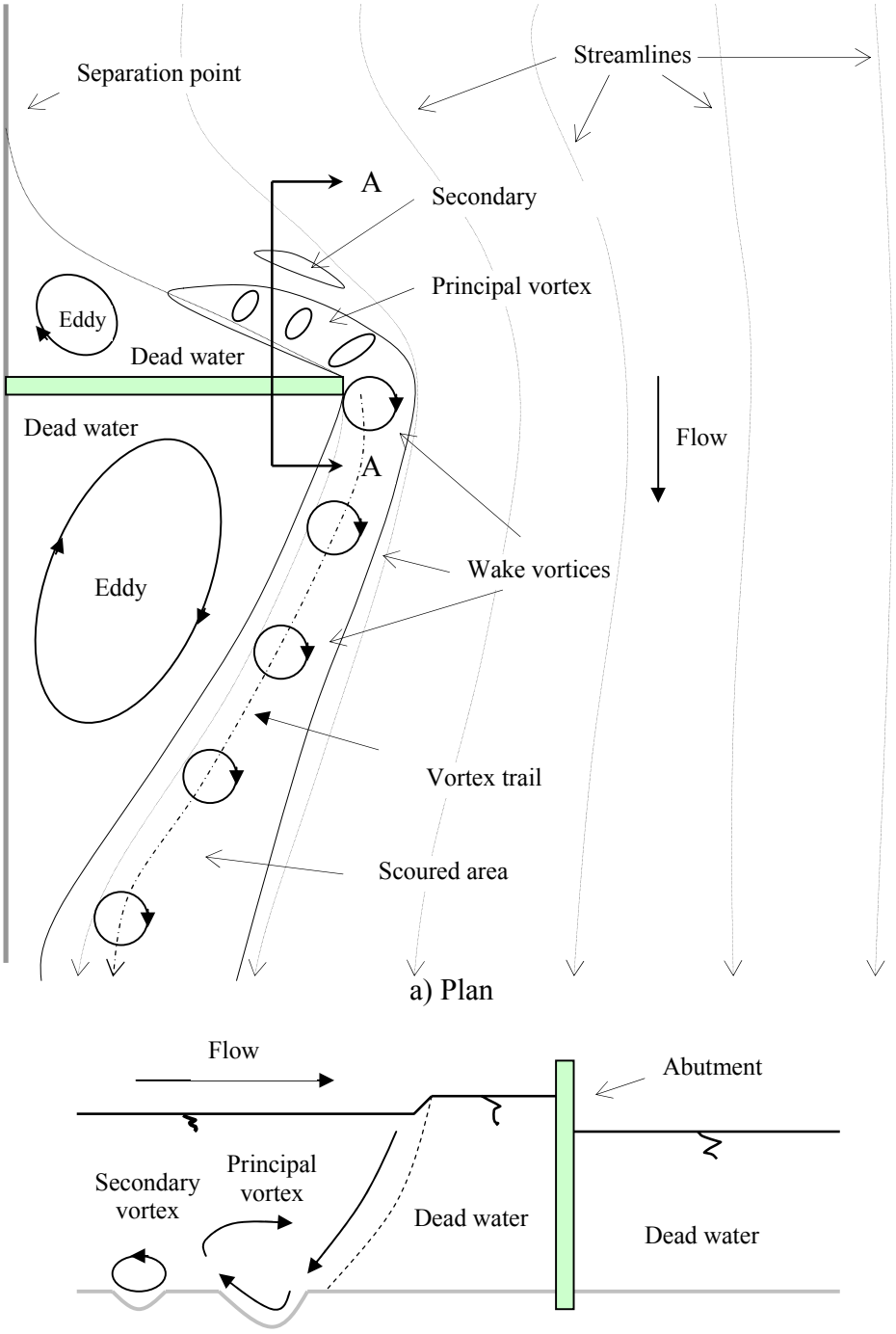

Figure 2-3: Flow patterns around an abutment
(After Breusers & Raudkivi, 1991; Hoffmans & Verheij, 1997; Raudkivi 1998)

2.5 Concluding remarks

Local scour is a major engineering problem as it can cause the undermining of hydraulic structures and their possible eventual collapse. The phenomenon is extremely difficult to analyse and predict due to the complex multidirectional flow fields. This chapter attempted to describe the basic processes. The next chapter focuses on the scale of the problem in South Africa.

Chapter 3
Bridge scour damage in South Africa

3.1 Introduction

The purpose of this chapter is to give an order-of-magnitude estimate of the extent to which bridge scour at river crossings is a problem in South Africa. It commences with a historical overview of scour damage to major river crossings. This is followed by a short description of the methodology that was followed in this study to estimate the prevalence of various types of scour damage and the annual cost of scour damage to provincially managed bridges in South Africa. The findings follow.

3.2 Historical overview

3.2.1 Recurrence of large floods and associated scour damage

Advances in flood hydrology are gradually improving the prediction of the magnitude and frequency of flooding in South Africa. Historical records indicate, however, that extensive damage to engineering structures such as weirs and river bridges has continued in spite of improved flood prediction. Often a single structure has been damaged repeatedly by major floods over several decades.

The coastal roads of KwaZulu-Natal have a 150 year history of bridge failure and the large number of river bridges involved increases the probability of disruption to traffic. Records of scour-related bridge failure in Natal rivers date back to 1868, when floods caused the failure of the iron plate girder Queens Bridge over the Umgeni River near Durban. The bridge had been built only four years earlier to replace the Connaught Bridge which failed during 1856 floods. The Queens Bridge was founded in a clayey river bed on 5 to 10m long timber piles. Although the Queens Bridge was constructed with much larger openings than the Connaught Bridge and the bridge was not overtopped, the river velocities between the piers reached an estimated 6.7 to 8.9m/s. After the floods, the piles at the southern end of the bridge had disappeared, whilst the remaining piles were exposed by scour (Van Bladeren, 1992).

During the 1959 floods in Natal, one pier on the Lovu River Bridge sank by 2.74m and three bridge spans were destroyed. In March 1976, one pier settled by 1.83m. Damage to bridges on the Natal South Coast during the 1976 floods was estimated at R50 million (R950 million in 2004 terms).

Scouring around piers and piles was noted as one of the most common causes of bridge failure during the 1987 Natal floods (Van Bladeren & Burger, 1989). A total of 130 bridges were destroyed or severely damaged during these floods including the John Ross / N2 Bridge over the Tugela River. Change in the river's course and/or lateral erosion also led to the failure of a number of bridges and gauging weirs. The approaches of the Edendale bridge over the Msunduse River and N2 bridge over the Mdloti River

were badly eroded, whilst a gauging weir and bridge situated on a meander of the Mhlatuze River were endangered by lateral migration of the meander. Van Bladeren & Burger (1989) noted that outflanking of the weir and undermining of the bridge abutment is to be expected in future floods.

Recent flooding in February 2000 in the north and north-eastern regions of South Africa caused extensive damage to infrastructure, and disrupted economic activity in Mpumalanga and the Northern Province. Approximately 200 bridges and other drainage structures were washed away or severely damaged during floods in the Northern Province alone. The value of damage to provincial roads and bridges alone was estimated at R1.269 million (R1.960 million in 2004 terms) (Chabane *et al*., 2000). This excludes extensive damage to local streets and drainage structures falling under local government authorities. An additional R25.6 million (R40 million in 2004) damage was estimated to have been sustained by dams and bridges in the Kruger National Park. Damage to river crossings was mostly caused by erosion of the approaches as backflow occurred on the downstream side of the bridge approach fills. In a discussion of these floods, Van Bladeren and Van der Spuy (2000) list twelve previous flood events in the region dating back to 1909 which caused damage of comparable magnitude to that experienced in the 2000 floods. The N1 route to Beit Bridge has been "seriously disrupted" by floods on five occasions in the past 42 years (Alexander, 2000).

In an investigation into January 1981 floods in the South Western Cape, Kovács (undated) stated that the erosion of soil and subsequent deposition of sediments is probably the most prevalent form of flood damage affecting the drier areas of South Africa. During this event, severe scouring downstream of man-made river constrictions, dams and river confluences led to deposition of a 0.5 m deep layer of sediment over 700 000 m^2 of cultivated land downstream of Laingsburg. Further downstream of the town, approximately 9.2 Mm^3 of soil was deposited in the Floriskraal Dam reducing its original capacity by 23%.

Scour damage to bridge foundations is certainly not limited to structures in rural areas. Uncanalised rivers receiving fast flowing water from impermeable surfaces, concrete pipes and lined channels also encounter scour problems. During the February 2000 floods, bridges in many golf courses in Gauteng were affected by flood damage. Foundations of bridge piers and abutments in the Jukskei River at the Dainfern Golf Course were undercut, bridge approaches were washed away, and sediment deposits left on the fairways (Arup, 2000). Fast flowing runoff from impervious urban areas may present a threat to golf courses in which rivers are not canalised to enhance their aesthetic appeal.

It is important to realise that scour is often difficult to detect and the maximum scour depths attained under peak flood conditions cannot be measured with ease. From investigation of the 1978 floods in Natal, Van Bladeren & Burger (1989) concluded that time scales for scour are short. Sedimentation in scour holes may occur within a few hours after the flood peak and the maximum scour depth concealed. For example, scour at the Pondoland Bridge on the Mzimvubu River at Port St Johns during the 1978 floods

caused the failure of one pier and the collapse of two spans. The scour depth at the bridge was estimated at 19.5m by depth soundings but had diminished to 0.4m two years later (Van Bladeren, 1992).

3.2.2 Consequences of scour damage

i) Disruption of communications

Substantial economic losses may result from transport routes and communication links which are lost due to floods. The floods affecting the Transkei and Natal Coastline in 1913 severely disrupted communications south of Durban. Eight railway crossings could not be used as the bridges had failed and/or the approach embankments were washed away. Less severe floods in 1985 again disrupted road and railway links with an estimated R2 to R3 million in damage (R13 to R20 million in 2004). Two spans were lost from the Mpambanyoni River road bridge in a manner which suggests that the pier supporting these spans was undermined by scour. During the 2000 floods, some routes in the Northern Province carrying in excess of 4000 vehicles per day were cut off for long periods of time. Temporary bypasses were vulnerable to smaller floods occurring after the main event and were sometimes unsuitable for use by heavy vehicles. Alternative routes had to be found for rail transport and an additional 600 km had to be travelled on some routes.

ii) Disruption of services

Pipe bridges or pipelines attached to road and rail bridges can also be vulnerable to scour damage. Water supply to rural communities, in particular in the Northern Province and Mpumalanga, was severely disrupted by the February 2000 floods. Damage to weirs, pump stations and pipelines affected water supply to more than 2.1 million of the 3.5 million people normally served by this infrastructure (Muller, 2000). Damage sustained by many bridges also resulted in damage to pipelines supported by these structures.

iii) Loss of flow data

Scour is often responsible for outflanking of gauging weirs. The reason for the failure of the recording towers, which are usually located on the river floodplains, may however be difficult to establish. The failure may be due to hydrodynamic and debris loading, or alternatively to local and general scour undermining the foundations of the tower. Furthermore, the recording stations may be partially or entirely submerged when failure occurs so that the failure event cannot be witnessed by an observer. In an investigation following the 1981 floods in the Buffels River in the South Western Cape, which affected the town of Laingsburg, many of the flow measuring stations installed on various bridges and weirs could not be used for this purpose due to serious damage or a complete wash-away of the structure and/or recording station. Excessive erosion and debris accumulation at contracted bridge sections also rendered the bridge unsuitable for use in flood flow

calculations (Kovács, undated). During the 1984 Domoina floods in Northern Natal, 19 recording towers and gauge plates were washed away at river measuring stations (Kovács *et al*., 1985). Many more stations sustained damage. The value of damage to river gauging equipment was approximately R600 000 (R4.3 million in 2004). Extensive damage was again incurred by the Natal flow gauging network during the 1987 floods. Flood damage reports were prepared for 68 stations of which 34% were destroyed and a further 18% suffered structural damage. The total damage to the provincial flow gauging network was estimated at R1.2 million (R6.2 million in 2004) which was equal to the total annual budget of the Natal Directorate of Hydrology for that year (Van Bladeren & Burger, 1989). Of the 100 flow measurement sites employed in flow calculations for this flood event, only one was a bridge contraction site as all other potential bridges were considered unsuitable. They had been washed away, severely damaged, loaded with excessive amounts of debris or experienced excessive, unquantifiable scour of the riverbed at the constriction.

Damage to the flow gauging network of the Department of Water Affairs and Forestry (DWAF) during the 2000 floods in the northern provinces of South Africa was estimated at R32 million (R50 million in 2004). In addition, invaluable and irretrievable flow data was lost. Gauging weirs were frequently outflanked, recorder towers overturned, and recording instruments washed away. At the time, it was expected to take more than five years to reinstate the damaged weirs and recording equipment (Muller, 2000).

3.2.3 Importance of scour as a failure mechanism in river crossings

Relatively few investigations of major flood events have included studies into the cause of damage to structures in rivers. Indeed, the assessment of damage has not even formed part of the terms of reference of many reports. Instead, in many technical reports (e.g. Kovács, 1978; Du Plessis, 1984; Du Plessis & Bain, 1987), emphasis has rather been placed on calculation of the recurrence interval of the flood and estimation of the peak flow. In the few studies where a damage assessment has however formed part of the study, scour has been reported as a leading cause of damage.

In investigative reports into major flood events in South Africa, both Kovács (undated) and Van Bladeren and Burger (1989) noted the prevalence of scour and sedimentation processes in damage sustained by engineering infrastructure in rivers. In their documentation of the 1987 Natal floods, they include a comprehensive study of bridge failures resulting from the floods. The cause and mechanism of failure was determined for a total of 31 structures. Scour damage to the bridge foundations or approach embankments was reported at 21 of these sites. Scour directly undermining bridge foundations was identified as the reason for catastrophic failure of six bridges. In a review of bridge failure and damage occurring during the 2000 floods in the northern and north-eastern regions of South Africa, Sheasby (2000) reported that that the bridge crossing failures were predominantly due to scour and that very few structural collapses occurred where the piers were properly founded.

Although flood hydrology analyses are essential to improving future flood prediction, investigation into the damage-causing mechanism is equally important.

3.3 Methodology adopted by this study

An attempt was made in this study to estimate the prevalence of various types of scour damage, and the annual cost of scour damage to provincially managed bridges in South Africa. This section describes the sources of information, some details regarding the field survey, the identification of the most prevalent scour types, and how the costs of repairing the scour damage were estimated.

3.3.1 Sources of information

The information used for this study came from three different sources; the provincial Bridge Management Systems, investigative studies and design reports undertaken by consultants, and technical reports on historical floods. The study is not comprehensive; it focuses largely on bridges under the authority of the various Provincial Governments. Bridges on National Roads are covered only in general terms via the technical reports on historical floods, whilst those under the jurisdiction of Local Government are not covered at all owing the enormous difficulty in obtaining information on them.

The condition of road bridges in most provinces is monitored through Bridge Management Systems (BMSs). These are electronic or hardcopy database systems containing information about the road bridges in each province falling under the jurisdiction of the Provincial Government. This information is collected during routine bridge inspections and typically includes the following:

- Location, geometry and dimensions of the bridge and description of the structural system.
- Information relating to the condition of various structural elements of the bridge, the condition of the waterway, and traffic volumes on the route.
- Numerical ratings for the severity and extent of existing distress of structural components and identification of potential damage which may occur in future.
- Estimates of repair costs and an indication of the urgency of these repairs.
- Photographs of the bridge in general and specific elements needing repair.

Some electronic BMSs are also linked to a GIS environment so that a specific structure or route can be located with ease. A search function enables the user to identify all bridges which, for example, are subject to a particular type of damage, or all those which have a priority rating above some user-specified value. The information contained in the BMS is collected during routine bridge inspections which take place every five years or as resources permit. They are managed by the provincial transport / roads authority or consulting engineers appointed by the provincial authority.

Table 3-1: Status of the Bridge Management Systems in South Africa (as at July 2004)

Province	BMS Format	No. of Structures in BMS
Eastern Cape	Electronic system linked to GIS	1400
Free State	Hardcopy system with detailed maps	1800
Gauteng	Electronic system	680
KwaZulu-Natal	Electronic system	400*
Limpopo Province	Electronic system	800
Northern Cape	Electronic system	500
Western Cape	Electronic system linked to GIS	2200

* Of the 3200 bridges in KwaZulu-Natal, only 400 had been inspected at the time of the study.

The status of BMSs in South Africa is summarised in Table 3-1. The status of the BMS in Mpumalanga was not determined owing to difficulties encountered in locating the person responsible for the system. In the North-West Province, a bridge inventory study had yet to commence at the time of the study. A search for the keyword "scour" was run in the available BMSs for each province to identify all structures currently subject to scour damage. In some systems, the search was also performed for the nature of damage to extract bridges with damage described as "undermining" or "erosion" for example. The search function was also employed, in some instances, to identify components associated with scour repair using keywords such as "gabions", "backfill" and "underpin".

Investigative reports and bridge design reports produced by consulting engineers for bridges at which particularly severe or recurrent damage has occurred were also reviewed. These reports constituted about 15% of the data collected and were obtained and reviewed upon the recommendation of engineers involved in bridge repairs and BMSs. No thorough search for such reports was undertaken. The findings, therefore, do not include all the bridges at which special investigations have been undertaken.

A Technical Report is produced by the Department of Water Affairs and Forestry (DWAF) after each major flood event in South Africa (see Section 3.2). These Technical Reports primarily contain hydrological data, but some also include an assessment of the damage caused by the flood event. The majority of these reports document floods affecting KwaZulu-Natal and the former Transkei region of the Eastern Cape. The information was treated differently to that from the more current BMSs and Consultant's reports as it was generally not as detailed, particularly with respect to scour types and costs. Although estimates of the total cost of flood damage are provided in most documentation, the fraction of this cost which may be attributed to scour damage had to be estimated. The precise cause of the failure of a bridge under extreme flood conditions was also usually difficult to determine. It was also not possible to draw conclusions about the prevalent types of scour from historical information.

3.3.2 Field survey

A total of 121 sites in seven of South Africa's nine provinces were investigated in detail as part of this study. Visits were made to 56 of these sites, and the remaining 65 were investigated by means of a desk study (Table 3-2 and Figure 3-1). Two sites were weirs whilst the remainder were road bridges. They were selected on the basis of the relevance of the nature of distress to this study, the severity of scour damage and location of the structure. Where priority ratings were employed in the BMS, bridges with higher priority or urgency ratings were selected in preference to others. Structures were otherwise selected based on photographs stored in the BMS or on the recommendation of the person responsible for the system.

Table 3-2: Distribution of survey sites by province

Province	Number of structures investigated		
	Field & desk study	Desk study only	Total
Eastern Cape	20	2	22
Free State	0	31	31
Gauteng	0	3	3
KwaZulu - Natal	15	14	29
Limpopo Province	2	13	15
Mpumalanga	0	0	0
North - West	0	0	0
Northern Cape	1	2	3
Western Cape	18	0	18
Total	**56**	**65**	**121**

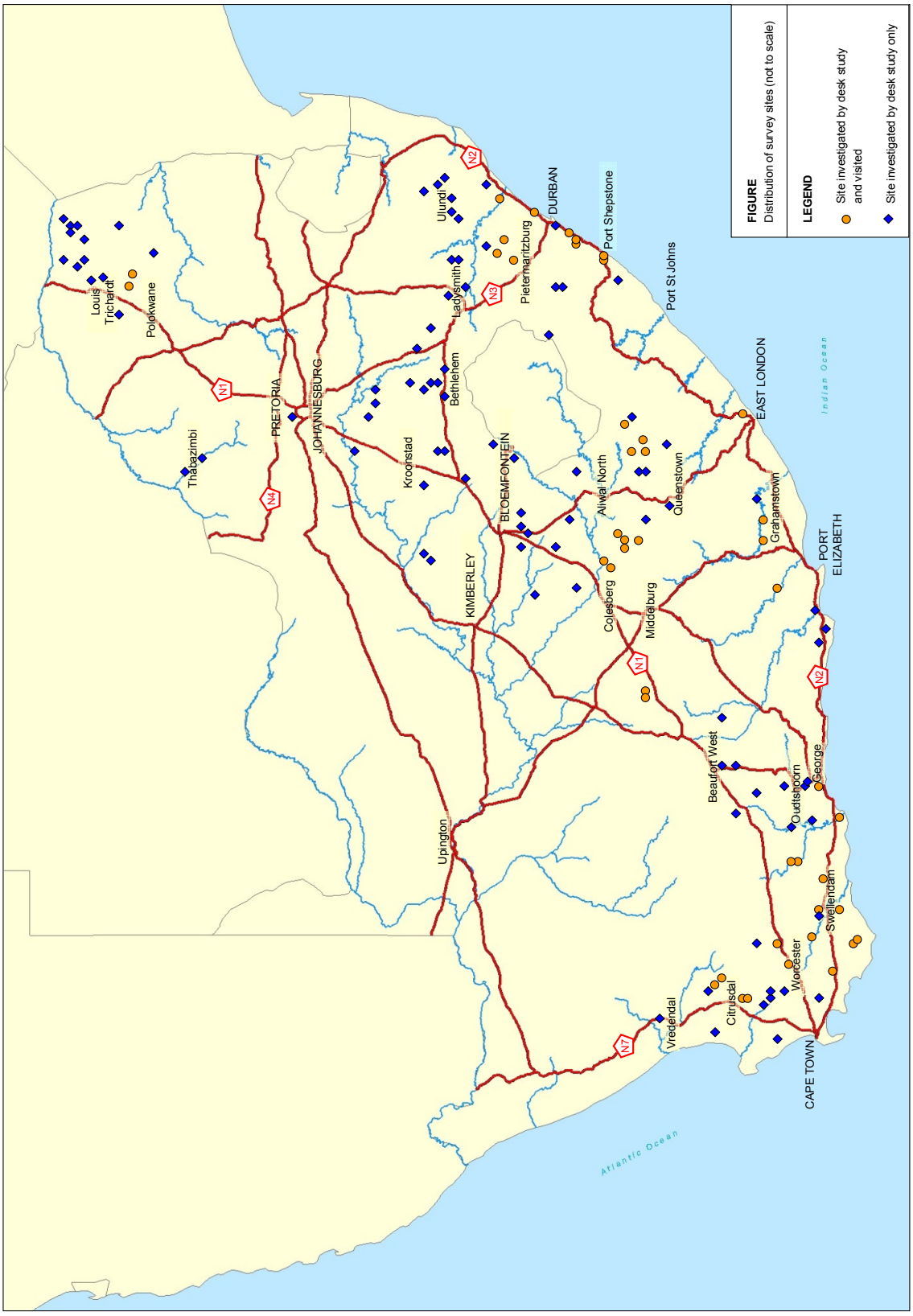

Figure 3-1: Distribution of survey sites

3.3.3 Identification of most prevalent scour type

Photographs taken and notes made during the field survey and information gathered in the desk study were used to classify the observed scour condition into the following five categories

i) **General scour** due to changes in the flow and the river's sediment load. A river's longitudinal profile adjusts over time in response to the flow and sediment load of the stream. For the purpose of this study, general scour was considered as scour which is not caused or affected by the presence of a bridge.

ii) **Constriction scour** where the cross-sectional area of the stream is reduced and flow velocity raised by narrow bridge openings. The presence of narrow bridge openings may also cause outflanking of the approach embankments under flood conditions due to the afflux resulting from the damming effect on the river.

iii) **Local scour** around bridge foundations such as piers, abutments and other local obstructions to the river flow. The formation of vortices around these obstructions leads to scouring immediately adjacent to the foundations.

iv) **Outflanking** where the approach embankments of a bridge have been scoured and water flows around the bridge.

v) **No scour evident** or the type of scour was concealed by water or dense vegetation.

More than one type of scour was evident at most sites. Emphasis was placed on those types of scour, such as general, local and constriction scour, which attack bridge foundations directly. Erosion of earth embankments at bridge approaches was not considered in detail, although outflanking is a common failure mechanism at river crossings.

Only 105 of the 121 sites surveyed revealed sufficient information for the determination of the most prevalent types of scour.

3.3.4 Costs of repairing scour damage

Estimates of the annual value of scour damage occurring at road bridges in South Africa were obtained or estimated from data in the Provincial BMSs and adjusted to 2004 values. Bridge inspections typically take place at 5 year intervals and maintenance and repair should be completed before the next inspection. The cost estimates thus generally reflect the value of damage which has been sustained by structures on an ongoing basis rather than that caused by extreme events. For calculation purposes, it was assumed that the value of the damage recorded in the BMSs occurred over a period of 5 years prior to

the last inspection and thus the total scour repair cost calculated for each province was divided by 5 to obtain the annual value of scour damage.

Estimates of the repair costs for four bridges which failed during the 1987 floods in Natal were available from the KwaZulu-Natal Department of Transport. These help to give an indication of the extent by which the inclusion of extreme events might increase the annual value of scour damage occurring in South Africa. The contribution of these historical failures to the annual value of scour damage occurring in South Africa was estimated by dividing the current cost of repairing the damage by the recurrence interval, *RI*, of the flood at the bridge location. This makes the simplistic assumption that the *RI* of the flood flow is equal to the *RI* of the damage.

As the cost data for each province was presented in slightly different ways, some interpretation was required to bring all the data onto a common base.

i) Eastern Cape, Gauteng and Northern Cape

Reliable cost data was obtained from the relevant BMSs for the Eastern Cape, Gauteng and Northern Cape provinces. The scour cost was calculated as the total value of repair activities associated with scour damage. The repair activities which were included are listed in Appendix A.

To produce realistic estimates of scour costs, an estimate had to be made of the fraction of each individual cost that was as a result of scour. For example, in the case of the item "reconstruct pier", it was assumed that 70% of the repair cost was incurred as a result of scour damage.

The percentage of bridges exhibiting some form of scour damage and approximate cost per scour-damaged bridge is given in Table 3-3.

Table 3-3: Prevalence and costs of scour damage in the Eastern Cape, Northern Cape and Gauteng

Province	Proportion of bridges with scour damage (%)	Cost per scour-damaged bridge (R)
Eastern Cape	26	R46 000
Northern Cape	20	R23 000
Gauteng	16	R3 000

ii) Free State

Comprehensive maintenance cost data was obtained for 31 severely scoured bridges in the Free State. The scour repair cost for each bridge was estimated from the total cost based on the severity of scour damage observed in photographs of each structure. The average cost per scoured bridge was then reduced to 80% of the calculated value as the 31 bridges analysed represent the more severe cases in the province. This reduced the

cost per scour-damaged bridge to R22 000 which is similar to the rate calculated for the Northern Cape. This is a conservative estimate as the Free State is a wetter province than the Northern Cape. It was also assumed that, as in the Northern Cape, 20% of bridges in the Free State were subject to scour damage.

iii) KwaZulu-Natal, Limpopo Province and Western Cape

From the provincial BMS it was determined that scour damage is evident at 28% of bridges in KwaZulu-Natal. Owing to the lack of sufficient data, the costs of scour damage in KwaZulu-Natal, Limpopo Province and the Western Cape were based on the more detailed information from the Eastern Cape and Free State. As, however, the rivers and therefore bridges in KwaZulu-Natal are larger than those in the Eastern Cape, the cost per scour-damaged bridge was estimated as R52 000 – which is slightly more than that calculated for the Eastern Cape.

In Limpopo Province, it was assumed that 24% of bridges currently experience scour damage and that the repair cost per bridge is R36 000. These values are intermediate between those for the Free State and Eastern Cape.

As the Western Cape is more mountainous than Limpopo Province a rate of R38 000 per scour-damaged bridge was assumed. It was again assumed that 24% of bridges in the Western Cape are subject to scour damage.

iv) Mpumalanga and North-West

The number of bridges in Mpumalanga and the North-West Province was unknown and therefore had to be estimated from the available data from neighbouring provinces. The area, population and Gross Geographic Product (GGP) of Limpopo Province were compared to that of the North-West and Mpumalanga. The GGP appeared to be a poor indication of the number of transport links and hence bridges so, in the end, only the area and population figures were used. In Mpumalanga, for example, the number of bridges in the province was calculated as follows:

$$B_{MP} = \frac{1}{2}\left(\frac{A_{MP}}{A_{LP}} + \frac{P_{MP}}{P_{LP}}\right)B_{LP} \tag{3.1}$$

The subscripts *MP* and *LP* refer to Mpumalanga and Limpopo Province respectively. *B* is the number of bridges, *A* the area, and *P* the population of the province.

It was assumed that scour occurs at 24 and 22% of bridges in Mpumalanga and the North-West respectively. The cost per scour-damaged bridge was estimated at R38 000 in Mpumalanga. A value of R24 000, similar to that of the Free State, was assumed for the North-West Province.

3.4 Types of scour observed

3.4.1 General scour

General scour occurs as a response to changing flow and sediment loads in a river. Sites at which general scour has taken place are shown in Figures 3.2 to 3.11. This is often a natural process but may be accelerated by mining of the riverbed (Figures 3.10 and 3.11). General scour may expose piles or caissons which are less streamlined than the bridge piers and local scour may then commence at these obstacles as shown in Figures 3.3 and 3.9. General scour was observed at 22% of the 105 bridges analysed.

3.4.2 Constriction scour

Bridge openings are usually narrower than the natural width of the river to reduce the bridge length and cost of the structure. The reduced cross-sectional area of the river at the bridge increases the flow velocities creating a potential for scour of the riverbed in the contracted section and immediately downstream of the bridge. Constriction scour was evident at 44% of the bridges studied.

Figure 3-2: General scour, occurring as the river naturally erodes downwards, has exposed the piles at some pier footings at bridge ZB1103 near Dalton, KwaZulu-Natal.

Figure 3-3: This exposed pile is now subject to local scour

Figure 3-4: Water flows under the bridge piers as a general lowering of the bed has occurred at B2763 near Glendale, KwaZulu-Natal. This bridge is also subject to excessive sedimentation at times.

Figure 3-5: Evidence of local scour at the piles in the sandy riverbed.

Figure 3-6: The Mzimkulu River at Port Shepstone, KwaZulu-Natal, has a long history of flooding.

Figure 3-7: The piles of this bridge near the Mzimkulu river mouth have been exposed to a significant depth.

Figure 3-8: Caissons below the N2 Bridge at Port Shepstone are exposed.

Figure 3-9: The Palmiet River in the main street of Grabouw, Western Cape, no longer flows parallel to the bridge piers. This may have initiated scouring under the bridge and exposure of the piles.

Figure 3-10: A local entrepreneur produces concrete bricks from this bridge site in KwaZulu-Natal.

Figure 3-11: Although repair of the scouring under this bridge is not urgent, mining of river sand downstream of structures can initiate head-ward erosion which could undermine the foundations.

Figure 3-12: Constriction of the flow at this culvert near Riebeeck East, north-west of Grahamstown, Eastern Cape, has led to high velocity water exiting the downstream end. The riverbed has been severely scoured for a long distance downstream.

Figure 3-13: Same culvert as Figure 3-12 from the downstream side.

Figure 3-14: Same culvert as Figure 3-12 looking downstream.

Figure 3-15: Scour of the riverbed immediately under the bridge openings may indicate constriction scour. Many bridges such as this have puddles of stagnant water under the structure where scour took place during floods. (Photo: Free State Department of Transport)

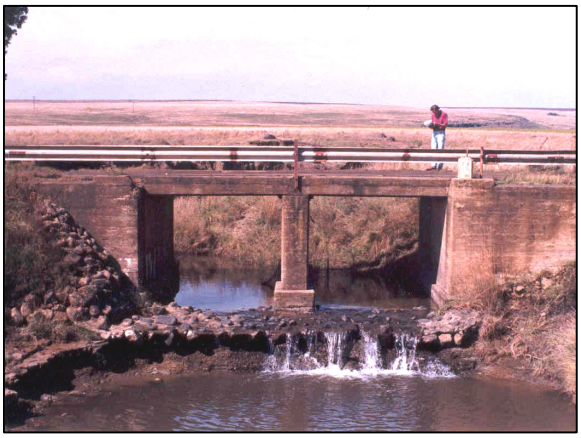

Figure 3-16: Scour downstream of B1972 in the Free State (Photo: Free State Department of Transport)

Figure 3-17: The above bridge is in a critical state as constriction scour has eroded the riverbed under and downstream of the structure, exposing the foundations completely. (Photo: Free State Department of Transport)

Figure 3-18: The bridge piers are not founded on piles or caissons and are resting only on small quantities of directly-compressed material. (Photo: Free State Department of Transport)

Figure 3-19: Bridge B5007, between Ladismith and Riversdale over the Touws River, in the Western Cape demonstrates the action of constriction on a large scale. Scour occurred under and immediately downstream of the bridge. Deposition of the sediment is evident further downstream where the river channel is more vegetated.

Figure 3-20: A local scour hole has developed at the closer pier in the soft riverbed rock at this bridge south of Aliwal North, Eastern Cape

Figure 3-21: Detail of the local scour hole at pier shown in Figure 3-20.

Figure 3-22: Local scour holes are not often visible as they may be under water or filled with sediment after floods. The local scour hole at a pier of this bridge near the Gariep Dam is clearly visible (bridge inset).

Figure 3-23: This bridge in the town of Heidelberg, Western Cape, failed as the foundations were undermined. The fact that piers on the *upstream* side failed suggests that local scour was responsible.

Figure 3-24: Local scour holes at the Touws River Bridge between Ladismith and Riversdale, Western Cape. Some differential movement between the piers and bridge deck has occurred (inset).

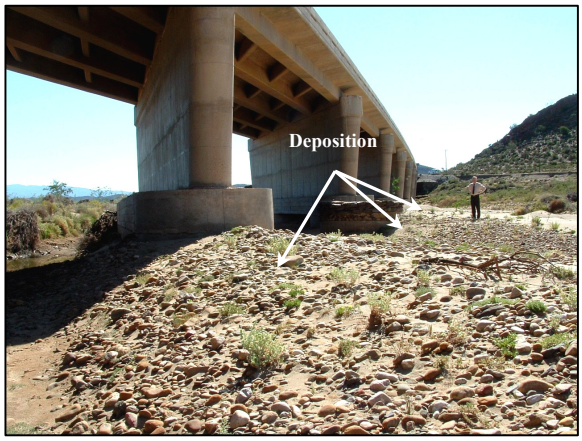

Figure 3-25: Deposition downstream of one of the bridge piers shown in Figure 3-24

Figure 3-26: Local scour downstream of the bridge abutment erodes the approach embankment behind the wing-wall of bridge B0896, Free State. (Photo: Free State Department of Transport)

Figure 3-27: Channelling of stormwater from the road or bridge surface into the river channel may aggravate the effects of local scour behind abutments shown in the previous figure, NB0960, Limpopo Province.

Figure 3-28: The river approaches the abutment rather than the opening of culvert NB241 in Limpopo Province.

Figure 3-29: The abutment has been undercut laterally by about 1.5m.

Figure 3-30: The above abutment and one bridge span failed as the abutment was undercut. (Photo: Free State Department of Transport)

Figure 3-31: Poor alignment of this bridge in Swellendam, Western Cape, has led to local scour upstream of the abutment.

Figure 3-32: The approach embankments of a bridge in Dainfern Golf Course, Gauteng, were washed away during 2000. (Photo: Arup, 2000)

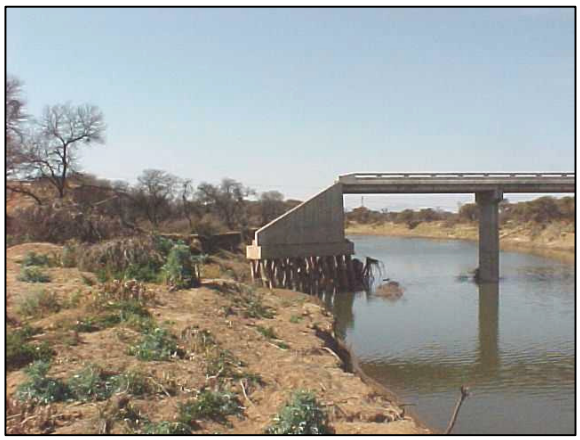

Figure 3-33: Outflanking of the bridge abutments and scour of the riverbed has exposed the piles anchoring the abutment at this bridge in Limpopo Province. (Photo: Leporogo Specialist Engineers)

Figure 3-34: Bend scour on this meander of the Gouritz River near Gouritsmond, Western Cape, is threatening the bridge abutment and approach fill on the far side.

Figure 3-35: Lateral erosion on the meander has shifted the natural river bank quite some distance beyond the bridge abutment. The bridge is in danger of being outflanked in future floods.

Figures 3-12 to 3-19 illustrate constriction scour. This form of scour is typically characterised by a lowered riverbed under the bridge and immediately downstream. In some cases, scour caused by constriction was evident for a significant distance downstream (Figure 3-14).

Constriction is also linked to outflanking and local scour. A very narrow opening will cause excessive afflux, overtopping and erosion of the approach fill. Water which exits a constriction at a high velocity may also cause significant local scour as backflow occurs at the downstream abutments (Figure 3-26).

Scour at man-made river constrictions has also aggravated sediment deposition further downstream during floods. The sediment load of a stream increases at the constricted section. Further downstream, the flow velocity decreases and sediment is deposited on agricultural land, in dams and on human settlements. This type of damage occurred in Laingsburg in 1981.

3.4.3 Local scour

The presence of flow obstructions such as piers causes turbulence and local scouring around foundation elements. Local scour was witnessed at 60% of the surveyed sites and was found to be the most prevalent form of scouring.

Local scour is not usually visible, particularly under flood conditions. Scour holes may be concealed by turbid water and vegetation which has grown in stagnant pools under bridges. As the field survey was undertaken during July, the east coast and interior of South Africa were experiencing a dry season. Evidence of local scouring was thus observed in several dry riverbeds and in shallow, clear water (Figures 3-21, 3-22 and 3-23).

Sedimentation of local scour holes takes place as the flow in a river wanes after a flood. Circular patterns in the sand around caissons at the N2 Bridge at Port Shepstone suggest that local scour holes had formed there and were subsequently filled in (Figure 3-8).

Local and constriction scour were found to occur simultaneously at 37% of sites. At the Touws River Bridge (Figure 3-19), typical patterns of local scour upstream (Figure 3-24) and downstream of the piers (Figure 3-25) were also seen.

Local scour on the downstream side of a bridge abutment takes place as backflow against the wingwall and approach fill occurs as illustrated in Figures 3-26 and 3-27. Scour on the upstream side of an abutment occurs when the oncoming flow is not aligned with the bridge opening. Good examples of this are shown in Figures 3-28, 3-29 and 3-31.

3.4.4 Outflanking

Outflanking of bridges and weirs was not the focus of this investigation but is linked to constriction scour as discussed in Section 3.4.2. Some examples of bridges which have been outflanked or may be outflanked in future are shown in Figures 3-32 to 3-35.

3.4.5 Predominant scouring mechanisms

The predominant mechanism of scour observed was local scour followed by constriction scour. The prevalence of each type of scour is summarised in Table 3-4. The table indicates the number of structures at which each scour type was evident, but does not provide any indication of the severity of the problem.

Table 3-4: Predominance of different types of scour at South African river bridges

Province	**Number of structures analysed**	**Type of scour**				
		General	Local	Constriction	Outflanking	Other / None
Eastern Cape	19	4	11	11	0	2
Free State	31	7	18	20	1	3
Gauteng	3	1	3	0	1	0
KwaZulu-Natal	31	5	17	11	0	13
Limpopo	19	4	11	5	8	4
Northern Cape	3	0	2	3	0	0
Western Cape	18	4	12	7	0	3
Total	105	21	63	46	10	23
Total %	**100**	**20**	**60**	**44**	**10**	**22**

3.4.6 Severity of different types of scour

In general the constriction scour observed was considered more severe than the local scour evident, presenting a greater threat to the structural integrity of the affected bridges. This assessment may, however, be invalidated when considering the major flood events which cause the catastrophic failure of large bridges. The depth of local scouring under these extreme conditions might be several orders of magnitude greater than that witnessed under low flow conditions during the dry season.

3.5 Financial costs of scour damage

3.5.1 Annual costs of scour damage

Calculations for the costs of scour damage are detailed in the Appendices. The estimates presented in Table 3-5 are intended to indicate the order of magnitude of the value of scour damage rather than to serve as reliable and accurate costs. The provinces are listed in descending order of the cost of scour damage in the region. As expected and indicated by historical records, the area of most concern is KwaZulu-Natal. The value of scour damage currently experienced in KwaZulu-Natal accounts for 42% of the total damage in South Africa.

Table 3-5: Estimates of the value of annual scour damage

Province	Total number of bridges	Total scour repair cost (R)	Annual scour repair cost (R)
KwaZulu-Natal	3 200	R46 200 000	R9 200 000
Western Cape	2 200	R20 100 000	R4 000 000
Eastern Cape	1 400	R16 600 000	R3 300 000
Free State	1 800	R8 000 000	R1 600 000
Limpopo Province	800	R6 900 000	R1 400 000
Mpumalanga	600*	R5 500 000	R1 100 000
North-West	650*	R3 400 000	R690 000
Northern Cape	500	R2 300 000	R460 000
Gauteng	680	R300 000	R67 000
Total		**R 109 000 000**	**R22 ,000 000**

* Number of bridges estimated

As the damage caused by major historical flood events is not contained in the figures presented above, the annual cost of R22 million can certainly be considered to be a conservative underestimate of the cost of scour damage. These figures furthermore reflect only the financial costs associated with repair of the affected structures. Quantification of the economic costs associated with failure of a vital transport link would further inflate the values.

3.5.2 Contribution of extreme historical floods to annual scour damage costs

The contribution of large-scale bridge failures during extreme flood events to the above scour costs needs to be quantified. The costs in Table 3-5 were extracted from BMSs which will not reflect costs associated with urgent repairs to vital routes necessitated by large floods as the BMSs are only updated every 5 years.

Comprehensive cost data for historical floods is not readily available. Table 3-6, however, gives an indication of the contribution which a large flood event such as the 1987 floods in Natal may make to the annual cost of scour damage in South Africa. Cost data was available for the four scour-damaged bridges listed in the table.

Table 3-6: Selected bridge repair costs for the 1987 floods in Natal

Bridge & River	Cost (Rm) 1987	Cost (Rm) 2004	Recurrence Interval*	Annual scour cost (Rm)
John Ross Tugela River	6.0	31.1	45	0.7
Scottburgh Mpambanyoni River	3.0	15.5	33	0.5
Josephines Bridge Mkomaas River	2.0	10.4	200	0.1
Batstones Drift Mzimkulu River	1.0	5.2	70	0.1

* Kovács (1988)

On the assumption that large flood events take place every few years somewhere in the country, it seems reasonable to add an average of, say, R5 million to the annual scour damage costs, increasing the total average annual scour damage costs to R25 to R30 million. The consequential damages, primarily as a result of traffic delays and the cost of re-routing traffic via alternative routes, may very well be higher than this. It should also be noted that the investigation only included those bridges administered by the provincial authorities. Inclusion of bridges administered by the National Road Agency and local authorities might greatly increase the figure.

3.6 Concluding remarks

The scour damage observed at most bridges investigated in the field study was not considered to be severe to the extent that the structural integrity of the bridges was under threat, although evidence of severe scouring during past floods was seen at a few sites. Scour damage does, however, constitute a sizeable proportion of the maintenance costs. For example, approximately 26% of bridges in the Eastern Cape currently require scour-related repair work accounting for approximately 17% of the total cost of bridge maintenance in the province. Scour damage to provincial road over river bridges in South Africa amounts to approximately R25-30 million per annum. About 42% of this cost is attributed to scour damage in KwaZulu-Natal. This estimate excludes damage to bridges maintained by local authorities and the economic costs associated with the disruption caused by the failure of major transport links.

Local and constriction scour are the two mechanisms occurring most frequently at bridge sites. Local scour was observed at 60% of the 105 bridges investigated and constriction scour at 44%. The severity of the constriction scour observed in the field study was generally greater than the local scour. It might thus be concluded that excessive constriction of the flow poses the greatest threat to South African river bridges. It must, however, be noted that local scour is hard to observe and occurs where the bridge is most vulnerable i.e. around the foundations. It is quite possible that it becomes the main mechanism of failure during periods of extreme floods. The combined effect of local and constriction scouring also requires attention as this combination was observed at 37% of the sites investigated.

Chapter 4
Numerical methods for the prediction of local scour

4.1 Introduction

In the past, hydraulics and sedimentation engineering problems were generally investigated with the aid of physical models. Physical models are often, however, expensive because they almost always require a lot of manpower and time to construct and test, whilst the results may be distorted by scale issues. Recently, however, the phenomenal increase in the power of the desk-top computer has made it increasingly attractive to use Computational Fluid Dynamics (CFD), either as a complement to physical modelling or as a replacement for it. CFD is the name given to the numerical modelling of fluid flow and related processes (Versteeg & Malalasekera, 1995; Olsen, 1999).

Over the last few years, many commercial and general-purpose CFD codes have been developed to solve a multitude of different engineering problems. There are, however, no simple design methodologies for the prediction of scour and deposition phenomena. Various approaches, using an assortment of CFD codes, have been used to model the scouring processes around engineering structures constructed in fluvial environments. Some examples are reported by Olsen & Melaaen (1993), Kogaki *et al.* (1997), Olsen & Kjellesvig (1998), Richardson & Panchang (1998), Biglari & Sturm (1998), Yen *et al.* (2001), Kothyari & Raju (2001), Ali & Karim (2002), Chen *et al.* (2002), Armitage & McGahey (2003), Chrisohoides *et al.* (2003), Armitage & McGahey (2004), Kimura *et al.* (2004), Salaheldin *et al.* (2004), Yanmaz (2004). Whilst there has been definite progress, gross simplifications are still required to overcome the huge computational demand required to analyse these sorts of problems.

This chapter summarises the mathematical principles behind CFD, reviews some of the approaches to modelling local scour adopted by various researchers over the past decade or so and then compares two codes in current use – one a well-known general code (FLUENT), and the other a commercial code developed specifically for the solution of open channel flow problems (TELEMAC), to show the limitations of both approaches.

4.2 Overview of the main numerical solution techiques

The four main numerical solution techniques used in CFD codes are (Versteeg & Malalasekera, 1995):

i) Finite Difference Method
ii) Finite Volume Method
iii) Finite Element Method
iv) Spectral Method

These will now be briefly described in turn.

4.2.1 Finite Difference methods

Finite Difference Methods make use of truncated Taylor series to approximate differential equations governing the fluid flow problem. The differential terms appearing in the governing equations are replaced by finite differences yielding algebraic equations for the unknown values of variables at each grid point in terms of the values at neighbouring grid points. More details can be found in John (1995).

4.2.2 Finite Volume methods

The Finite Volume Method was originally developed as a special Finite Difference Method. The governing equation of fluid flow is integrated over the finite control volumes of the computation domain. These integral equations are converted into a system of algebraic equations by substituting a variety of finite-difference-type approximations for the terms in the integral equations representing flow processes such as convection, diffusion and sources. Iterative methods are then used to solve the algebraic equations.

The Finite Volume Method for the solution of steady and unsteady flow problems can be formulated in various different ways according to the method used to generate algebraic equations from the integral equations in the process of discretisation. The Central Differencing Scheme based on truncated Taylor series is suitable for diffusive steady state problems. The Upwind Differencing Scheme, Hybrid Differencing Scheme, Power-law Scheme, and QUICK scheme are generally suitable for solution of problems of steady-state convection-diffusion. Various techniques such as SIMPLE, SIMPLER, SIMPLEC and PISO algorithms are used for pressure-velocity coupling. Further details may be found in Versteeg & Malalasekera (1995).

4.2.3 Finite Element methods

In Finite Element Methods, which are more complex than either Finite Difference or Finite Volume techniques, variations of the unknown flow variables are approximated by simple piecewise functions (e.g. linear or quadratic) valid on the boundaries of the elements. Ordinary or partial differential equations describe the domain geometry, physical properties of the fluid and boundary conditions. Since the assumed piecewise functions will not satisfy the governing equations precisely, there will be some errors in the solution. The integrated values of these errors or residuals are minimised after multiplication by suitable weighting functions. A system of algebraic equations for the coefficients in the assumed piecewise functions is derived from the integral equations. The system of algebraic equations is solved with the appropriate boundary conditions (Balden, 2003).

The Finite Element Method can be formulated in different ways according to the weighting functions used for minimising the residuals or errors in the solution. In the Galerkin formulation, the trial (piecewise) functions are used as weighting functions. This is a weak formulation as, during the formulation of the algebraic equations, there are no

restrictions other than the requirement that the derivative of the unknowns must exist at the boundary between the elements (unlike with the original differential equations). The main advantage of the weak formulation is that mass continuity need not to be satisfied automatically in the solution procedure (Olsen, 1999).

4.2.4 Spectral methods

The Spectral Method approximates the unknown fluid flow variables by means of truncated Fourier series or series of Chebyshev polynomials. This approximation is valid throughout the entire computational domain. The constraints that lead to the algebraic equations for the coefficients of the Fourier or Chebyshev series are provided by weighted residuals similar in concept to the techniques used in the Finite Element Method, or by making the approximate function coincide with the exact solution at a number of grid points (Versteeg & Malalasekera, 1995).

4.2.5 Discussion

Each method has its advantages and disadvantages (Versteeg & Malalasekera, 1995; Olsen, 1999; Balden, 2003), a discussion of which is beyond the scope of this study. In general, however, the Finite Difference and Finite Volume Methods (a modified form of Finite Difference) are widely used owing to their simplicity when compared to the others. In the Finite Volume Method there are clear relationships between the numerical algorithm and the underlying physical conservation principles, making this technique readily understandable and therefore attractive to the user. By contrast, the complex mathematics associated with Finite Element Methods may at times obscure the underlying physical processes involved. In order to solve the system of algebraic equations using Finite Elements, a large matrix needs to be inverted and thus often results in a slower rate of computation compared with Finite Volume Methods. Moreover, implicit solvers and high order upstream schemes are difficult to formulate with Finite Elements. Various techniques are employed in the Finite Element programs to overcome these problems with varying degrees of success. Debate continues as to which of the two main approaches is better, but it is telling that almost all commercial general-purpose three-dimensional CFD codes use the Finite Volume approach (Olsen, 1999). The Spectral Method is a special Finite Element method where the approximation of the unknowns is valid throughout the entire computational domain rather than over elements.

4.3 Fundamental equations used in CFD

All CFD codes are based on the principles of conservation of mass (continuity), momentum (Newton's second law) and energy (first law of thermodynamics). These principles are formulated into a set of governing equations containing the viscous stress components. In many three-dimensional fluid flows, the viscous stresses can be expressed

as functions of the local deformation rate, which is comprised of the linear deformation rate and the volumetric deformation rate. In the case of a Newtonian fluid, the viscous stresses may be replaced with rate of deformation using two proportionality constants; the (first) dynamic viscosity, μ, relating stresses to linear deformations, and the second viscosity, λ, relating stresses to the volumetric deformation. This yields the Navier-Stokes equations (Versteeg & Malalasekera, 1995). Many hydrodynamic and sediment transport CFD codes used to predict scour and deposition around engineering structures are based on the Navier-Stokes equations, which are solved together with the transport equations (convection-diffusion).

The equations describing the conservation of mass, momentum and energy, which are common to all CFD codes, are introduced in Sections 4.3.1, 4.3.2 and 4.3.3 respectively. The derivations are not presented but may be found in Patankar (1980), Versteeg & Malalasekera (1995) or White (1991). The equation governing transport of a general scalar quantity is then given in Section 4.3.4. Owing to its popularity as a simple sediment transport model, the Van Rijn (1987) sediment transport formula is presented in Section 4.3.5.

4.3.1 Mass conservation equation

The principle of conservation mass may be stated as, "*The rate of increase of mass in fluid element is equal to the net rate of flow of mass into the fluid element*". The unsteady three-dimensional mass conservation equation for a compressible fluid is (Versteeg & Malalasekera, 1995):

$$\frac{\partial \rho}{\partial t} + \frac{\partial (\rho u)}{\partial x} + \frac{\partial (\rho v)}{\partial y} + \frac{\partial (\rho w)}{\partial z} = 0 \tag{4.1}$$

where ρ is the density of the fluid and u, v and w are the velocity components in the x, y and z directions respectively. The above equation can be expressed in the more compact vector notation:

$$\frac{\partial \rho}{\partial t} + div(\rho \mathbf{u}) = 0 \tag{4.2}$$

where $\mathbf{u}$ is the velocity vector and $div\mathbf{u} = \frac{\partial u}{\partial x} + \frac{\partial v}{\partial y} + \frac{\partial w}{\partial z}$ in a Cartesian co-ordinate system.

For an incompressible fluid Equation 4.2 may be reduced to:

$$div\mathbf{u} = 0 \tag{4.3}$$

4.3.2 Momentum and Navier-Stokes equations

The momentum equation is based on Newton's second law and may be stated as, "*The rate of increase of momentum of fluid particle is equal to the sum of forces on fluid particle*". The components of the momentum equation in the three co-ordinate directions are (Versteeg & Malalasekera, 1995):

$$\text{x-component: } \rho\frac{Du}{Dt} = \frac{\partial(-p+\tau_{xx})}{\partial t} + \frac{\partial\tau_{yx}}{\partial y} + \frac{\partial\tau_{zx}}{\partial z} + S_{Mx}$$

$$\text{y-component: } \rho\frac{Dv}{Dt} = \frac{\partial\tau_{xy}}{\partial x} + \frac{\partial(-p+\tau_{yy})}{\partial y} + \frac{\partial\tau_{zy}}{\partial z} + S_{My}$$

$$\text{z-component: } \rho\frac{Dw}{Dt} = \frac{\partial\tau_{xz}}{\partial x} + \frac{\partial\tau_{yz}}{\partial y} + \frac{\partial(-p+\tau_{zz})}{\partial z} + S_{Mz} \tag{4.4}$$

where in the viscous stress τ_{ij}, the suffixes i and j indicates that the stress component acts in the j-direction on a surface normal to the i-direction. The sign associated with pressure p is opposite to that associated with the normal viscous stress because the usual sign convention takes a tensile stress to be the positive normal stress. S_{Mx}, S_{My} and S_{Mz} indicate body forces. If gravity is the only body force, S_{Mx}, = 0, $S_{My} = \rho\mathbf{g}$ and $S_{Mz} = 0$ where $\mathbf{g}$ is the gravity vector.

As previously discussed, the viscous stresses are proportional to the rates of deformation in a Newtonian fluid. If the fluid is also incompressible, these stresses are:

$$\tau_{xx} = 2\mu\frac{\partial u}{\partial x} \qquad \tau_{yy} = 2\mu\frac{\partial v}{\partial y} \qquad \tau_{zz} = 2\mu\frac{\partial w}{\partial z}$$

$$\tau_{xy} = \tau_{yx} = \mu\left(\frac{\partial u}{\partial y} + \frac{\partial v}{\partial x}\right) \qquad \tau_{xz} = \tau_{zx} = \mu\left(\frac{\partial u}{\partial z} + \frac{\partial w}{\partial x}\right) \qquad \tau_{yz} = \tau_{zy} = \mu\left(\frac{\partial v}{\partial z} + \frac{\partial w}{\partial y}\right) \tag{4.5}$$

Substituting for the body force and the viscous stresses, all momentum equations shown above can be re written in indicial notation as (Versteeg & Malalasekera, 1995):

$$\rho \frac{D\mathbf{u}}{Dt} = \rho \mathbf{g} - \nabla p + \frac{\partial}{\partial x_j}\left[\mu\left(\frac{\partial u_i}{\partial x_j} + \frac{\partial u_j}{\partial x_i}\right)\right] \tag{4.6}$$

This is the Navier-Stokes equation for an incompressible Newtonian fluid. It must be noted that in general the viscosity, μ, varies with temperature, pressure and position.

4.3.3 Energy equation

The energy equation is derived from the first law of thermodynamics and may be stated as, "*The rate of change of energy of a fluid particle is equal to the rate of heat transfer to the fluid particle plus the rate of work done on the particle*". The rate of change of specific energy of a fluid particle per unit volume is expressed by the following:

$$\rho \frac{DE}{Dt} = -divp\mathbf{u} + \frac{\partial(u\tau_{xx})}{\partial x} + \frac{\partial(u\tau_{yx})}{\partial y} + \frac{\partial(u\tau_{zx})}{\partial z} + \frac{\partial(v\tau_{xy})}{\partial x} + \frac{\partial(v\tau_{yy})}{\partial y} + \frac{\partial(v\tau_{zy})}{\partial z} + \frac{\partial(w\tau_{xz})}{\partial x} + \frac{\partial(w\tau_{yz})}{\partial y} + \frac{\partial(w\tau_{zz})}{\partial z} + div(k_T gradT) + S_E \tag{4.7}$$

where the specific energy E is sum of internal energy i and kinetic energy $(u^2 + v^2 + w^2)/2$ such that $E = i + (u^2 + v^2 + w^2)/2$; k_T is the coefficient of thermal conductivity; T is temperature and S_E is a source of energy per unit volume per unit time due to the body force.

The equation for the rate of change of kinetic energy of a fluid particle is:

$$\rho \frac{D\left[\frac{1}{2}\left(u^2 + v^2 + w^2\right)\right]}{Dt} = -\mathbf{u} \bullet grad\, p + u\left(\frac{\partial \tau_{xx}}{\partial x} + \frac{\partial \tau_{yx}}{\partial y} + \frac{\partial \tau_{zx}}{\partial z}\right) + v\left(\frac{\partial \tau_{xy}}{\partial x} + \frac{\partial \tau_{yy}}{\partial y} + \frac{\partial \tau_{zy}}{\partial z}\right) + w\left(\frac{\partial \tau_{xz}}{\partial x} + \frac{\partial \tau_{yz}}{\partial y} + \frac{\partial \tau_{zz}}{\partial z}\right) + \mathbf{u} \bullet S_M \tag{4.8}$$

The rate of change of internal energy of a fluid particle is:

$$\rho\frac{Di}{Dt}=\tau_{xx}\frac{\partial u}{\partial x}+\tau_{yx}\frac{\partial u}{\partial y}+\tau_{zx}\frac{\partial u}{\partial z}+\tau_{xy}\frac{\partial v}{\partial x}+\tau_{yy}\frac{\partial v}{\partial y}+\tau_{zy}\frac{\partial v}{\partial z}$$
$$+\tau_{xz}\frac{\partial w}{\partial x}+\tau_{yz}\frac{\partial w}{\partial y}+\tau_{zz}\frac{\partial w}{\partial z}+div(k_T gradT) \tag{4.9}$$

where $i=cT$ for an incompressible fluid, with c as the specific heat of the fluid.

The equation of the rate of change of internal energy of a fluid element can be rewritten in terms of the dissipation function, Φ (Yang & Song, 1979; Armitage & McGahey, 2003):

$$\rho\frac{\partial i}{\partial t}=\Phi+div(k_T gradT)-\rho(\mathbf{u}\bullet gradcT) \tag{4.10}$$

where Φ can be expanded as follows:

$$\Phi=\mu\left[2\left(\left(\frac{du}{dx}\right)^2+\left(\frac{dv}{dy}\right)^2+\left(\frac{dw}{dz}\right)^2\right)+\left(\frac{du}{dy}+\frac{dv}{dx}\right)^2+\left(\frac{du}{dz}+\frac{dw}{dx}\right)^2+\left(\frac{dv}{dz}+\frac{dw}{dy}\right)^2\right] \tag{4.11}$$

If the fluid can be regarded as isothermal, then the applied unit steam power can be written as (Armitage & McGahey, 2003):

$$P_t=\Phi=\tau_{ji}\frac{\partial u_i}{\partial x_j}=\rho\frac{Di}{Dt}=\rho\frac{\partial i}{\partial t} \tag{4.12}$$

The letter P is used as a reminder that the above is a power term, whilst the subscript t indicates that the power is used to overcome shear stresses.

4.3.4 Transport of a scalar quantity

The general transport equation for a general scalar quantity, ϕ, according to the Finite Volume formulation is (Versteeg & Malalasekera, 1995):

$$\frac{\partial(\rho\phi)}{\partial t} + div(\rho\phi\mathbf{u}) = div(\Gamma grad\phi) + S_\phi \tag{4.13}$$

This equation accounts for the various transport processes involved in fluid flow: the ***rate of change*** term and the ***convective*** term on the left hand side and the ***diffusive*** term and the ***source*** term respectively on the right hand side. Γ is the diffusion coefficient.

4.3.5 Van Rijn sediment transport equations

Scour modelling requires that additional equations be added that describe the conditions under which sediment will be entrained or deposited by the flow. There are a number of different approaches to sediment transport modelling of a scour bed:

- Defining the incipient condition at which point the particles are only just stable (Chien & Wan, 1999; Armitage & McGahey, 2003).
- Adding a source term to estimate the sediment pick-up rate at the bed cells.
- Specifying an equilibrium sediment concentration close to the bed.

The third approach is currently the most popular in commercial CFD codes (e.g. TELEMAC). The Van Rijn (1987) presents a commonly used formula for the calculation of the equilibrium sediment concentration, c_{bed}, at each of the bed cells, which can in turn be used in the solution of the convection-diffusion equations (transport equation) of sediment transport.

$$c_{bed} = 0.015\frac{d^{0.3}}{a}\frac{\left[\frac{\tau_0 - \tau_c}{\tau_c}\right]^{1.5}}{\left[\frac{\rho_s - \rho_w}{\rho_w \nu^2}\right]^{0.1}} \tag{4.14}$$

Here d is the sediment particle diameter, a is a reference level set equal to the roughness height, τ_0 is the bed shear stress, τ_c is the critical bed shear stress for movement sediment particles, ρ_w and ρ_s are the respective densities of water and sediment and ν is the kinematic viscosity of water.

The suspended and bed load components of sediment transport are often treated separately. The Van Rijn (1987) formula to calculate the bed load q_b of uniform sediment (median diameter d_{50}) in the absence of suspension is:

$$\frac{q_b}{d_{50}^{1.5}\sqrt{\frac{(\rho_s-\rho_w)g}{\rho_w}}} = 0.053\frac{\left[\frac{\tau-\tau_c}{\tau_c}\right]^{1.5}}{d_{50}^{0.3}\left[\frac{(\rho_s-\rho_w)g}{\rho_w\nu^2}\right]^{0.1}} \tag{4.15}$$

So-called "bed forms" are commonly found in alluvial channels. Bed forms are relief features such as dunes or ripples which change the effective roughness of the bed thereby affecting the sediment transport process. Van Rijn (1987) suggests the following formula for the bed form height Δ for uniform sediment:

$$\frac{\Delta}{y} = 0.11\left(\frac{d_{50}}{y}\right)^{0.3}\left(1-e^{-\left[\frac{\tau-\tau_c}{2\tau_c}\right]}\right)\left(25-\left[\frac{\tau_0-\tau_c}{\tau_c}\right]\right) \tag{4.16}$$

where y is the water depth. The effective roughness $k_{s+\Delta}$ is then calculated using the following relationship:

$$k_{s+\Delta} = 3d_{90} + 1.1\Delta\left(1-e^{-\frac{25\Delta}{L}}\right) \tag{4.17}$$

where L is the bed form length which is typically equal to $7.3y$ and d_{90} is the sieve size passed by 90% of the sediment by mass. For uniform sediments, d_{90} is approximately the same as d_{50}.

4.4 Domain description and boundary conditions

The definition and description of a suitable flow domain is the first step in numerical analysis. Suitable boundary conditions must be imposed to replicate the conditions found in reality.

4.4.1 Domain description

Normally a two-phase domain containing the flow of water in a channel with a region of air above is considered. Many current commercial CFD codes can solve multi-phase fluid flow. The depth of the air portion should be large enough to avoid any effects from the boundary conditions at the top of the domain. Salaheldin *et al.* (2004) found that if the

ratio between the initial depths of the air and the water is one-third or larger, the uppermost boundary has not affect on the water flow. To be conservative, they used a ratio 0.5 or more for their numerical analysis.

A finer mesh is required near solid boundaries, such as a channel wall or pier, in order to resolve the flow and scour details near these. A finer mesh is also required at the air-water interface. Unfortunately, although the finer mesh ensures better computational accuracy, it also increases the computational time. Salaheldin *et al.* (2004) suggested that the size of the cells should satisfy the limits of walls distance $11.225 < y^+ < 30$. The lower value of y^+ was chosen to avoid calculation in the laminar sub-layer whilst the upper value was to ensure the law of wall for velocity was applicable. The wall unit distance y^+ is defined as:

$$y^+ = \frac{u_* y}{\nu} \tag{4.18}$$

where y is the vertical distance from the node or centre of the wall-adjacent cell to the boundary and ν is the kinematic fluid viscosity. The shear velocity u_* is given by:

$$u_* = \sqrt{\frac{\tau_0}{\rho}} \tag{4.19}$$

4.4.2 Boundary conditions

The flow properties at the inflow boundary must be selected to represent fully-developed turbulent open channel flow to enable the shortening of the entrance length and thereby reduce computational time. Care should be taken to ensure that the integrated flow over the input face equals the total flow that will be modelled (Armitage & McGahey, 2003). Salaheldin *et al.* (2004) specified two separate inlets for air and water that were a sufficient distance from the pier to ensure fully-developed flow. They also specified two separate outflows for air and water at the downstream end. An overall mass balance correction and zero diffusion flux for all flow variables were defined at the downstream boundary. The water level at the outlet was not defined and was allowed to change in response to the changes in hydrodynamic pressure calculated at all boundaries inside the domain. Ali & Karim (2002) placed the inflow and outflow faces $3.0R$ and $6.0R$ from centre of the pier respectively, where R was the radius of pier.

In the case of two-dimensional flow and with flow around symmetrical structures such circular piers, symmetry can be employed to reduce computational cells and hence computational costs. Of course this concept could not be applied if accurate simulation of the Von Kármán vortex street and its effects on scouring were of interest. It is normal

practice to impose a no-slip boundary condition, setting the velocity to zero at the solid boundaries such as the channel bed, channel walls and pier.

4.5 Turbulence and free surface modelling

Turbulent flow around engineering structures is both complex in nature and highly variable. It is characterised by high frequency velocity and pressure fluctuations over a wide range of length and time scales. Modelling of such flow details is one of the most complex aspects of CFD modelling and contributes substantially to computational expense. The free surface profile is also not physically horizontal as gradually or rapidly varied flow always occurs in the vicinity of structures. In recent years, commercial CFD codes have incorporated models for simulating turbulent flow, as well as calculating the free surface profile. These two aspects (turbulence and free surface) are interactive (Sarkar & Rhodes, 1999). The turbulence model, influential in developing the internal flow structure of a fluid phase, affects the development of free surface profile through, *inter alia*, the resistance and energy losses that it predicts. The free surface profile in effect defines the flow geometry of the water phase and thus the solution domain within which the turbulence model is applied.

4.5.1 Turbulence modelling

There is a direct correspondence between accuracy and computational cost. The most accurate turbulence models attempt Direct Numerical Simulation (DNS) of the unsteady Navier-Stokes equations (Section 4.3.2) using Finite Difference techniques, Finite-Element Methods and so on at a scale that is capable of resolving the smallest meaningful turbulent eddies without requiring additional closure equations. A high Reynolds number turbulent flow domain might contain eddies (bursts) as small as 10 to 100 μm. This implies that up to 10^{15} eddies could be observed in a 1m x 1m x 1m flow domain requiring a similar number of cells and the associated very fine time step (Versteeg & Malalasekera, 1995). Consequently, although the DNS solution is the most accurate of all, it is computationally the most expensive. This approach is thus presently limited to application to simple problems and flows with small Reynolds numbers (*Re*). By way of illustration, Speziale (1991) stated that DNS of a turbulent pipe flow at a Reynolds number of 5×10^5 would have required a computer which was 10 million times faster than the CRAY supercomputer that was then available. Hoffman & Johnson (2003) noted that to accurately resolve a turbulent flow at $Re = 10^6$ using DNS would require in the order $Re^3 = 10^{18}$ mesh points in space-time, and thus would be impossible on any presently foreseeable computer. On the other hand, DNS at $Re = 10^2$ on a personal computer and at $Re = 10^3$ on a supercomputer is possible.

In order to reduce the unacceptably high computational loads of DNS, commercial CFD codes approximate turbulent processes in various different ways. One approach is to model the turbulent eddies as individual units, inferring the small-scale

turbulent process from behaviour of the large scale eddies. These types of models are called Large Eddy Simulation (LES) or Very Large-Scale Eddy Simulation (VLES) models. The larger is the size of the eddy, the greater is the degree of approximation.

As LES and VLES are still computationally intensive, the most common computational methods generally approximate the Navier-Stokes equations with the so-called Reynolds-Averaged Navier-Stokes equations (RANS). These express the various fluid parameters such as velocity and pressure as the sum of mean and fluctuating components (Armitage & McGahey, 2003). The revised governing equations can be solved through the estimation of the turbulent or eddy viscosity.

There are various methods for estimating the eddy viscosity. Some of more common methods are the following:

i) The **Reynolds Stress Model (RSM)**, also known as the second-order or second-moment closure model. This model introduces exact Reynolds stress transport equations to account for the directional effects of the Reynolds stress field. The six equations for Reynolds stress transport are solved along with a model equation for the scalar dissipation rate ε.

ii) The **Algebraic Stress Model (ASM)** is also a six-equation model. This model is an economical way of accounting for the anisotropy of Reynolds stresses without going to the full length of solving the Reynolds stress transport equations by neglecting the convection and diffusion terms altogether.

iii) **Two-equation Models**. These models, of which the k-ε model is one, introduce equations for the transport of kinetic energy and the rate of viscous dissipation, which are used to approximate the velocity and length scales, which in turn are used to calculate eddy viscosity. The transport equations contain a number of empirically derived constants that are applicable to certain situations. There are different types of k-ε models are available in the various CFD codes such as the standard k-ε model, the RNG (re-normalised group) k-ε model and the realizable k-ε model.

iv) The **One-equation Prandtl Eddy Model**. This model relates the eddy viscosity to a length scale.

v) The **Zero-equation Model** which assumes a constant eddy viscosity

There is a wide range of turbulence models available in commercial CFD codes and the choice of model is dependant on the particular application. Much research is currently underway to find the most simple but effective turbulence model (Park & Sung, 1997; Perot & Moin, 1996). The k-ε model (Launder & Spalding, 1972) is probably the most widely used owing to its simplicity and effectiveness considering computation time. The transport equations for turbulent kinetic energy, k, and dissipation rate, ε, are (Versteeg & Malalasekera, 1995):

$$\frac{\partial}{\partial t}(\rho k)+\frac{\partial}{\partial x_i}(\rho k u_i)=\frac{\partial}{\partial x_j}\left[\left(\mu_l+\frac{\mu_t}{\sigma_k}\right)\frac{\partial k}{\partial x_j}\right]+G_k+G_b-\rho\varepsilon-Y_M+S_k \tag{4.20}$$

$$\frac{\partial}{\partial t}(\rho \varepsilon)+\frac{\partial}{\partial x_i}(\rho \varepsilon u_i)=\frac{\partial}{\partial x_j}\left[\left(\mu_l+\frac{\mu_t}{\sigma_\varepsilon}\right)\frac{\partial \varepsilon}{\partial x_j}\right]+C_{1\varepsilon}\frac{\varepsilon}{k}(G_k+C_{3\varepsilon}G_b)-C_{2\varepsilon}\rho\frac{\varepsilon^2}{k}+S_\varepsilon \tag{4.21}$$

where t is time, ρ is the fluid density, u_i is the velocity in the x_i direction, μ_l and μ_t are the respective dynamic molecular and turbulent viscosities and σ_k and σ_ε are the turbulent Prandtl numbers for k and ε. G_k and G_b represent the generation of turbulent kinetic energy due to mean velocity gradients and buoyancy respectively and S_k and S_ε are source terms. The turbulent viscosity is computed by combining k and ε as follows:

$$\mu_t=\rho C_\mu\frac{k^2}{\varepsilon} \tag{4.22}$$

The constant terms in Equations 4.20-22 have the following typical default values (Rodi, 1984; FLUENT, 2003):

$$C_{1\varepsilon}=1.44,\ C_{2\varepsilon}=1.92,\ C_\mu=0.09,\ \sigma_k=1.0,\ \sigma_\varepsilon=1.3$$

Biglari & Sturm (1998), Richardson & Panchang (1998), Ali & Karim (2002), Chen *et al.* (2002), Armitage & McGahey (2004) and Salaheldin *et al.* (2004), all used various types of k-ε turbulence models to predict flow and scour pattern around engineering structures and verified their results with experimental and field data. They all found reasonable agreement between the experiment and numerical results.

Salaheldin *et al.* (2004) examined the performance of several turbulence models in simulating a three-dimensional separated complex flow field around circular piers. The computation was performed using several variants (Standard, RNG and Realizable) of the k-ε Model and the Reynolds stress model (RSM) for turbulence closure. The computation results were compared to reliable experimental data. The results showed that all the k-ε Models overestimated the velocity field near the bed. The overestimations produced by the Standard and the RNG k-ε Models were however only slight. The Realizable k-ε Model, on the other hand, overestimated considerably. It was also found that the k-ε

models overestimated the area of scour initiation. Again, the Realizable k-ε Model gave the poorest results. The RSM performed satisfactorily for estimation of the velocity field, bottom shear stress distribution and water level variation around the pier for the initial condition as well as for equilibrium scour.

Figure 4-1 illustrates the relationship between cost and accuracy of the most commonly used turbulence models.

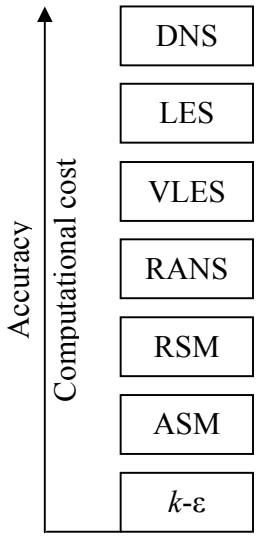

Figure 4-1: Relationship between computational cost and accuracy of turbulence models

(The figure does not reflect the actual accuracy or computational cost)

4.5.2 Free surface models

In recent years a number of commercial CFD packages have incorporated routines for calculating the free surface profile in open channels whilst simultaneously solving the internal flow structure of the water phase. Some of more common methods are:

i) 1D backwater computation: This method is based on friction loss computed by Manning's formula. The water surface is then calculated using energy balance between surface points.

ii) 2D depth-averaged approach: This method assumes a hydrostatic pressure distribution with water depth.

iii) 3D pressure field: This method calculates the pressure at water surface by linear extrapolation from the surface cells. This method is only suitable for small water surface slopes.

iv) Lagrangian grid methods: A Lagrangian grid is embedded in and moves with free surface. Many Finite Element codes use this approach because if grid and fluid move together, the grid automatically tracks free surface. This method cannot track surfaces that break apart or intersect.

v) Marker-and-Cell (MAC) method: This method is based on a fixed Eulerian grid of control volumes. The location of fluid within the grid is determined by a set of marker particles that move with the fluid and indicate the free surface. This method has been used primarily for two-dimensional simulations because it requires considerable memory and CPU time to accommodate the necessary number of marker particles. Typically, an average of about 16 markers in each grid cell is needed to ensure an accurate tracking of surfaces undergoing large deformations.

vi) Volume-of-Fluid (VOF) method. The VOF method is based on multiphase flow theory. Water and air phases share the same velocity and pressure fields and therefore the same set of equations describes the flow field of the air-water two-phase flow as the single-phase flows. The VOF method has proven to be a good method for tracking the free surface based on a time-dependent simulation. The gas/liquid fraction is usually set at 1:2 (Salaheldin *et al.*, 2004).

4.6 Previous work in the modelling of local scour

The rapid improvement of computational power has made the numerical modelling of scour increasingly attractive. Owing to the great complexities arising from the three-dimensional nature of local scour, most development work has focused on two simple situations: circular piers and rectangular plate abutments.

4.6.1 Computational modelling of local scour around a pier

Olsen & Melaaen (1993) attempted to compute the geometrical shape of a scour hole around a circular pier with the aid of a Finite Volume numerical model. The bed deformation was carried out in stages based on the assumption that the flow at each stage was steady. The bed shear stresses computed at each stage was used to compute the bed changes. The computations were carried out for 10 stages, giving a scour hole shape very similar to what was obtained in a physical model study. The steady Navier-Stokes equations for the three-dimensional flow field on a general non-orthogonal grid were solved at each stage. The k-ε turbulence model was used to solve for the Reynolds stresses. There was no mention of the approach used to model the free surface. The flow field gave the shear stress on the boundaries, which in turn was used to estimate the sediment concentration for the bed elements. The diffusion-convection equation for the sediment concentration was then solved, and changes in the bed elevation were calculated

from sediment continuity. A new flow field was then determined using the modified bed topology, and the above sequence repeated until the depth of the calculated scour hole was identical to that measured in a separate physical model study. Once the scour depth was correct, the shape of the computed scour hole compared quite well with that measured in the physical model. However, neither the CFD nor the physical model tests were run to equilibrium scour conditions.

Olsen & Kjellesvig (1998) predicted the water flow using the Reynolds-averaged transient Navier-Stokes equations together with the k-ε turbulence model. The location of the water surface was calculated by extrapolating the pressure from the inner cells. The pressures in the surface cells were then compared to a fixed reference pressure located on the downstream boundary. If there were any discrepancies between the two values, the water surface was adjusted accordingly. The sediment transport was calculated using the convection-diffusion equation for sediment concentration except for the cells closest to the bed. In these cells, the bed concentration, c_{bed} was calculated using a formula presented by Van Rijn (see Section 4.3.5) with the reference level, a, set to 5% of the water depth. The critical bed shear stress, τ_c, was adjusted for sloping beds using a formula presented by Brooks (1963). The level of the bed was then adjusted for the next time step (100 seconds). The heights of the cells were continuously adjusted in proportion to the height difference between the bed and the water surface. The flow field for a steady solution with a horizontal non-moving bed and water surface appeared to give realistic velocity vector and bed shear stress fields. The same problem was then run with the sediment concentration calculation procedure adjusting the location of the bed and the water surface after each time step. The scour hole and bar developed much as expected although it took an IBM-370 workstation nine weeks to simulate 208 hours of scour hole development. The maximum scour depth was obtained after about 104 hours. It was concluded that the maximum scour depth corresponded well with those predicted by four different empirical equations presented by Chitale (1962), Shen et al. (1969), Jain (1981) and Garde et al. (1993). The model predicted a maximum scour depth of 1.5m whereas the empirical equations gave 2.2m, 1.9m, 2.2m and 1.4m respectively. A relatively coarse grid was used in the model. As a consequence, the model did not simulate the wake vortices. An even coarser grid gave a significantly smaller scour hole indicating that the solution was grid-dependent. The shape of the scour hole was also very sensitive to the angle of repose. Another problem was that the rate of scour development was dependent on the empirical parameters in the Van Rijn equation. It was thus impossible to tell how well the numerical model predicted the development of scour hole without resort to confirmation from some sort of physical modelling.

Encouraged by the work of Olsen & Melaaen (1993), Richardson & Panchang (1998) used FLOW-3D to model the flow field past a circular pier for which physical model results were available. Three steady-state flow conditions were modelled; with the initial flat bed, the intermediate scour hole, and the equilibrium scour hole. The model of Richardson & Panchang (1998) was based on the transient three-dimensional Navier-Stokes equations. The computations were performed using two different turbulent closure

schemes: Prandtl's mixing length theory and the RNG k-ε model. A qualitatively more realistic velocity vector field appeared downstream of the pier using the RNG k-ε model, but in general the results of both schemes were largely similar. All of the boundaries were rigid, i.e. no free surface or scour routines were employed. The shape of the scour hole was approximated by the frustum of a cone. The computed flow velocities were broadly in agreement with the laboratory observations. Particle tracking showed that sediment movement through the scour holes was also much as expected. Each simulation required approximately 168 hours of CPU time on a desktop SUN workstation.

Yen *et al.* (2001) developed a morphological model consisting of a three-dimensional flow field model and a scour model to simulate the bed evolution around a circular pier and compared the simulated results with experimental results. They incorporated the large eddy simulation (LES) with Smagorinsky's subgrid-scale (SGS) turbulence model to simulate the flow and bed shear field. The bed shear stress was calculated using following equation:

$$\tau_{ij} = \mu\left(\frac{\partial \overline{u}_i}{\partial x_j} + \frac{\partial \overline{u}_j}{\partial x_i}\right) \tag{4.23}$$

where μ and $\overline{u}$ are the dynamic fluid viscosity and time-averaged velocity respectively. The computation of the bed shear was carried out with the aid of a Taylor series approximation of the velocity profile. The flow field was not recomputed as the bed deformed. Instead, the bed shear stress field computed for the flat bed was modified progressively as the bed deformed. This was done to save computational time. It was assumed that the velocity profile near the pier was logarithmic and the Taylor series expansion was applied to the profile to obtain a relationship between the shear and mean velocities before deformation and the shear and mean velocities after deformation. This allowed a relationship to be developed relating the bed shear stresses before deformation and to those after deformation. The sediment continuity equation with sediment transport relation was solved imposing open and solid boundary conditions to simulate the evolution of the scour hole. The effect of the local bed slope of the scour hole on the direction of sediment particle motion was incorporated into the model as part of the effective shear stress. The bed-load sediment transport for course bed materials was calculated using the Van Rijn (1987) formula as follows:

$$q_s = 0.053\sqrt{(S_s - 1)g}\,d^{1.5}\,\frac{T_*^{2.1}}{D_*^{0.3}}$$

$$\text{where} \quad T_* = \frac{\tau_0 - \tau_c}{\tau_c}, \quad D_* = d\left(\frac{\rho^2 S_s' g}{\mu^2}\right)^{1/3}, \quad S_s' = S_s - 1 \tag{4.24}$$

where T_* and D_* are the characteristic parameters for excess bed shear stress and particle diameter respectively, q_s is the sediment volume transport rate per unit width, S_s is specific gravity of the sediment, g is the gravitational acceleration, d is the sediment particle diameter, τ_0 is the bed shear stress, τ_c is the critical shear stress and μ is the dynamic viscosity. The scouring effect of the downflow in front of the pier was simulated using the following relation:

$$\frac{d_j}{b} = \alpha \cdot \left(\frac{w_m}{u_o}\right)^{0.48} \cdot \left(\frac{t \cdot u_o}{b}\right)^{\gamma} \tag{4.25}$$

where d_j is the downflow scour depth, b is the pier diameter, w_m is the maximum downflow velocity, u_o is the mean velocity of the approaching flow, t is the time, γ is an exponent depending on w_m and α is a coefficient that is calibrated in the model. Equation 4.25 was adopted from the submerged vertical jet flow scour relations proposed by Clarke (1962). Experimental data of the scour depth evolution at the pier nose and the scour depth contours around the pier were compared to the numerical results and good agreement was obtained.

Ali & Karim (2002) used FLUENT V4.3 to predict the three-dimensional flow field around a circular cylinder and compared the numerical results to an experimental model. Solutions were obtained for rigid beds and for scour holes of different sizes for different time durations. The numerical results were used to predict the variation of bed shear stress around the cylinder using two different turbulence models – the Standard *k-ε* and RNG *k-ε*. The calculated bed shear stresses were then used in the sediment continuity equation to obtain an expression for the variation of scour depth with time. As FLUENT V4.3 could not simulate a free surface, the water surface was modelled by means of a 'rigid-lid' boundary. The maximum scour depth was found to depend on three dimensionless numbers: the pile Reynolds number which accounts for the effect of the pile diameter, the dimensionless particle diameter which accounts for the effect of sediment size and the duration number which accounts for temporal effects. The flow field predicted by FLUENT V4.3 compared favourably with limited available experimental results. The results obtained using the RNG *k-ε* model were virtually identical to those produced by the Standard *k-ε*. FLUENT V4.3 was not capable of modelling the 'turbulent bursts' that are widely observed in the physical phenomena, and are capable of enlarging the scour hole through the removal of sediment from the bed.

Armitage & McGahey (2003) developed Unit Stream Power and Movability Number models for the prediction of local scour in rivers. In their study, CFX V4.3 was used to predict the scour potential upstream of a vertical weir, at an abutment and two piers. The results were then compared to the observed equilibrium scour patterns measured in small-scale laboratory models. The simulations were carried out using

relatively coarse meshes to reduce both the CPU time and the size of the data files that were manipulated in the post-processor. CFX-V4.3 did not contain a free surface modelling routine. Three alternatives were therefore considered for the modelling of the free surface; a symmetry or slip (no shear) boundary, a rigid-lid incorporating an air interface and a moving wall. The moving wall was chosen as it most accurately predicted the turbulent viscosity distribution with depth. Of the available turbulence models in CFX-V4.3, the Standard k-ε and the Low Reynolds Number k-ε models were found to provide the best predictions of the turbulent shear stresses for the two- and three-dimensional flow-fields respectively. Additional FORTRAN subroutines were written to determine the Movability Numbers and the Unit Stream Power values. A Unit Stream Power or Movability Number higher or lower than the critical value indicated potential for scour or deposition respectively. The scour potential, Ω, was defined as the difference between Movability Number, Mn (Liu, 1957), calculated by the program, and the critical Movability Number $Mn_{c(\beta,\gamma)}$ (adjusted to account for bed-slope where relevant):

$$\Omega = Mn - Mn_{c(\beta,\gamma),}$$

$$\text{where} \quad Mn = \frac{u_*}{v_{ss}} = f(Re_*)$$

$$\text{and} \quad Mn_{c(\beta,\gamma)} = \psi Mn_c \tag{4.25}$$

The subscripts (β,γ) and (0) indicate a sloped bed and a horizontal bed respectively. u_*, v_{ss}, Re_* and ψ are the shear velocity, particle settling velocity, particle Reynolds number and correction factor for bed slope respectively. The scour potential is a measure of the amount of deformation the channel bed will undergo before an equilibrium scour hole is established. Determination of this equilibrium position could theoretically be computed iteratively with the scour potentials being recalculated after each boundary adjustment. The final solution would be obtained once all scour potentials were close to zero. In CFX-V4.3, however, this could not be automated. Instead of generating new geometries manually for each iteration, Armitage & McGahey (2003) chose simply to compute the scour potential for the initial and final scoured states and compared these with the physical model. Despite the limitations of CFX-V4.3, the agreement between numerical and physical results was sufficiently encouraging to suggest that there is potential for the use of their method for scour prediction.

Salaheldin *et al.* (2004) used FLUENT V5.0 to model the separated turbulent flow around vertical circular piers in clear water and compared the results with several sets of physical data. The three-dimensional Reynolds-Averaged Navier-Stokes equations were solved using the Finite Volume technique. The two-phase domain (water in the channel with a region of air on the top) was represented using the Volume of Fluid (VOF) method coupled with a multiphase formulation solver in order to resolve the variation of the water surface around the pier. The ratio between the initial depths of air to the initial

depth of water was set equal to 0.5 or larger to avoid any effect from the boundary condition at the top of the domain on the water flow. Two continuity equations were solved to account for each phase although the momentum and general transport equations were shared by both phases. The size of the cells adjacent to solid boundaries was chosen to satisfy the limits of the wall unit distance $11.225<y^{+}<30$. The law-of-the-wall for the mean velocity, modified for roughness, was utilized to calculate the bottom shear stress. Three variants of the *k-ε* Model were used in the study; Standard, Renormalization Group (RNG) and the Realizable *k-ε* model. Despite the high computational effort and time required, the Reynolds Stress Model (RSM) was also used in their study. The RSM was found to give satisfactory estimates for the flow velocity field, shear stress distribution, and water level variation around the pier in the case of flat bottom, and for estimating the velocity field and water level variation in the case of equilibrium scour. The vertical distributions of the streamwise velocity, *u*, obtained using the standard *k-ε,* RNG *k-ε* and the RSM models were also close to the experimental data. The vertical velocities, *v*, however deviated significantly from the experimental data near the bed and near the water surface because of the no-slip boundary condition. It was noticeable that the three *k-ε* Models, (Standard, RNG and Realizable) overestimated the area in which the computed bed shear stress exceeded the critical bed shear stress compared to that suggested by the physical data. This overestimation of bottom shear stress may have resulted from the overestimation of the streamwise velocity near the bottom by these turbulence models. The pressure coefficient, C_p, was used as a surrogate for the water level variation at the pier. C_p is related to the static pressure as follows:

$$C_p = \frac{p_x - p_0}{0.5\rho U^2} \tag{4.26}$$

where p_x is the local static pressure at position x in the flow direction, p_0 is the upstream undisturbed static pressure, U is the upstream approach velocity and ρ is water density. With the exception of the RSM, the computed pressure coefficients deviated substantially from the physical data. Salaheldin *et al.* (2004) concluded that the RSM available in FLUENT-V5.0 is an effective tool for predicting the complex flow around bridge piers.

4.6.2 Computational modelling of local scour around an abutment

There have been many attempts to construct a numerical model for the flow around abutments.

Tingsanchali & Maheswaran (1990) modelled the flow around a groyne using the program TEACH developed by Gosman & Pun (1973) and later modified by Rodi *et al.* (1981). The 2D depth averaged steady Navier-Stokes equations were solved utilising a hybrid Finite Difference scheme and an iterative method. The *k-ε* model was used for turbulence closure. A correction factor was applied to the dissipation term $C_{2\varepsilon}\rho(\varepsilon^2/k)$ in

the ε transport equation (Equation 4.21) to improve the agreement between the computed and experimental data of the velocities and streamline pattern in the vicinity of the groyne tip. A further 3D correction factor helped to improve the prediction of bottom shear stresses. Molls & Chaudhry (1995), using another code that also utilised the 2D depth-averaged equations, obtained similar results for the same problem.

Ouillon & Dartus (1997) appear to have been the first to publish work on the 3D modelling of the flow around a groyne. They solved the RANS equations using a hybrid Finite Volume scheme based on the SIMPLE algorithm and a k-ε turbulence model. The porosity method was used to track the free surface. They did not attempt to model scour hole development. Instead, by comparing the computed bed shear stress with the critical bed shear stress for a particular problem that had been previously been the subject of a physical model investigation, they were able to identify potential scour and deposition zones with reasonable accuracy.

Biglari & Sturm (1998) also used a 2D, depth-averaged, k-ε model – this time for the prediction of the flow around bridge abutments situated in compound channels. Clear-water equilibrium maximum scour depths near the upstream corner of the abutment face were then estimated using an empirically determined relationship between the dimensionless scour depth and the excess velocity ratio. Although this method satisfactorily explained the general relationship between measured values of equilibrium scour depth and the different abutment lengths and discharges tested, there were shortcomings. Biglari & Sturm concluded that more work was needed to identify the influence of additional local hydraulic variables that could only be predicted accurately by 3D numerical turbulence models. Additional criticisms are that the method only predicts the maximum equilibrium scour depth, and it is likely that the empirical relationship between the dimensionless scour depth and the excess velocity ratio will change for different abutment arrangements and flow conditions.

Kothyari & Raju (2001) developed a model to predict scour around spur dikes and bridge abutments using the concept of an analogous pier. This concept is based on the premise that an abutment or spur dike may be represented by a circular pier with an equivalent diameter such that the pier will produce the same equilibrium scour depth as the abutment or the spur dike under similar hydraulic conditions. Laboratory data from several clear-water and live-bed scour experiments were analysed and used to develop a relationship for determining the diameter of the analogous pier. The temporal variation of scour depth and the equilibrium scour depth at the spur dike and the abutment were then computed using a pier scour model with the size of the analogous pier being taken as the pier diameter. The pier scour model used was developed by Kothyari *et al.* (1992) and is an algorithm based on analytical and semi-empirical relationships which relate particle movement to time. Satisfactory agreements were observed between model and laboratory results of equilibrium scour depth and temporal variation of scour depth for both clear-water and live-bed scour conditions.

Kimura *et al.* (2004) investigated the flows around submerged skewed spur dikes using a three-dimensional numerical model. Their model could reproduce the three-dimensional flow patterns including the water exchange between the spur dykes zone and the mainstream affected by the inclination angle. However, the flow near the bed with upstream inclined spur dikes was not captured well. Kimura *et al.* (2004) therefore developed the numerical model further and used it to compute the three-dimensional turbulent flow structures around submerged spur dikes under various hydraulic conditions. The governing differential equations (composed of continuity, momentum and k-ε equations) were solved with a Finite Volume Method on a full-staggered grid system. A total of 15 computational cases were performed under different hydraulic conditions, of which 7 cases coincided with available laboratory tests. Special attention was given to the three hydraulic parameters; the inclination angle, the ratio of the length interval between two spur dikes to the length of each spur dike and the ratio of the height of the spur dikes to the depth of flow. The numerical results showed that the flow near the bed, which is particularly important for sediment transport, was affected by both inclination angle and the ratio of height of spur dikes to flow depth. The results showed that unsteady vortex shedding in downstream inclined spur dikes were generated from the first spur dike and the period was determined by the feedback effect of impinging shear layer.

Chrisohoides *et al.* (2003) developed a CFD model for solving the unsteady three-dimensional Reynolds-Averaged Navier-Stokes (URANS) equations closed with the k-ω turbulence model (Wilcox, 1988) and used it to describe the flow field around flat-bed abutments. The URANS equations were formulated in Cartesian coordinates and then transformed to generalised, non-orthogonal curvilinear coordinates to facilitate the numerical treatment of the body-fitted, curvilinear grids used to discretise the computational domain using Finite Volume methods. The main objective of their investigation was to clarify the qualitative general three-dimensional flow field around the abutment rather than to obtain a quantitative description. Their simulations showed the existence of a recirculating eddy in the junction region between the abutment and sidewall on the upstream side as investigated by Melville (1997). Their simulation further revealed that the mean flow in that region was highly three dimensional and unsteady. The surface flow consists of several counter-rotating eddies rather than single recirculating eddy. New eddies were generated continuously due to the complex interaction between existing eddies and the surrounding walls. These merged to form large new eddies, which in turn broke up into smaller eddies which initiated new cycles. It was noted that the spatial extent of this recirculating flow region was not fixed in time but showed large-scale unsteady fluctuations. These temporal fluctuations affect the scouring process as they change the dynamics of the flow in the vicinity of scour hole. The model results also revealed a massively separated wake consisting of large-scale eddies extending up to five to six abutment lengths downstream of the abutment.

It is no surprise that work on the development of a numerical model for the computation of local scour around abutments has lagged behind that for piers. The

additional plane of symmetry through the centreline of a circular pier simplifies the problem by permitting only half of the domain to be modelled. This greatly reduces computational expenses.

4.7 A comparison of CFD codes in current use

Many commercial codes are currently available for prediction of local scour in rivers. They fall into two main categories: general codes that have numerous user selected options that are designed to solve a wide range of fluid flow problems, and codes that are developed specifically for the solution of river problems. Some well-known examples are listed below. Some basic details on these programs, as published by the agents in September 2004, are to be found in Appendix B (General Codes) and Appendix C (Specialised River Codes). The codes presented are:

i) General Codes – FLUENT (B.1), CFX (B.2), Flo++ (B.3), STAR-CD (B.4), FIDAP (B.5), FLOW-3D (B.6), PHONICS (B.7).

ii) Specialized River Codes – Delft3D (C.1), MIKE 3 (C.2), TELEMAC (C.3), TABS (C.4), SMS (C.5), SSIIM (C.6), CCHE3D (C.7).

iii) Some common issues arising with available commercial CFD codes are the following:

- They tend to be difficult to use. This is inevitable given the complexity of the problems they are used to solve, but it does mean that operators have to go on fairly intensive training courses to become proficient in use of the programs.
- The source code is usually obscured for copyright purposes, making it difficult for the operator to determine what routines the code uses to solve each modelling problem.
- Many of the codes do not allow significant modeller input, making them unsuitable for development work.
- The licences are often extremely expensive although many offer substantial reductions for use in teaching and research.
- The software requires fast machines with large amounts of memory – the faster and larger the better. No machine is big enough to accurately solve every problem – nor is this likely to change in the foreseeable future.

Two codes, one a general code (FLUENT), and the other a specialized code for use in river modelling (TELEMAC), chosen on the basis of cost and flexibility, were tested to determine their potential capability for use in the solution of local scour problems and to illustrate typical problems.

4.7.1 Numerical modelling of local scour using FLUENT Version 6.2

Three-dimensional steady-state free surface flow around two circular piers and a rectangular abutment was modelled using FLUENT Version 6.2 with the incipient motion criteria at the channel bed defined by three different measures – the Movability Number (Liu, 1957), Shields Stress (Shields, 1936) and Applied Unit Stream Power (Yang, 1972). The Standard k-ε Model was employed for turbulent closure and the free surface was computed by the Volume of Fluid method. A user-defined function (UDF) was used to simulate scour hole evolution. It was assumed that bed deformation occurred in stages and flow conditions at each stage were steady. The URANS equations were solved iteratively at each stage until equilibrium conditions were attained (i.e. flow conditions were constant). Once equilibrium was attained, scour potentials at the bed were computed and the bed was deformed accordingly. The process was repeated until an equilibrium scour hole developed (i.e. the scour potential at each point on the bed was less than or equal to zero for successive stages). Numerical model solutions were compared to reliable experimental data generated in the civil engineering laboratory at UCT.

Transverse depth point profiles of the velocity, water volume fractions, k and ε were specified at both the upstream and downstream boundaries of the domain. The obstacles, top of the domain and channel bed were specified as no-slip walls. For each pier simulation, a symmetry plane was defined along the channel centreline and only half of the domain was modelled. The grids used consisted of approximately 175,000 and 220,000 quadrilateral elements respectively. In each case, the grid was generated to be roughly aligned with the flow expected near the pier to reduce numerical diffusion. The grid was unstructured in plan (x-z plane) but structured in the vertical (y) direction. A structured hexahedral grid of approximately 830,000 cells was used for the abutment. The rectangular geometry of the domain and obstacle in this case allowed the structured mesh to be easily generated.

The need to model air as well as water increases the computational demand. The VOF method in FLUENT requires that air is specified as the primary phase and it was found necessary to allow air to occupy at least three-quarters of the domain volume to prevent mixing of the phases. In addition, the air flow is more turbulent than the water flow so that a reasonably fine mesh must be generated in the air volume even though details of the air flow are not of interest for local scour prediction. The VOF method also requires use of reasonably low under-relaxation factors during the solution process for numerical stability. This slows convergence and increases computational cost. The variation of the free surface elevation around the pier and abutment modelled appear realistic (Figure 4-2) suggesting that the pressure variations around these obstacles can be reproduced by the numerical model. A very distinct interface between the two fluids is obtained provided the mesh is sufficiently fine near the free surface.

FLUENT facilitates easy input of user-defined functions allowing the model to be customised for a particular application. Sediment transport functions such as the Unit Stream Power were thus defined and used to produce output such as shown in Figure 4-3.

Good agreement between the numerical and experimental models was generally obtained. Care had to be taken to select the appropriate grid sizing near the channel bed to avoid unrealistic distortion of the computed flow velocity distribution as this is used as input into the incipient motion criteria for sediment in the numerical model.

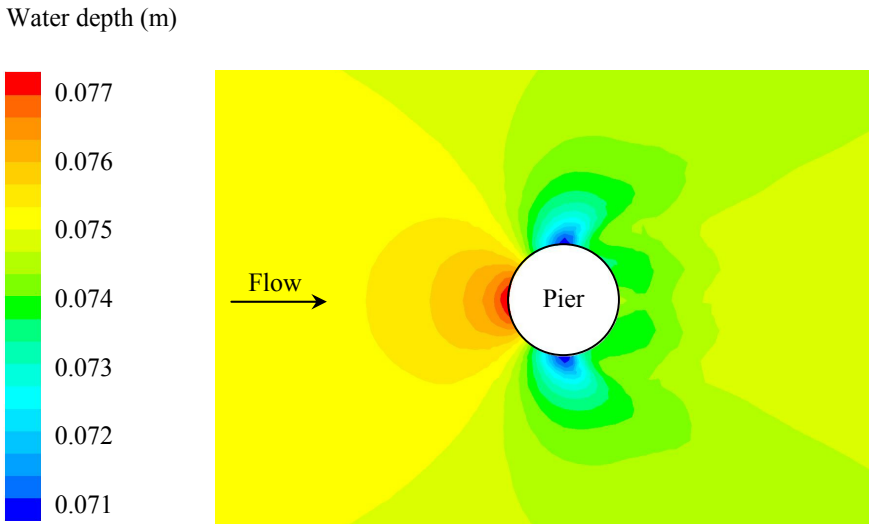

Figure 4-2: Plan view of the variation of the free surface around a circular pier (FLUENT)

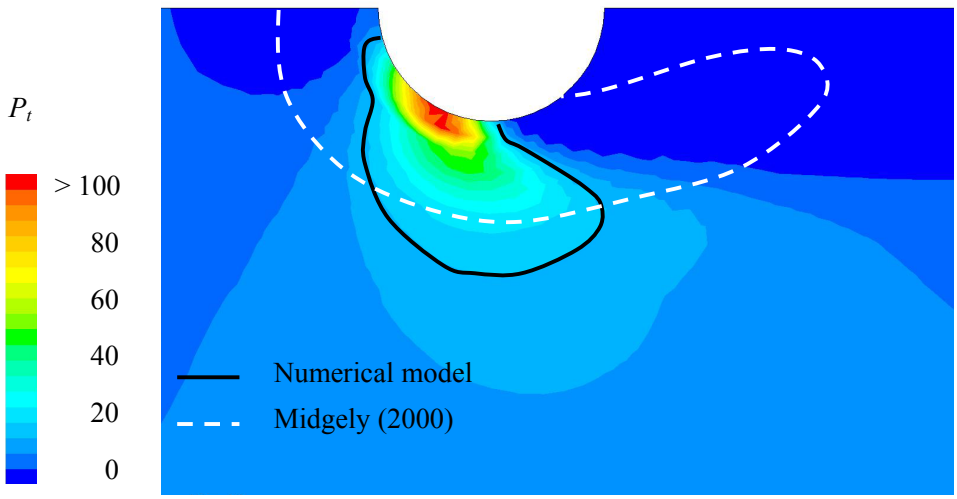

Figure 4-3: Plan view of the contours of applied unit stream power indicating the region affected by local scouring at a circular pier (FLUENT)

To obtain the water depths observed in the physical model studies, it was found necessary to fix the flow velocity distributions at both the upstream and downstream ends of the domain in addition to values of the turbulent kinetic energy k and dissipation rate ε. If only the upstream conditions were specified, the water depth was in some instances computed to be only half the physically measured value. Forcing the velocity distributions at both the upstream and downstream boundaries may, however, limit the formation of wake and recirculation zones downstream of the obstacles. Unfortunately, lists of point velocities, k and ε had to be provided to the program at the upstream boundary by the user as text documents which required tedious preparation.

Correct representation of flow velocity gradients near the channel bed, within the turbulent boundary layer, is essential for accurate scour prediction as many sediment transport parameters such as the bed shear stress, Movability Number, Shields stress and Unit Stream Power are functions of these velocity gradients. It was found that the values were very sensitive to the wall model and the associated choice of vertical cell size at the channel bed. The vertical height of the bed-adjacent cell is quantified using the wall unit y^+ such that

$$y^+ = \frac{u_* y}{\nu} \tag{4.27}$$

where u_* is the shear velocity, y is the distance from the bed to the wall-adjacent cell node and ν is the kinematic fluid viscosity. The following options were investigated; a coarse mesh enclosing the inner region of the boundary layer with $y^+ = 31$, an intermediate mesh using a cell size corresponding to $y^+ = 9.8$ and very fine mesh resolving the linear layer with $y^+ = 0.9$. Both the "standard" and "enhanced" wall treatment in the k-ε turbulence model offered by FLUENT V6.2 were explored. In standard wall treatment, the influence of the wall on the near-wall solution variables is accounted for using semi-empirical formulae referred to as wall functions. The formulae used are dependent on the value of y^+ e.g. a logarithmic law is used for the mean velocity if $y^+ > 11.225$ and a laminar stress-strain relationship is used when $y^+ < 11.225$. For enhanced wall treatment, resolution of the viscosity-affected inner region via a mesh is enabled by modifying the turbulence model. When the near-bed mesh is fine enough to be able to resolve the laminar sub-layer, a two layer approach is used. In the two layer model, the domain is subdivided into a viscosity-affected region and a fully-turbulent region. The equations for k, ε and μ_t remain the same for the turbulent region. The values of ε and μ_t within the viscosity-affected region, on the other hand, are estimated using a different approach. k is still determined using the transport equation but ε is determined from an algebraic equation and not a transport equation. In addition, the relationship used to determine μ_t is different. Also with the enhanced wall treatment, when the near-bed mesh is relatively coarse, "enhanced" wall functions are applied. Enhanced wall functions are functions used to represent the entire wall region (laminar, transitional and turbulent)

based on a "single wall law". FLUENT achieves this single wall law formulation by blending linear (laminar) and logarithmic (turbulent) laws-of-the-wall. Figure 4-4 shows the variation of shear stress with depth for different wall models for the case of uniform flow in an infinitely wide channel. The distribution is theoretically linear.

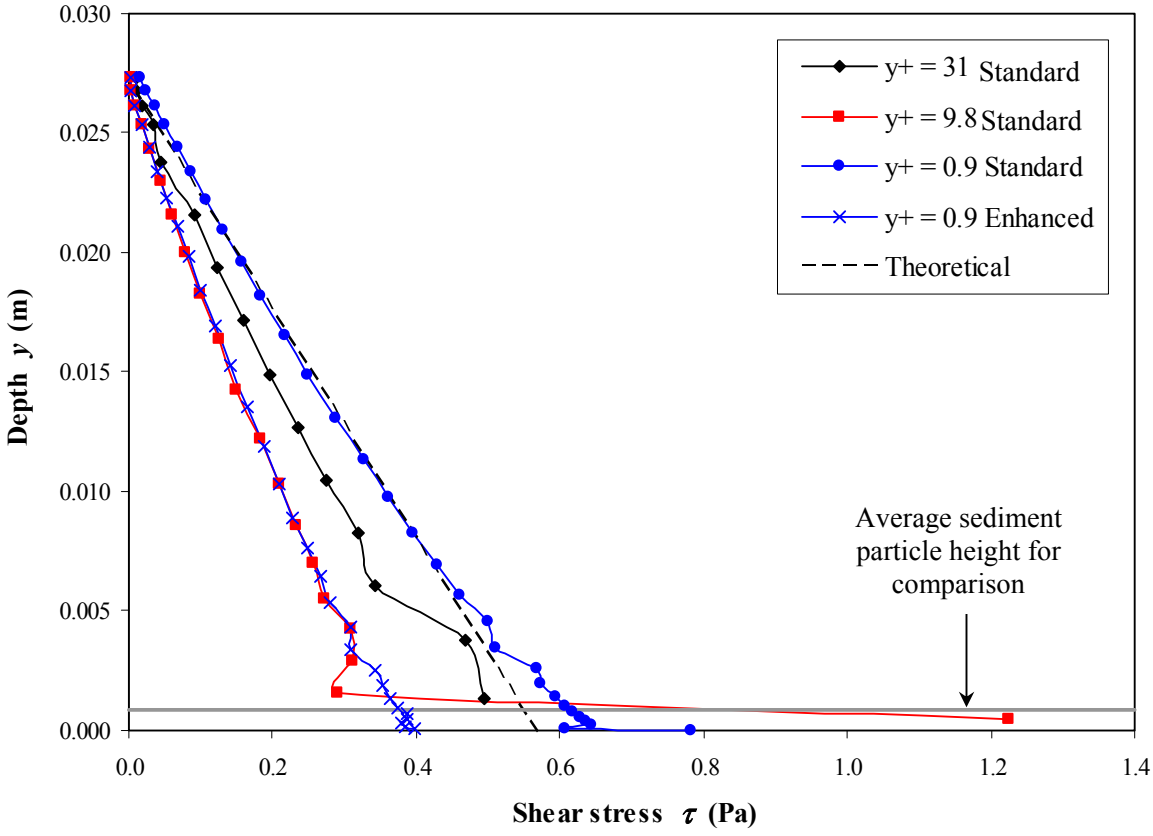

Figure 4-4: Distribution of shear stress with depth for different wall models

It is evident from Figure 4-4 that the choice of wall model has a significant impact on scour prediction. Even though the general approach for turbulent flows is to select a y^+ value between 30 and 300 for standard wall functions, it appears that a fine mesh with $y^+ = 0.9$ and standard wall treatment is the best option as it gives a shear stress profile closest to the theoretical distribution. The mesh with $y^+ = 0.9$ is, however, very difficult to implement in practice. If the mesh is refined to give very small cells in the vertical direction of the order 10^{-4} to 10^{-5} m as is typically required, refinement of a similar magnitude is necessary in the horizontal plane to prevent excessive skewness / very high aspect ratios in the bed-adjacent cells. This is impractical as the mesh then almost inevitably consists of many millions of cells. Difficulty has been encountered when attempting to simulate flow through a domain containing more than one million cells using an Intel P4 chip with a clock speed of 2.8 GHz and with 2 GB RAM. The time taken to simulate steady flow and incipient sediment motion at a cylindrical pier on a flat

bed with a symmetry plane on the channel centreline was typically 5 hours with 220 000 cells, whilst simulation of flow around a rectangular abutment was typically 22 hours with 830 000 cells.

As previously mentioned, bed deformation was modelled in stages. An automated procedure for modelling bed deformation not only requires that the face mesh representing the bed be deformed at the end of every stage but also the domain mesh be modified to ensure that the solution at the next stage is accurate. FLUENT has dynamic mesh capabilities which can be used to control mesh behaviour during simulations. The dynamic mesh capabilities can however only be used in conjunction with the URANS equations. Transient simulations are therefore inevitable when simulating steady-state flows. For steady flows, the flow conditions are monitored until equilibrium is attained. Once equilibrium is attained a steady solution is deemed to have been obtained. Two user defined functions were created; one for bed mesh modification and the other for domain mesh adaptation. Both functions were called when a solution for a particular stage was obtained, the bed mesh modification UDF first followed by the domain mesh adaptation UDF. In the bed mesh routine, movability numbers for the bed nodes are computed using variables from the bed adjacent cells and the scour potential at each node is determined using Equation 4.25. Those bed nodes with scour potentials greater than zero were displaced in the vertical direction to reflect scouring. A linear relationship was assumed between node displacement and scour potential. The node displacements were determined according to the following equation:

$$\Delta y = C\Omega \tag{4.28}$$

Where Δy is the node displacement, C is a deformation constant and Ω is the scour potential. The nodes were displaced proportionally with the maximum displacement being limited to 3 mm. The constant in Equation 4.28 is determined at each stage using the maximum scour potential and the maximum allowed displacement. The value of C is determined in a manner such that the maximum node displacement approaches 0 as the scour potential values reduce to very small values. After the bed nodes have been displaced, a smoothing algorithm is employed to ensure that the maximum angle each bed mesh face makes with the horizontal is less than the sediment angle of repose.

After the bed mesh has been modified to reflect scour, the domain mesh adaptation UDF is called. This UDF ensures that cell heights are appropriate for the next stage. Nodes below half the mean flow depth with the same horizontal coordinates are determined and their positions are set according to the following relationship:

$$R = e^{\frac{L}{n-1}(x-0.5)} \tag{4.29}$$

where R is the ratio between two successive node intervals, L is the distance from the bed to half the mean flow depth, n is the number of nodes and x is a user-specified constant. Half the mean flow depth was chosen as a reference level as it is expected that flow at this point is least affected by the bed and free surface and the mesh is generally coarsest in this region. The choice of an appropriate value of x ensures that the cells closest to the bed are least affected by the bed deformation. The value of x selected needs to be less than 0.5 to ensure that cell sizes progressively increase from the bed towards the mean flow depth. The smaller the value of x, the smaller the size of the cells close to the bed and the smaller the effect of bed deformation on bed adjacent cells. The value of x should be such that bed adjacent cell heights are consistent with the wall treatment approach being used.

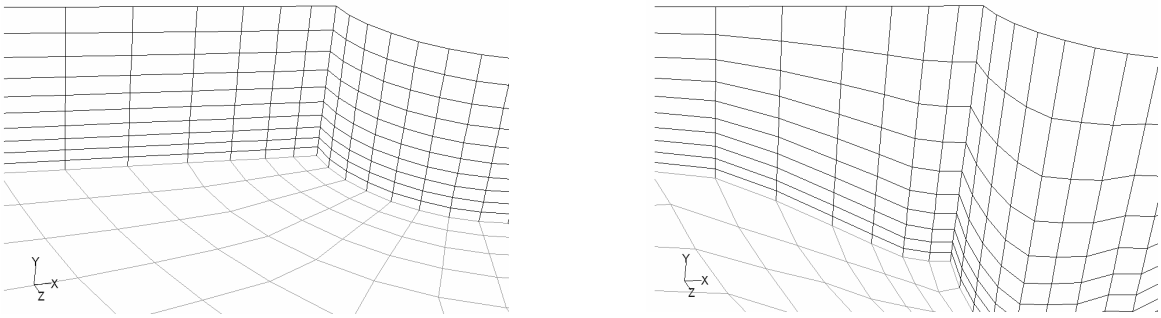

Figure 4-5: Illustration of mesh adaptation (FLUENT)

The automated procedure was used to simulate scour hole evolution around a circular pier. This simulation was based on a scour experiment carried out at the Civil Engineering Hydraulics laboratory of the University of Cape Town. The flow had a mean velocity An Intel P4 chip with a clock speed of 2.8 GHz and with 2 GB RAM was employed and the domain consisted of approximately 170,000 cells. The standard k-ε model was employed using standard wall treatment. It took approximately 118 hours for an equilibrium scour hole to develop. Figure 4-6 illustrates the different stages in scour hole development that were predicted by the numerical model. The maximum scour depth, $d_{s,}$ at each stage is indicated at the top of the plot. The different colours represent different bed elevations with deep blue corresponding to the lowest elevation at each stage and red corresponding to the highest elevation. As can be seen, the scour hole starts from the sides of the pier and migrates to the front where it continues to grow deeper. This pattern is in accordance with what was observed in the laboratory.

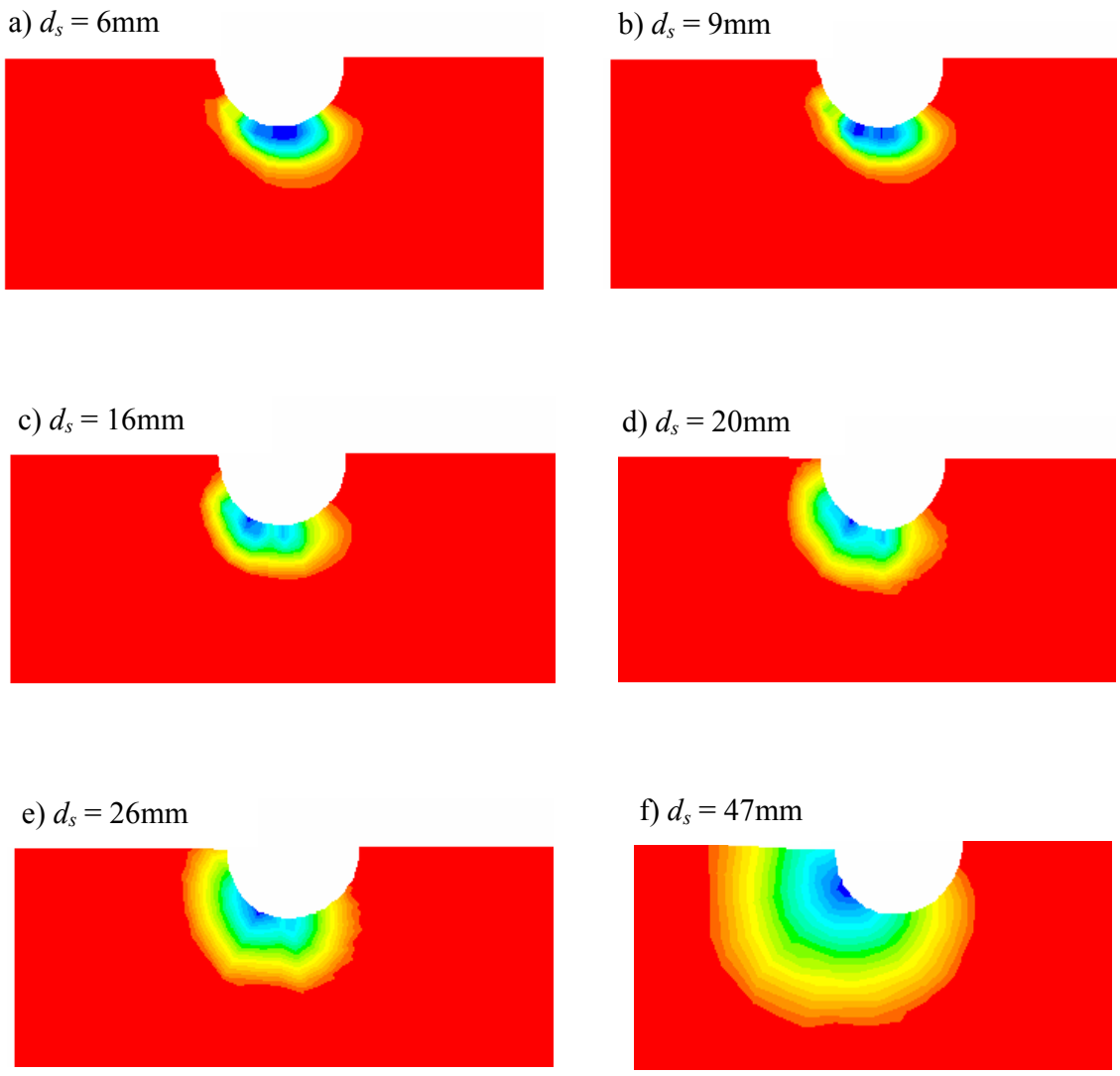

Figure 4-6: Stages in scour hole development (FLUENT)

It can be seen from Figure 4-7, which shows the variation of maximum scour depth with stage, that the maximum clear-water scour depth profile predicted by the model is similar to the theoretical profile (Figure 2-1). One difference, however, is that the profile predicted by the model rises to a definite maximum scour depth whereas the theoretical profile approaches the maximum scour depth asymptotically. Figure 4-8 indicates the movability numbers in the equilibrium scour hole. The critical movability number for sediment transport on a flat bed for a turbulent boundary is 0.17. A slope correction factor is applied to this figure for sloping beds. As expected, the movability numbers in front of the pier are close to zero indicating that the computed scour potentials

were approximately equal to or less than zero. The movability numbers along the side of the pier are quite high. The maximum value is about 0.16. The critical movability number in this region will however be greater than 0.17 since the bed slopes upwards in the direction of flow. The scour potential values computed in this region will therefore be less than zero.

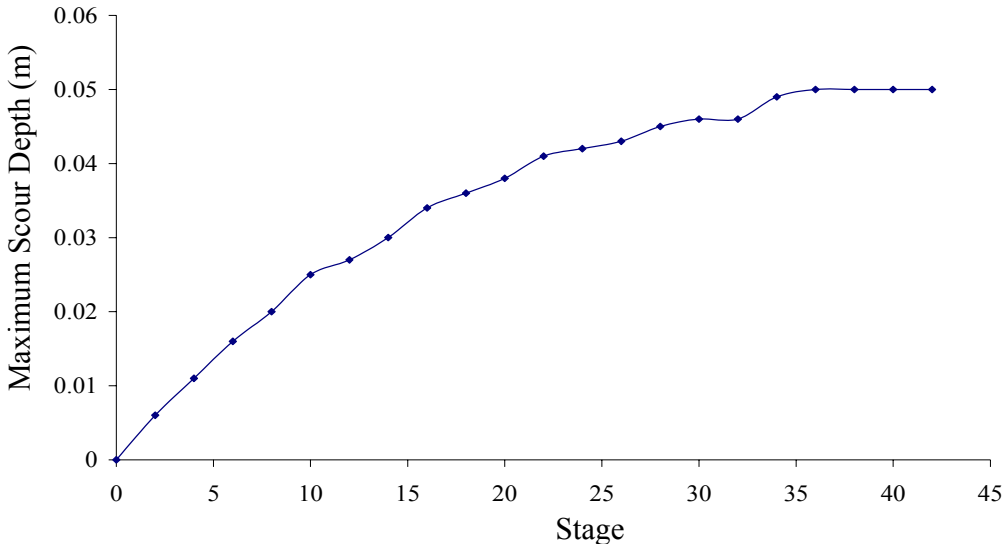

Figure 4-7: Variation of maximum scour depth with stage (FLUENT)

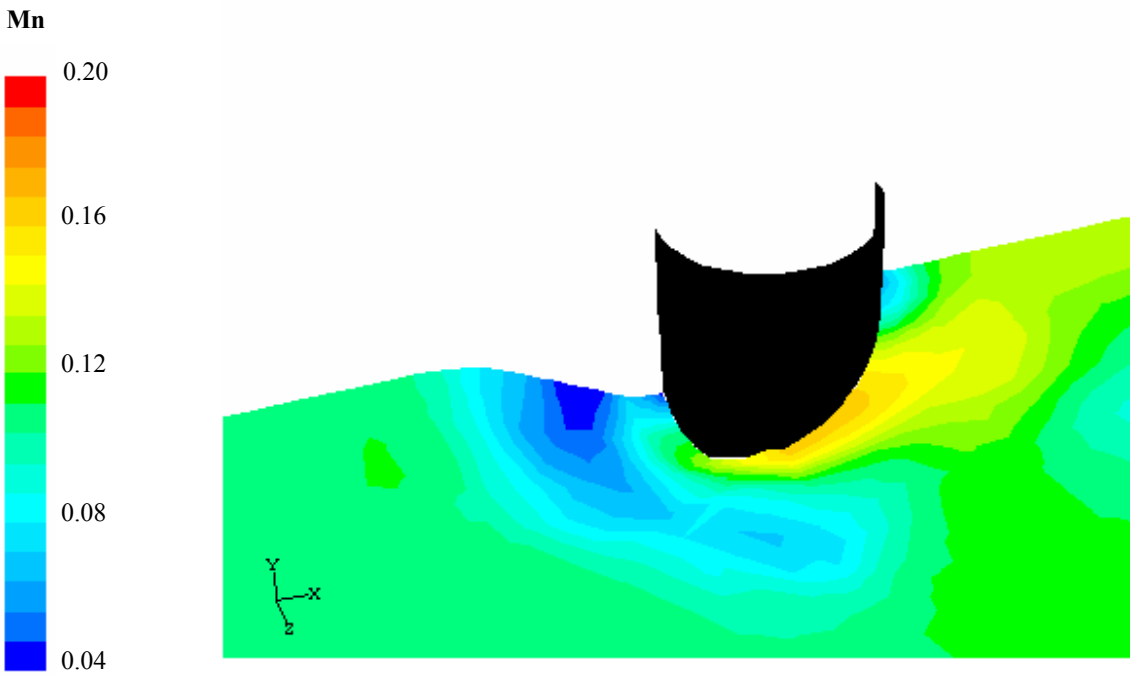

Figure 4-8: Movability numbers at equilibrium scour hole (Mn_{c0} = 0.17) (FLUENT)

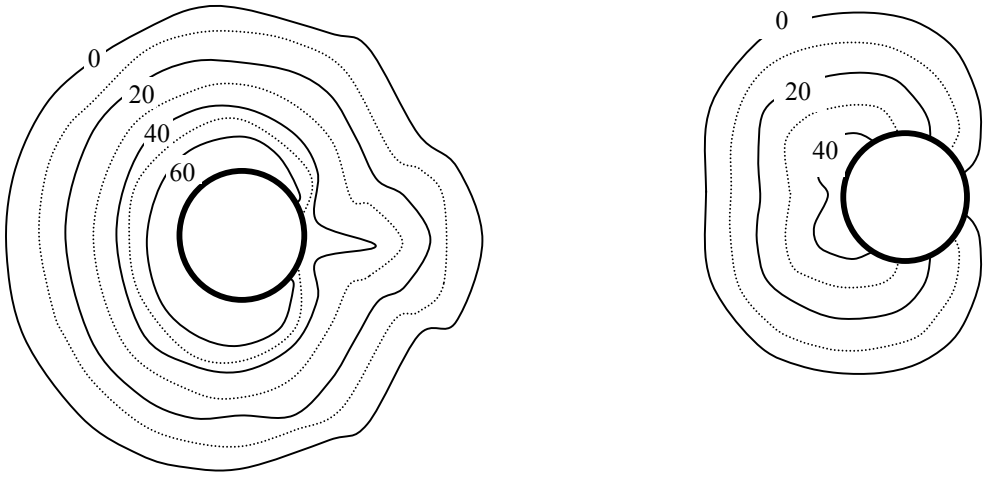

Contours of scour hole - laboratory

Contours of scour hole – FLUENT

Figure 4-9: Contours of scour hole from laboratory experiment and numerical model

Figure 4.9 shows the contours of scour holes from both the physical and numerical models. The numerical model predicted a maximum scour depth of 50 mm whereas the physical model gave a depth of 68 mm. The maximum scour depth predicted by the numerical model occurred at an angle approximately 30º to the channel centreline. This was in agreement with the location of the maximum scour depth in the physical model. The shape of the scour hole predicted by the numerical model was however not in concurrence with that observed in the laboratory indicating that the estimation of the sediment transport parameter (movability number in this case) at the bed was inaccurate. It has already been shown in Figure 4-4 that none of the modelling approaches that were assessed correctly predicted the bed shear stress. It is evident that for an accurate scour hole to develop, scour prediction at the bed has to be accurate. Thus, in order for the developed model to be a viable option with the current generation of PCs, a suitable modelling approach, which accurately predicts the near-bed velocity gradients, needs to be found.

4.7.2 Numerical modelling of local scour using TELEMAC Version 5.4

The TELEMAC system is an integrated modelling tool comprising different simulation modules principally designed for open channel flow problems. All modules have been compiled using standard FORTRAN 90. The code primarily uses the Finite Element Method (Section 4.2.3) although the Finite Volume Model (Section 4.2.2) can be used for simulating the two-dimensional (2D) hydrodynamic module, and the non-cohesive sediment transport module, SISYPHE. Figure 4-5 shows some of the different modules available in the TELEMAC system.

The grid generation and definition of suitable boundary conditions are usually carried out in the pre-processing module MATISSE, although the boundary conditions can also be defined using FORTRAN programming or using a MS DOS-based parameter file. The 2D unstructured mesh usually consists of triangular elements (Figure 4-6a), whilst the 3D mesh is generated automatically from the 2D unstructured mesh by defining a number of horizontal planes (Figure 4-6b). In effect the 2D mesh is repeated along each horizontal plane to form layers of prisms.

TELEMAC-2D solves the depth-averaged free surface flow equations proposed by Saint-Venant in 1871. The main outputs are water depth and the depth-averaged velocity components at each node of the computational mesh. The module can correctly predict the higher velocity field that exists at the sides of the circular pier normal to the dominant flow direction which cause the high tractive forces at the base of this region (Figure 4-7). It cannot, however, predict the downflow at the pier nose which develops due to the reversed stagnation pressure gradient. Moreover this module cannot predict the horseshoe vortex flow field or wake behind the structure.

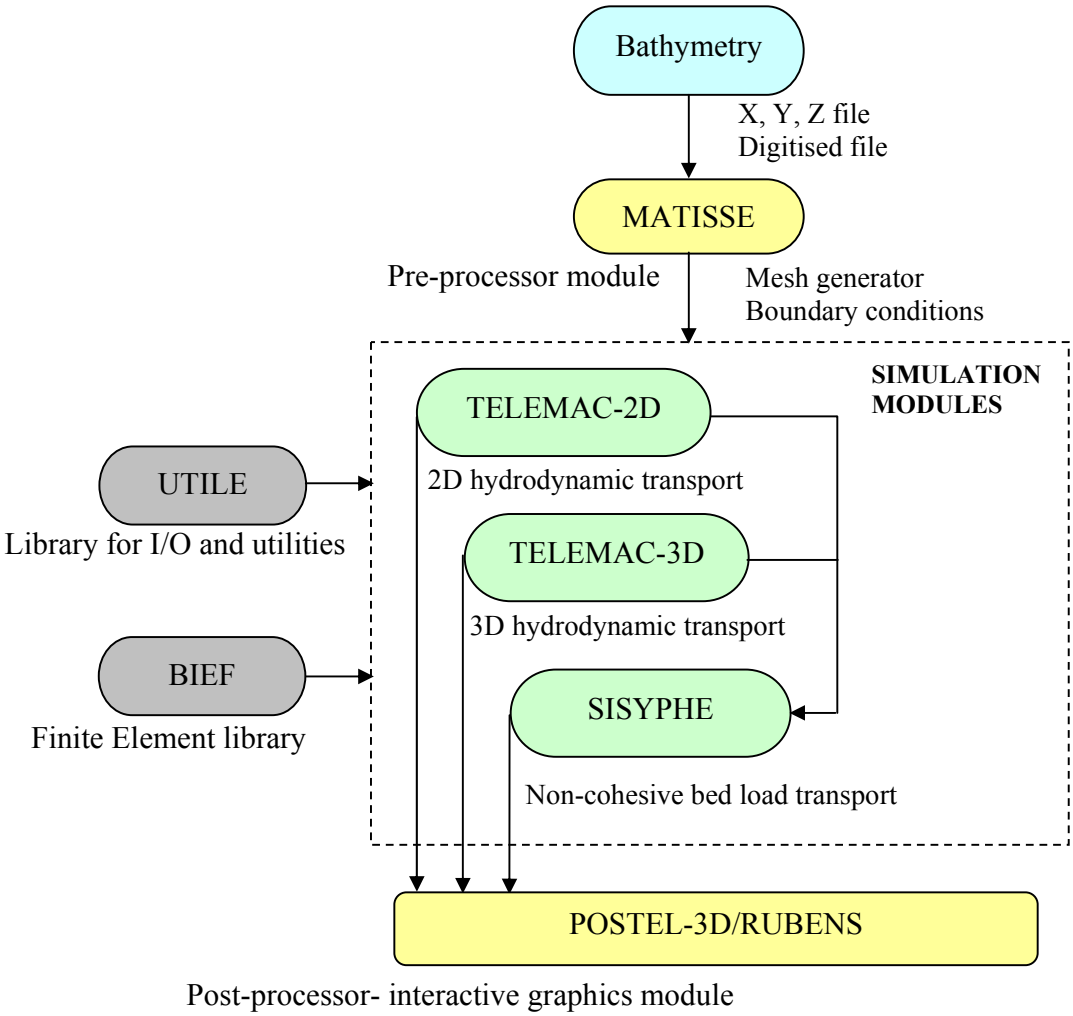

Figure 4-10: Modules of TELEMAC system used to model local scour

In TELEMAC-3D the three-dimensional Reynolds-Averaged Navier-Stokes equations are solved with the assumption of hydrostatic pressure conditions and time-dependent surface. The k-ε model is used for turbulence closure. During each time step, the vertical positions of the mesh points in each horizontal plane (vertical y-coordinates) change according to the free surface elevation and bed topography. The distances between each horizontal plane are in proportion to the local water depth (distance between bottom and free surface). The main outputs of the module are the three-dimensional velocity field (u, v, w), the position of the free surface and the elevation of the bottom resulting from scour and deposition. The module is specially designed for the simulation of the interaction between the hydrodynamic flow field and local features. It can predict the vertical down flow at the leading edge of the circular pier. Moreover it may also able capture the horseshoe vortex wrapped around the pier and wake vortices behind the pier. Unfortunately, the user-interface is currently not that well developed and

the module is also not that well coupled with other modules in the TELEMAC suite. There is, however, flexibility for the addition of user-defined subroutines programmed in FORTRAN 90 if so required.

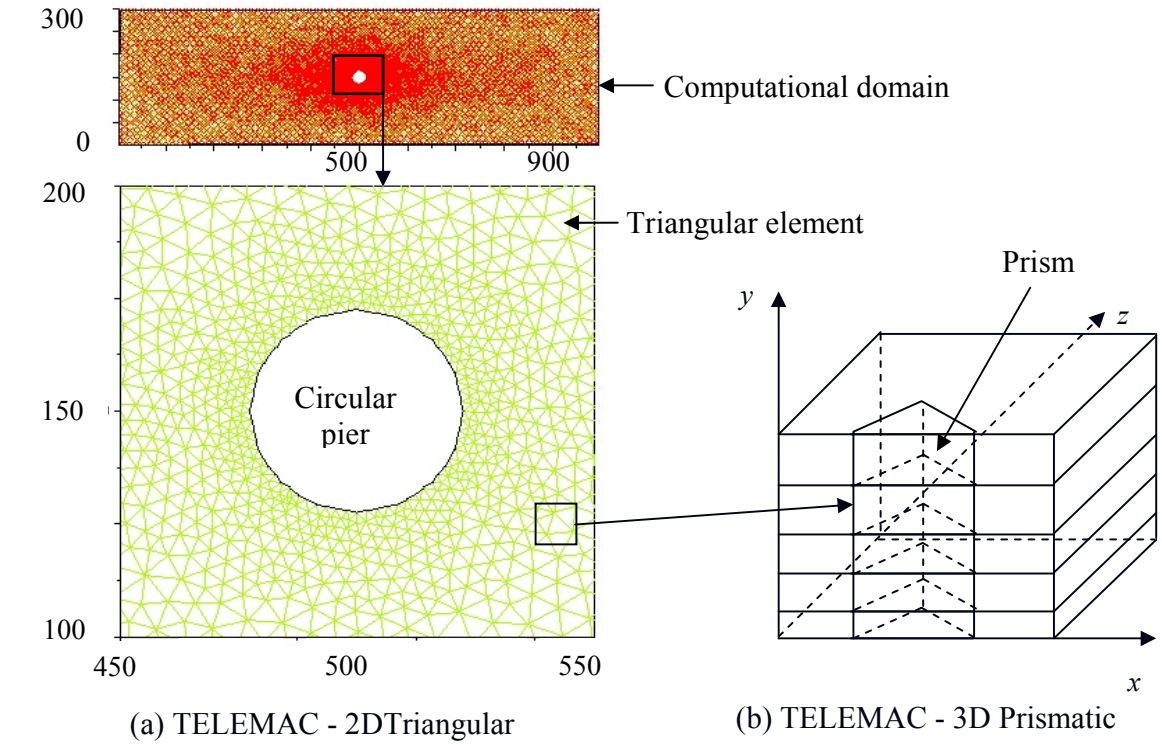

Figure 4-11: TELEMAC Two-dimensional (2D) and three-dimensional (3D) mesh

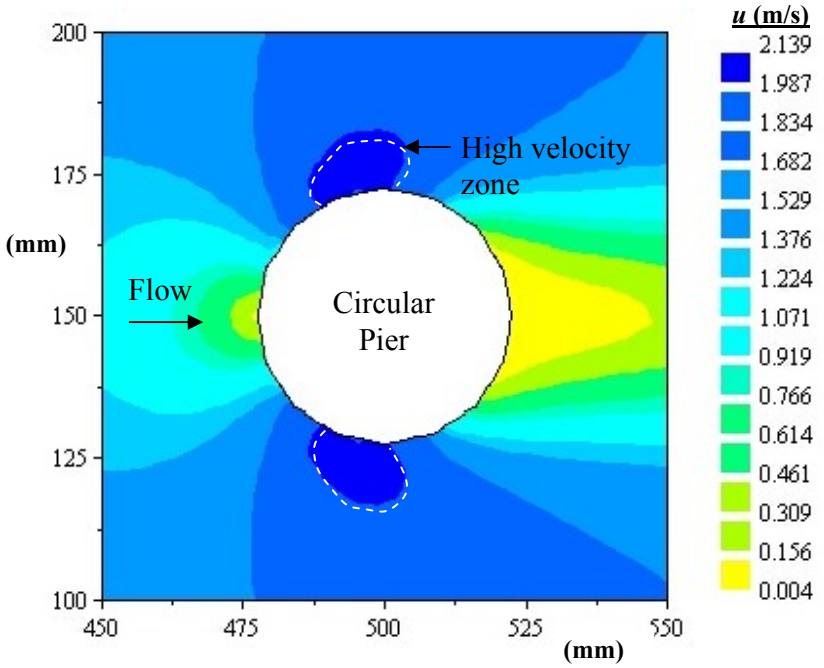

Figure 4-12: Scalar x-velocity contours around circular pier (TELEMAC-2D)

The SISYPHE sediment transport module has been designed to calculate the bed-load transport rate for sand according to either embedded empirical formulae, or user-defined subroutines. The empirical formulae mainly relate to non-cohesive sediment with a uniform grain-size distribution. The module can account for the effect of the bottom slope, rigid beds and layers of different particle sizes. It is usually coupled to TELEMAC-2D, in which case SISYPHE is directly called from TELEMAC and the two programs share memory. The main outputs of the module are the bottom elevations as a result of scour and deposition, and the solid transport rate at each node of the bed cells.

Graphics visualisation in TELEMAC is achieved with the aid of the post-processor module RUBENS, which is a two dimensional graphics visualization software package. TELEMAC -3D also requires the additional interface POSTEL-3D. POSTEL-3D enables results from TELEMAC-3D to be displayed in RUBENS. A limitation is that these modules are unable to do flow animations.

As with FLUENT, the program was used to model the initiation of scour in non-cohesive uniform sediment around a circular bridge pier. Both the 2D and 3D modules were used to simulate the hydrodynamic flow field around the structure. The 2D module was also coupled to the SISYPHE module so that the scour and deposition could also be modelled using the various options embedded in the code. During the TELEMAC-2D/SISYPHE simulation, scour was only observed at the sides of the circular pier normal to the dominant flow direction in line with the maximum tractive forces calculated by the

2D simulation (Figure 4-7 and 4-8) This is because a 2D simulation cannot model the vertical down-flow on the upstream of the pier or the horseshoe vortex that subsequently develops at the foot of this. A simulation of 30 hours of real time took approximately 34 hours using an Intel P4 chip with a clock speed of 3.0 GHz and 2 GB RAM. TELEMAC-3D was able to predict the three-dimensional flow patterns, but unfortunately deficiencies in the program prevented coupling with SISYPHE.

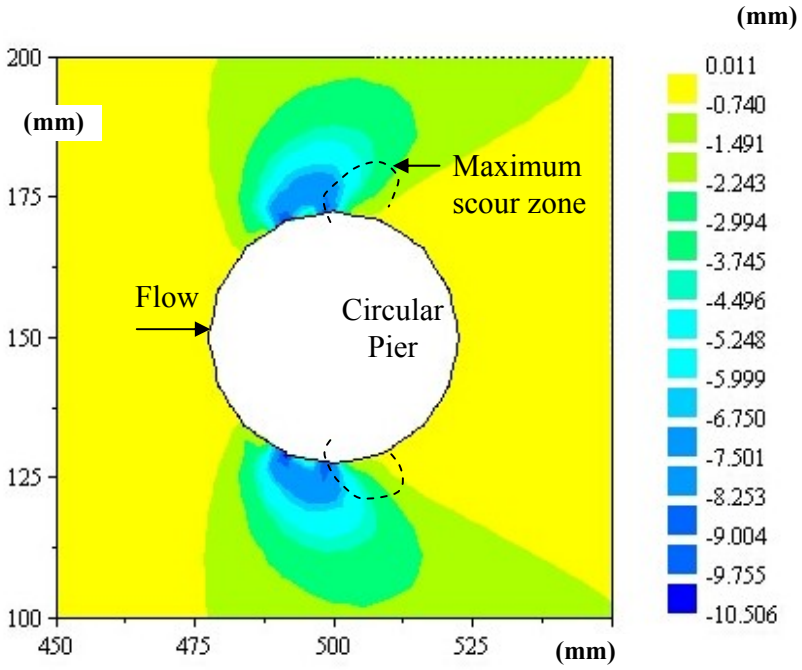

Figure 4-13: Scoured bottom topography around circular pier (TELEMAC-2D)

The main advantage TELEMAC has over a general code such as FLUENT is that it is already configured to deal with open channel flow problems, whilst general codes are often quite weak in this area. For example, FLUENT does not have a suitable boundary adjustment routine for use in scour / deposition models – this has to be written in by the user. On the other hand, in the specific case of TELEMAC versus FLUENT, the user interface has been much better developed in the case of the latter making it much easier to use. The documentation in FLUENT is also much better than that in TELEMAC, particularly since most of TELEMAC's documentation is only available in French – and much of it is out of date. In both programs, the current generation of PCs struggle to cope with the large number of cells required to accurately model the three-dimensional flow phenomena occurring in the vicinity of a structure – even with relatively simple turbulence models such as any of the k-ε versions. Clearly, scour modelling is still in its infancy.

4.8 Concluding remarks

This chapter set out to summarise the mathematical principles behind CFD and its use to model local scour. It is evident that, whilst the tools exist, their efficient application has been hindered by the huge computational demand that is still somewhat beyond the current generation of PCs. The situation is rapidly changing though, and there is real hope that numerical modelling will shortly become a viable option.

Chapter 5
Conclusions and recommendations for future research

5.1 Conclusions

5.1.1 Introduction

It is important that the reader appreciates that local scour is but one type of scour. Scour, whether it is in the form of long-term bed degradation, constriction scour, bend scour, confluence scour or local scour, is a major engineering problem as all forms of scour have the potential to undermine hydraulic structures and possibly cause their collapse. This report focuses only on local scour; for the reason that it is one of the greatest threats to hydraulic structures whilst simultaneously being one of the most difficult to analyse as a result of the three-dimensional vortex formation and dissipation around these structures.

Even in the context of a discussion of local scour, this report is still constrained. It deals with only two aspects: the extent of the problem in South Africa, and the state of the art of numerical modelling.

When dealing with the extent of the problem in South Africa, the focus is on provincially maintained road-over-river bridges. Other types of structure e.g. pipe bridges, weirs, spillways, dikes, intake structures, canoe chutes, etc. are largely ignored. Even road bridges, bridges along National roads and roads maintained by local authorities are effectively ignored. Furthermore, estimates of local scour damage are restricted to repair costs with no attempt made to determine consequential costs e.g. delays or the additional maintenance and running costs associated with the temporary deviation of traffic.

In the discussion on the state of the art of numerical modelling, the report assumes the use of commercially available software running on desktop personal computers. Clearly a lot more can be done if the modelling is carried out on supercomputers or high-speed clusters of machines, but these options are not generally available for routine engineering work.

Ultimately the report is designed to give a snap-shot of the situation as it currently stands at the present from the perspective of technology that is readily available to all consulting engineers. It is clear, however, that the rapid improvements in the speed of personal computing and the associated rapid development of software will render this document dated within a relatively short period of time.

5.1.2 The extent of the problem in South Africa

Scour damage is generally associated with extreme flood events. A study of current scour damage at road bridges in South Africa has indicated that severe scour damage is seldom evident at bridges under "normal" flow conditions. Evidence of severe scouring during past floods was, however, seen at several sites. An estimate of the direct cost of repair of scour-related damage on provincially maintained bridges is approximately R22 million per annum. About 42% of this cost is on bridges in KwaZulu-Natal. This cost excludes the damage incurred in extreme flood events and the economic costs associated with the disruption caused by the failure of major transport links. Inclusion of scour damage during extreme floods events may increase the estimate to between R25 million and R30 million per annum.

The severity of the constriction scour observed in the field study was generally greater than the local scour. It might thus be said that excessive constriction of the flow poses a greater threat to South African river bridges. It must, however, be remembered that local scour cannot be readily observed or measured, particularly during extreme flood events, and the holes are rapidly filled by sediment after the peak flow has passed, which might lead to an underestimate of the impact of local scour. Furthermore, the two types of scour usually act in conjunction so one cannot be studied in the absence of the other.

Local and constriction scour are the two mechanisms occurring most frequently at bridge sites. Local scour was observed at 60% of the 105 bridges investigated whilst constriction scour was observed at 44% of them. The local and constriction scouring were combined at 37% of the sites investigated. The prediction and mitigation of local scour is thus an important area for research.

5.1.3 The state of the art of numerical modelling

The complex nature of real flow phenomena has historically made physical modelling attractive. However, the construction, modification, and operation of physical models can make them extremely expensive which is encouraging engineers to look toward numerical simulation using CFD either as an adjunct to, or as a replacement for, physical models. The main problems associated with CFD relate to the transfer of the underlying physics to the numerical solvers. This is made difficult because of complex interaction of many different factors coupled with the severe limitations in the computational power of the current generation of desk-top machines.

The first step in numerical analysis involves the identification and description of a suitable flow domain. The domain is then divided into finite volumes or finite elements by means of two- or three-dimensional meshes. The choice of domain is extremely important. An adequate length of channel upstream and downstream of the structure must be modelled to ensure that any inadequacies in the boundary conditions have been smoothed out in the region of interest in the vicinity of the structure. In the case of

symmetrical flows around symmetrical structures such as circular piers, the computational time can be greatly reduced by defining the line of symmetry and modelling only half the channel width – although this will obscure such physical phenomena such as the von Kárman vortex street. This analytical trick cannot, however, be applied to models around asymmetrical structures such as a spur dike. Finer meshes generally give a more accurate solution compared with coarser meshes, but they are computationally time intensive. Considerable skill is required to determine the optimum mesh size taking into account the computational time and model accuracy. At present, there are no generally agreed guidelines for mesh refinement – especially close to the structure, the river bed and the air-water (free-surface) interface.

The selection of the turbulence model is a key factor in numerical modelling. Each turbulence model has its advantages and disadvantages depending on the type and nature of the flow field to be modelled. The more accurate turbulence models such as Direct Numerical Simulation (DNS), Large Eddy Simulation (LES), Very Large Eddy Simulation (VLES), or Reynolds Averaged Navier-Stokes (RANS) improve accuracy (in decreasing order), but at an extremely high computational cost associated with the finer meshes and additional time steps required. As a consequence, the k-ε family of turbulence models are by far the most popular and extensively used for predicting the local scouring problems in spite of their well-documented limitations particularly in the separated zones.

Some commercially available CFD codes that could be used to solve scour problems are listed in Appendices B (General codes) and C (Specialised river codes). Trials using one example of each type of code; FLUENT – a general code – and TELEMAC – a specialized river code – quickly revealed limitations with both. They were chosen on the basis of relatively low cost, good software support, and flexibility (they both allow for user-defined routines). FLUENT had an excellent user interface and great flexibility, but was not originally designed for open channel work so features such as sediment transport and boundary adjustment had to be specially programmed into the code. The Volume of Fluid method was used to determine the position of the free surface, which was reasonably accurate, but computationally intensive. TELEMAC was designed for open channel work so there were already modules for sediment transport / boundary adjustment, but the three-dimensional module was effectively a multiple two-layer model which was too coarse to pick up some of the small scale vortices that are set up in the vicinity of structures. The default free surface routine assumed hydrostatic pressure variation – which is not the case in the vicinity of a structure. A major shortcoming of TELEMAC was that it had a poor user interface, whilst the documentation was out of date – or in French. Both models demonstrated limitations in the modelling of the velocity gradients (and hence all other parameters such as shear stress that are dependent on the velocity gradient) in the boundary layer near the water / solid interface – unfortunately the most critical area for scour modelling.

5.2. Recommendations for future research

The following recommendations are intended to guide further investigations into scour damage in South Africa and research into numerical scour prediction methods:

- Further investigation needs to be made into the extent of the scour damage around bridges resulting from major historical flood events with particular emphasis on the causes of failure, and the associated economic costs. These costs need to include consequential damages such as the cost of providing temporary services or the additional fuel, maintenance and time cost of travelling additional distances over detours. The investigation should focus particularly on KwaZulu-Natal as the costs associated with scour damage in this province are estimated to account for 42% of the total value of scour damage in South Africa. This is a consequence of KwaZulu-Natal having the highest average rainfall and largest number of bridges of the nine provinces.
- A more extensive review of the causes of failure of other hydraulic structures, e.g. intake structures, weirs and dikes, is necessary to give a better indication of the extent to which scour damage is a contributory factor.
- Local scour is a priority for further research as the severity of scour resulting from this mechanism under flood conditions is difficult to predict – or measure. Local scour was identified as the most prevalent form of scour damage observed at provincial road bridges during this study. More research into the combined effects of local and other forms of scouring should however be undertaken.
- A review of appropriate scour protection measures needs to be undertaken. This would have to be linked to the types of structures and environments found in South Africa.
- More research could also be undertaken into the impacts of deposition – particularly with regard to potential blocking of intake structures.
- Computing power is increasing very rapidly. Current high end PCs are capable of performing between 12-15 GFLOPS (10^9 floating point operations per second). Trends in computational power appear to follow Moore's Law which translates to an average increase in performance of just over 1% every week. This is in turn leading to a rapid improvement in the available software. Ongoing research is thus required to ensure that South African engineers keep pace with the development of suitable codes for the prediction of local scour and deposition that will, *inter alia*, enhance their capacity to design safe and durable hydraulic structures. Some aspects that require further attention include:

- the optimum choice of incipient motion / sediment transport model in association with the appropriate numerical wall model for boundary adjustment
- the impact of non-cohesive and/or non-uniform bed material
- the impact of sediment load on flow properties (density, viscosity etc.)
- live bed scour
- rate of scour development
- deposition
- the potential use of discrete granular phase modelling as an alternative to empirical formulae (such as Van Rijn, 1987 etc.) to make the CFD model more closely related to the physical processes and thus more generally applicable

- The possible linkages between high definition 3D hydrodynamic models and other types of models e.g. 2D river models, river ecology models etc. need to be explored. For example, 2D river models are ideally suited for the modelling of long river reaches where the flow is predominantly two dimensional. If these 2D models could be linked to a suitable 3D model, they would help to better describe the boundary conditions of the latter model – and thus its ability to predict scour and/or deposition. Meanwhile, ecologists have expressed great interest in modelling the hydraulic habitat of various organisms in an attempt to better understand how these affect the viability of these creatures.

References

Alexander, WJR (2000). "The failure of bridges during the floods – some issues that need to be discussed." *Proc. Conf. on South African Floods of February 2000*, University of Pretoria, May 2000.

Ali, KMH & O Karim (2002). "Simulation of flow around piers." *J. Hydr. Res.*, 40 (2):161-174.

Armitage, N & C McGahey (2003). "A unit stream power model for the prediction of local scour in rivers." *Water Research Commission of South Africa*, Report No. 1098/1/03, ISBN 1-86845-955-1, Pretoria, South Africa.

Armitage, N & C McGahey (2004). "Scour prediction using the mobility number criteria for incipient motion." *Proc. Second International Conf. on Fluvial Hydraulics, River Flow 2004*, Vol. 1: 511-519.

Arup (Pty) Ltd. Consulting Engineers (2000). "Dainfern Country Club Flooding: Engineering Review – Draft Document."

Balden, V (2003). "MEC563Z: Introduction to Finite Elements", MEC563Z Course Notes, CERECAM, University of Cape Town, Rondebosch, South Africa.

Biglari, B & TW Sturm (1998). "Numerical modelling of flow around bridge abutments in compound channels." *J. Hydr. Engrg. ASCE*, 124 (2): 156-164.

Breusers, HNC & AJ Raudkivi (1991). "Scouring." IAHR Hydraulic Structures Design Manual 2. AA Balkema.

Brooks, NH (1963). Discussion of "Boundary shear stress in curved trapezoidal channels" by AT Ippen and PA Drinker. *J. Hydr. Engrg., ASCE*, 89 (HY3): 327-333.

Chabane, C, S Phillips, I Kriel & S Mnisi (2000). "Flood damage to the road and bridge infrastructure in the Northern Province." *Proc. Conf. on South African Floods of February 2000*, University of Pretoria, May 2000.

Chen, Q, G Dai & H Liu (2002). "Volume of fluid model for turbulence numerical simulation of stepped spillway overflow." *J. Hydr. Engrg. ASCE*, 128 (7): 683-688.

Chien, N & Z Wan (1999). "Mechanics of sediment transport." ASCE Press.

Chiew, Y-M (1995). "Mechanics of riprap failure at bridge piers." *J. Hydr. Div., ASCE*, 121 (9): 635-643.

Chitale, SV (1962). Discussion of "Scour at Bridge Crossings." by Laursen E.M. *Trans., ASCE*, 217 (I): 191 – 196.

Chrisohoides, A, F Sotiropoulos & TW Sturm (2003). "Coherent structures in flat-bed abutment flow: computational fluid dynamics simulations and experiments." *J. Hydr. Engrg. ASCE*, 124 (3): 177-186.

Clarke, FRW (1962). "The Action of Submerged Jets on Movable Material." Ph.D. Dissertation, Imperial College, London, UK.

Committee of State Road Authorities (1994). "Guidelines for the Hydraulic Design and Maintenance of River Crossings", TRH 25, Department of Transport, Pretoria, South Africa.

Dargahi, B (1987). "Flow field and local scouring around a cylinder." *Bulletin TITRA-VBI-137*, Department of Hydraulics Engineering, Royal Institute of Technology, Stockholm, Sweden.

Dey, SB, KS Sujit & LN Ghandikota (1995). "Clear water scour at circular piers: a model." *J. Hydr. Engrg. ASCE*, 121 (12): 869-876.

Du Plessis, DB (1984). "Documentation of the March – May 1981 floods in the South Eastern Cape". Technical Report TR 120, Department of Water Affairs, Pretoria.

Du Plessis, DB & SC Bain (1987). "Dokumentasie van die 1974-vloede in die Oranje- en Groot-Visrivier". Tegniese Verslag TR 132, Departement van Waterwese, Pretoria.

Ettema, R (1980). "Scour at bridge piers." School of Engineering Report No. 216, University of Auckland, New Zealand.

Fluent (2003). "Fluent Users' Guide." Fluent Inc., UK.

Garde, RJ, KG Ranga Raju & UC Kothyari (1993). "Effect of unsteadiness and stratification on local scour." International science publisher, NY, USA.

Gosman, DA & WM Pun (1973). Lecture notes for course entitled "Calculation of recirculating flow." *Report HTS/74/2*, Heat Transfer Section, Imperial College, London.

Graf, WH (1998). "Fluvial Hydraulics: Flow and transport processes in channels of simple geometry." John Wiley & Sons.

HEC-18 (1995). "Evaluating scour at bridges." Third edition, *US Department of Transportation, Federal Highway Administration Publication*, No. FHWA HI-96-031, Hydraulic Engineering Circular No. 18, 204 pages.

Hoffman, J & C Johnson (2003). "Adaptive DNS/LES: A new agenda in CFD." CIMS, New York University, USA.

Hoffmans, GJCM & HJ Verheij (1997). "Scour manual." AA Balkema.

Jain, SC (1981). "Maximum clear-water scour around circular piers." *J. Hydr. Engrg*, 107(5).

John, DAJ (1995). "Computational fluid dynamics: The basics with applications." McGraw-Hill, Inc. USA.

Kimura, I, T Hosoda & S Onda (2002). "Prediction of 3D flow structures around skewed spur dikes by means of a non-linear k-ε model." *Proc. International Conference on Fluvial Hydraulics, River Flow 2002*, Vol. 1: 65-73.

Kimura, I, T Hosoda, S Onda & A Tominaga (2004). "Computation of 3D turbulent flow structures around submerged spur dikes under various hydraulic conditions." *Proc. Second International Conference on Fluvial Hydraulics, River Flow 2004*, Vol. 1: 543-553.

Kogaki, T, T Kobayashi & N Taiguchi (1997). "Large eddy simulation of flow around a rectangular cylinder." *J. Fluid Dynamics Research*, 20 (1-6): 11-24.

Kothyari, UC, RJ Grade & KG Ranga Raju (1992). "Temporal variation of scour around circular bridge piers." *J. Hydr. Engrg., ASCE*, 118 (8): 1091-1106.

Kothyari, UC & KGR Raju (2001). "Scour around spur dikes and bridge abutments." *J. Hydr. Res.*, 39 (4): 367-374.

Kovács, ZPSJ (1978). "Documentation of the January, 1978 floods in Pretoria and in the Crocodile River catchment". Technical Report TR 88, Department of Water Affairs, Pretoria.

Kovács, ZP, DB Du Plessis, PR Bracher, P Dunn & GCL Mallory (1985). "Documentation of the 1984 Domoina Floods". Technical Report TR 122, Department of Water Affairs, Pretoria.

Kovács, ZP (1988). "Preliminary hydrological assessment of the Natal flood". Trans. SAICE, January 1988, 30 (1): 7-13.

Kovács, ZPSJ (undated). "Documentation of the January 1981 floods in the South Western Cape". Technical Report TR 116, Department of Water Affairs, Pretoria.

Launder, BE & DB Spalding (1972). "Lectures in mathematical models of turbulence." Academic Press, London, England.

Liu, H-K (1957). "Mechanics of sediment-ripple formation." *J. Hydr. Div. ASCE*, 83 (HY2): 23 pages.

Melville, BW (1997). "Pier and abutment scour: Integrated approach." *J. Hydr. Engrg. ASCE*, 123 (2): 125-136.

Midgley, M (2000). "Sediment movement around piers in open channel flow." BSc(Eng) thesis, University of Cape Town, Rondebosch, South Africa.

Molls, T & MH Chaudhry (1995). "Depth-averaged open-channel flow model." *J. Hydr. Engrg., ASCE*, 121 (6): 453-465.

Muller, A (2000). "Damage to DWAF infrastructure during the floods of February & March 2000." *Proc. Conf. on South African Floods of February 2000*, University of Pretoria, May 2000.

Olsen, NRB & MC Melaaen (1993). "Three dimensional calculation of scour around cylinders." *J. Hydr. Engrg. ASCE*, 119 (9): 1048-1054.

Olsen, NRB & HM Kjellesvig (1998). "Three dimensional numerical flow modelling for estimation of maximum local scour depth." *J. Hydr. Res.*, 36 (4): 579-590.

Olsen, NRB (1999). "CFD in Hydraulic and Sedimentation engineering", Department of Hydraulic and Environmental Engineering, The Norwegian University of Science and Technology, Report Ref.: ISBN 82 7598-041-0.

Ouillon, S & D Dartus (1997). "Three-dimensional computation of flow around a groyne." *J. Hydr. Engrg., ASCE*, 123 (11): 962-970.

Park, TS & HJ Sung (1997). "A new low-Reynolds-number k-ε-f_μ model for predictions involving multiple surfaces." *J. Fluid Dynamics Research*, 20 (1-6): 97-113.

Patankar, SV (1980). "Numerical heat transfer and fluid flow." Taylor & Francis, UK.

Perot, B & P Moin (1996). "A new approach to turbulence modelling." *Proc. Summer Program 1996, Centre for Turbulence Research*, pp 35-46.

Raudkivi, AJ (1986). "Function trends of scour at bridge piers." *J. Hydr. Engrg., ASCE*, 112 (1): 1-13.

Raudkivi, AJ (1998). "Loose boundary hydraulics." AA Balkema.

Richardson, JE & VG Panchang (1998). "Three-dimensional simulation of scour-inducing flow at bridge piers." *J. Hydr. Engrg. ASCE*, 124 (5): 530-540.

Rodi, W (1984). "Turbulence models and their application in hydraulics." State of the art review, second edition revised, IAHR Section on Fundamentals of Division II: Experimental and Mathematical Fluid Dynamics, Germany.

Rodi, W, RN Pavlovic & SK Srivatsa (1981). "Prediction of flow and pollutant spreading in rivers." *Transport models for inland and coastal waters*. Academic Press Inc., New York.

Salaheldin, TM, J Imran & MH Chaudhry (2004). "Numerical modelling of three-dimensional flow field around circular piers." *J. Hydr. Engrg. ASCE*, 130 (2): 91-100.

Sarker, MA & DG Rhodes (1999). "Physical and 2D numerical models of free surface flow over weir, using standard and RNG k-epsilon models with power law and SMART schemes." *Proc. IAHR Symposium on River, Coastal and Estuarine Morphodynamics*, Vol. 2: 259-268.

Sheasby, PT (2000). "The design of flood-resilient bridges." *Proc. Conf. on South African Floods of February 2000*, University of Pretoria, May 2000.

Shen, HW, VR Schneider & S Karaki (1969). "Local scour around bridge piers." *J. Hydr. Engrg.*, 95 (6).

Shields, A (1936). "Anwendung der Aenlichkeitsmechanik und der Turbulenzforschung auf die Geschiebebewegung." Mitteilungen der Preussischen Versuchsanstalt für Wasserbau und Schiffbau, Heft 26 (in German). English translation by WP Ott and JC van Uchelen, Hydrodynamics Laboratory Publication No. 167, Hydrodynamics Lab., California Institute of Technology, Pasadena.

South African National Roads Agency Limited (1986). "Road Drainage Manual." First Partly Revised Edition, ISBN 0-908381-39-5, Department of Transport, Pretoria, South Africa.

Speziale, CG (1991). "Analytical methods for the development of Reynolds-stress closures in turbulence." Annual Revision of Fluid Mechanics, 23: 107-157.

Tingsanchali, T & S Maheswaran (1990). "2D Depth-averaged flow computation near groyne." *J. Hydr. Engrg., ASCE*, 116 (1): 71-86.

Van Bladeren, D (1992). "Historical Flood Documentation Series No. 1: Natal and Transkei, 1848 – 1989". Technical Report TR 147, Department of Water Affairs and Forestry, Pretoria.

Van Bladeren, D & CE Burger (1989). "Documentation of the September 1987 Natal Floods". Technical Report TR 139, Department of water Affairs, Pretoria.

Van Bladeren, D & D van der Spuy (2000). "The February 2000 Floods – The Worst in Living Memory?" *Proc. Conf. on South African Floods of February 2000*, University of Pretoria, May 2000.

Van Rijn, LC (1987). "Mathematical modelling of morphological processes in the case of suspended sediment transport." PhD Thesis, Delft University of Technology.

Versteeg, HK & W Malalasekera (1995). "An introduction to Computational Fluid Dynamics." Addison Wesley Longman Limited, Harlow, Essex, UK.

White, FM (1991). "Viscous Fluid Flow." Second Edition, McGraw-Hill Inc., New York.

Wilcox, DC (1988). "Reassessment of the scale determining equation for advanced turbulence model." *AAIA Journal*, 26 (1): 1299-1310.

Yang, CT (1972). "Unit stream power and sediment transport." *J. Hydr. Div. ASCE*, 98 (HY10): 1805-1826.

Yang, CT & CS Song (1979). "Theory of minimum rate of energy dissipation." *J. Hydr. Div. ASCE*, 105 (HY7): 769-784.

Yanmaz, AM (2004). "A reliable model for bridge abutment scour", *Turkish J. Eng. Env. Sci.*, 28: 67-83.

Yen, CL, JS Lai & WY Chang (2001). “Modelling of 3D flow and scour around circular piers.” *Proc. Natl. Sci. Counc., ROC(A)*, 25 (1): 17-.

Zanke, U (1978). “Zusammenhange zwischen Stromung und Sedimenttransport, Teil 1: Berechnung des Sedimenttransportes, -allgemeiner Fall-, Teil 2: Berechnung des Sedimenttransportes hinter befestigten Sohlenstrecken, -Sonderfall sweidimensionaler Kolk-.“ Mitteilungen des Franzius-Instituts der TU Hannover, Heft 47, 48.

Appendix A

Cost estimates of current scour damage in South Africa

A.1 Eastern Cape

Number of bridges in EC	1400
Number of hits for *scour* in BMS	357
Percentage of bridges with scour damage	26

Total value of all maintenance activities **R100 326 000**

Scour repair activity	**Cost (R)**	**Fraction due to scour**	**Scour repair cost (R)**
Backfill/Underpin of undermining at abutment	1 401 580	0.90	1 261 422
Embankment-Repair erosion damage	544 150	1.00	544 150
Stone pitching-New/repair	263 200	0.80	210 560
Gabion boxes (1mx1m)-New/repair	1 369 350	0.80	1 095 480
Gabion matresses-New/repair	1 098 000	0.80	878 400
Backfill/Underpin of undermining at pier	1 907 120	1.00	1 907 120
Re-construct pier	177 100	0.70	123 970
Gabion boxes - New/repair in waterway	5 602 725	0.80	4 482 180
Gabion matresses-New/repair in waterway	4 979 700	0.80	3 983 760
Bed and banks - Repair erosion damage	905 650	1.00	905 650
Concrete cut-off beam - New/repair	282 000	0.70	197 400
Concrete apron slab - New/repair	618 000	0.80	494 400
Stone pitching-New/repair in waterway	366 700	0.80	293 360
Remove silt/sand	397 988	0.50	198 994
Total cost of scour-related repairs			**R16 577 000**

Scour cost / Total cost	0.17
Scour cost per damaged bridge	R46 400

A.2 Gauteng

Number of bridges in GP	680
Number of hits for *scour* in BMS	107
Percentage of bridges with scour damage	16

Total value of all maintenance activities **R13 573 000**

Scour repair activity	**Cost (R)**	**Fraction due to scour**	**Scour repair cost (R)**
Embankment-Repair erosion damage	43 392	1.00	43 392
Embankmts : Grouted stone pitching New/rep	66 788	0.50	33 394
Waterway : Backfill to repair erosion damage	26 530	1.00	26 530
Waterway : Gabion mattresses New / replace	120 000	0.90	108 000
Waterway : Gabion boxes New / replace	57 900	0.80	46 320
Remove silt/sand	188 730	0.40	75 492
Total cost of scour-related repairs			**R333 000**

Scour cost / Total cost	0.02
Scour cost per damaged bridge	R 3 100

A.3 Northern Cape

Number of bridges in NC	500
Number of hits for *scour* in BMS	102
Percentage of bridges with scour damage	20

Total value of all maintenance activities **R28 715 000**

Scour repair activity	Cost (R)	Fraction due to scour	Scour repair cost (R)
Backfill/Underpin of undermining at abutment	246 750	1.00	246 750
Re-construct concrete abutment	659 800	0.70	461 860
Embankment-Repair erosion damage	41 490	1.00	41 490
Stone pitching-New/repair	35 925	0.80	28 740
Gabion boxes (1mx1m)-New/repair	61 065	0.80	48 852
Gabion matresses-New/repair	253 500	0.80	202 800
Re-construct pier	120 000	0.70	84 000
Gabion boxes - New/repair in waterway	62 685	0.80	50 148
Gabion matresses-New/repair in waterway	886 050	0.80	708 840
Bed and banks - Repair erosion damage	50 490	1.00	50 490
Concrete cut-off beam - New/repair	25 500	0.70	17 850
Concrete apron slab - New/repair	410 975	0.80	328 780
Stone pitching-New/repair in waterway	18 075	0.80	14 460
Remove silt/sand	56 280	0.50	28 140
Total cost of scour-related repairs			**R2 313 000**

Scour cost / Total cost	0.08
Scour cost per damaged bridge	R22 600

A.4 Free State

Bridge No.	Total maintenance cost (R)	Repair cost (R)	Estimated scour cost (R)	Scour cost / Total maintenance cost
322	214 527	136 847	127 154	0.59
333	5 975	5 265	4 853	0.81
418	39 961	14 791	13 612	0.34
589	112 213	22 416	17 208	0.15
595	21 485	17 320	12 778	0.59
627	4 272	4 027	4 014	0.94
675	39 727	10 116	7 466	0.19
863	26 088	6 420	6 110	0.23
877	51 630	17 515	10 715	0.21
896	70 940	25 490	14 245	0.20
949	85 535	31 370	24 615	0.29
963	106 688	6 131	4 566	0.04
1007	7 235	6 720	4 488	0.62
1068	46 560	40 190	37 335	0.80
1102	45 534	28 078	22 031	0.48
1143	292 400	122 880	100 416	0.34
1153	257 765	146 125	138 338	0.54
1156	33 462	11 850	7 965	0.24
1161	47 144	5 334	3 700	0.08
1171	34 515	8 140	4 542	0.13
1178	32 174	4 872	3 374	0.10
1197	29 577	27 680	18 720	0.63
1215	39 076	12 586	6 119	0.16
1524	80 384	62 520	56 364	0.70
1952	55 832	11 196	8 654	0.16
1972	5 868	4 762	3 705	0.63
2001	42 630	8 765	6 363	0.15
2006	134 035	42 784	34 957	0.26
2034	35 735	6 955	4 187	0.12
2040	53 797	3 740	3 444	0.06
2077	27 777	5 427	4 834	0.17
Total	**R2 497 000**	**R1 030 000**	**R860 000**	
Average	**R80 500**	**R33 200**	**R27 700**	**0.35**

Number of bridges in FS	1800
Number of scour-damaged bridges (estimated)	360
Percentage of bridges with scour damage (estimated)	20
Reduction factor for average scour cost	0.80
Scour cost per damaged bridge (assumed similar to NC)	R22 200
Total scour cost	**R7,992,000**

A.5 KwaZulu-Natal

Number of bridges in KZN	3200
Number of bridges in BMS	400
Number of hits for *scour* in BMS	111
Percentage of bridges with scour damage	28
Scour cost per damaged bridge (using EC rate + 10%)	R52 000
Total cost of scour-related repairs	**R46 176 000**

A.6 Limpopo Province

Number of bridges in LP	800
Number of scour-damaged bridges (estimated)	192
Percentage of bridges with scour damage	24
Scour cost per damaged bridge (estimated from EC & FS data)	R36 000
Total cost of scour-related repairs	**R6 912 000**

A.7 Western Cape

Number of bridges in WC	2200
Number of scour-damaged bridges (estimated)	528
Percentage of bridges with scour damage	24
Scour cost per damaged bridge (estimated from EC data)	R38 000
Total cost of scour-related repairs	**R20 064 000**

A.8 Mpumalanga

	Area (km^2)	Population (million)	No. of bridges
LP	123910	4.2	800
MP	79490	2.7	?
MP / LP	0.64	0.64	?

Area & population data from "Road Atlas of Southern Africa", Automobile Association of SA.

Assume: Number of bridges in MP = 0.64 x Number of bridges in LP

Number of bridges in MP (estimated)	600
Number of scour-damaged bridges (estimated)	144
Percentage of bridges with scour damage	24
Scour cost per damaged bridge (estimated from EC & FS data)	R38 000
Total cost of scour-related repairs	**R5 472 000**

A.9 North-West Province

	Area (km^2)	Population (million)	No. of bridges
NP	123910	4.2	800
NW	116320	3.0	?
NW / NP	0.94	0.71	?

Area & population data from "Road Atlas of Southern Africa", Automobile Association of SA.

Assume: Number of bridges in NW = 0.83 x Number of bridges in LP

Number of bridges in MP (estimated)	650
Number of scour-damaged bridges (estimated)	143
Percentage of bridges with scour damage	22
Scour cost per damaged bridge (estimated from FS & NC data)	R24 000
Total cost of scour-related repairs	**R3 432 000**

A.10 Summary of Scour Repair Costs

Province	Number of bridges	Scour-damaged bridges (%)	Cost per scour-damaged bridge	Total scour repair cost (R)	Annual scour repair cost (R)	Proportion of total scour cost (%)
KwaZulu-Natal	3200	28	R52 000	46 176 000	9 235 200	42.3
Western Cape	2200	24	R38 000	20 064 000	4 012 800	18.4
Eastern Cape	1400	26	R46 400	16 577 000	3 315 400	15.2
Free State	1800	20	R22 200	7 992 000	1 598 400	7.3
Limpopo	800	24	R36 000	6 912 000	1 382 400	6.3
Mpumalanga	600	24	R38 000	5 472 000	1 094 400	5.0
North-West	650	22	R24 000	3 432 000	686 400	3.1
Northern Cape	500	20	R22 600	2 313 000	462 600	2.1
Gauteng	680	16	R3 100	333 000	66 600	0.3
Total				**109 271 000**	**21 854 200**	**100**

Appendix B

General CFD codes that could be used to solve scour and deposition problems

The information given in Appendix B was obtained by the authors from the relevant suppliers and/or their websites and refers to the situation as at September 2004. Where the information is incomplete it is because it was not readily available.

B.1 FLUENT

The FLUENT framework includes; FLUENT 6, FLUENT 5 and FLUENT 4.

B.1.1 Supplier

Fluent Europe Ltd., Sheffield, UK

B.1.2 Initial price

FLUENT has a wide variety of pricing structures ranging from one stand-alone license to a multiple network license with a special discount for academic institutions. A license may be a perpetual license or an annual license. A perpetual license costs roughly three times the value of an annual license and an annual maintenance fee is payable for updates of the code. Holders of annual licenses automatically receive the updates.

B.1.3 Annual license fees

The initial and annual license fees are the same.

B.1.4 Hardware requirements

FLUENT runs on all the major UNIX platforms (HP, Sun, DEC, Linux, IBM, SGI) and on a Windows NT/2000/XP platform. At least 500 MB memory is recommended. For benchmarking, refer to http://www.fluent.com/software/fluent/fl5bench/index.htm.

B.1.5 Type of code

Finite Volume

B.1.6 Support

UK: Sheffield Business Park, Europa Link, Sheffield S9 1XU
Tel: 0114 281 8888, Fax: 0114 281 8818
Email: info@fluent.co.uk
Website: http://www.fluent.com/worldwide/europe/about/index.htm

Online support is available. In South Africa, support is provided by Danie de Kock (E-mail: djdekock@postino.up.ac.za). Training can also be provided.

B.1.7 Flexibility of program

Flexible; additional routines can be written into code.

B.1.8 Capabilities

FLUENT is a general CFD code. It is capable of modelling problems in the automotive industry, aerodynamics, combustion, power generation, water industries, steel industries, chemical industries and processing, glass making etc. Currently FLUENT 6 and FLUENT 4 are used.

Some general features of FLUENT are the following:

- It has complete mesh flexibility with solution-based mesh adaptation. It has a dynamic mesh capability for modelling flow around moving bodies. There is a parallel computing option for solving large problems more quickly with unstructured meshes.
- It can solve steady state, transient, inviscid, laminar, turbulent, Newtonian or non-Newtonian flows.
- There is range of turbulence models e.g. k-ε, second order closure Reynolds Stress (RSM) and large eddy simulation (LES).
- It can model the free surface of complex flows using the volume of fluid (VOF), Eulerian and mixture multiphase algorithms.
- The Lagrangian model facilitates tracking of particle trajectories for dispersed phase modelling (particles, droplets or bubbles).

B.1.9 Main users

FLUENT is used by many different users from all over the world. The University of Cape Town (UCT) currently uses FLUENT.

B.1.10 Programming language

C++

B.2 CFX

The CFX framework includes; CFX-5 Version 5.7 and CFX 4 Version 4.4.

B.2.1 Supplier

AEA Technology, UK

B.2.2 Hardware requirements

CFX 4 (Version 4.4) can run on Compaq, Hewlett Packard, IBM, SGI, SUN, Cray and NEC, Windows 2000/NT/XP and Linux computer platforms. Detailed hardware and

software requirements can be found at http://www-waterloo.ansys.com/cfx/products/cfx-4/system.htm.

The following table lists the latest known status of operating system and hardware compatibility for CFX-5 (Version 5.7 released in April 2004). Details may be found on the website http://www-waterloo.ansys.com/cfx/products/cfx-5/sysreq.htm.

Vendor	Operating System			Double Precision Solver	64-bit Memory Address Solver
	Compiled and tested on	Also formally tested on	Known to run on		
Sun MicroSystems	Solaris 8		Solaris 9	Yes	Yes
SGI	IRIX 6.5			Yes	Yes
Hewlett-Packard	HPUX-11i v1 (11.11)			Yes	Yes
IBM	AIX 5.1			Yes	Yes
HP-Compaq	TruUnix 5.1*			Yes	Yes
Microsoft Personal Computer (IA32)	Windows 2000	Windows XP	Athlon systems	Yes	No
Linux PC (IA32)	Redhat 9.0		Redhat 8.0 Redhat Enterprise Linux 2.1/3.0 Athlon systems Opteron systems (using 32-bit executables)	Yes	No
Itanium II (IA64)	Redhat Enterprise Linux 2.1 HPUX-11i v2 (11.23)			Yes	Yes

* Support on TruUnix 5.1 is for the batch solver only

B.2.3 Type of code

Finite Volume.

B.2.4 Support

Online support is available using e-mail at cfx-info-uk@ansys.com and detailed support information can be found on the website: http://www-waterloo.ansys.com/cfx/contact.

Canada: ANSYS Canada Ltd.
554 Parkside Drive, Waterloo, Ontario N2L 5Z4
Tel: (888) 827-2356, Fax: (519) 886-7580
Email: cfx-info-na@ansys.com

France: ANSYS France
Eric Bienvenu, Les bureaux de Sevres, 2 rue Troyon, Sevres, F-92316
Tel: +33 (0) 141148345, Fax: +33 (0) 141148346
Email: eric.bienvenu@ansys.com

Germany: ANSYS Germany GmbH
Staudenfeldweg 12, D-83624 Otterfing
Tel: +49 (0) 8024 9054-0, Fax: +49 (0) 8024 9054-17
Email: cfx-info-germany@ansys.com

India: CFX Limited
16 Jayamahal Main Road, Bangalore 560-046
Tel: +91-80-23634676, Fax: +91-80-23634255
Email: cfx-info-india@ansys.com

Japan: Ansys K.K.
16F Queen's TowerC, 2-3-5, Minatomirai, Nishi-ku, Yokohama 220-6216
Tel: +81.45.640.1616, Fax: +81.45.640.1617
Email: cfx-info-apac@ansys.com

UK: ANSYS Europe Ltd.
The Gemini Building, Fermi Avenue, Harwell International Business Centre, Didcot, Oxfordshire OX11 0QR
Tel: +44 (0)1235 448018, Fax: +44 (0)1235 448001
Email: cfx-info-uk@ansys.com

USA: ANSYS Inc.
Southpointe, 275 Technology Dr. Canonsburg, Pennsylvania 15317
Tel: (724) 746-3304, Fax: (724) 514-9494
Email: cfx-info-na@ansys.com

Local support is available from the online helpdesk based in Secunda, South Africa.

B.2.5 Flexibility of program

CFX is a highly flexible program. It can incorporate additional routines, do computations internally and write data to file for alternative post-processing options.

B.2.6 Capabilities

CFX-5.5 uses an implicit, pressure-based algorithm for all flow speeds, incompressible and compressible flow. Advection modelling based on upwind differencing scheme with 1st and 2nd order blend factor, and high-resolution bounded discretisation is possible. Coupled solution of the continuity, momentum and energy equations and multiphase flow modelling is available.

Standard features include:

- Unstructured meshing, solution on any mixture of tetrahedral, hexahedral, prismatic and/or pyramidal elements; generalised grid interface; import and connect multiple meshes from independent sources; solution-based mesh adaption; can generate moving and deforming mesh. Mesh morphing from prescribed surface or volume movement, explicit volume mesh movement via user defined FORTRAN routines.
- It can handle steady state, transient, laminar and turbulent flow for Newtonian, non-Newtonian fluids or multi-component fluids.
- Variety of turbulence models i.e.: zero-equation turbulence, k-ε, RNG k-ε, shear stress transport, k-ω, Reynolds Stress transport model (second moment closure), Detached Eddy Simulation (DES) turbulence model, Large Eddy Simulation (LES). Scalable wall functions and automatic near-wall treatment including integration to the wall.
- Kinetic theory viscosity and thermal conductivity models including Sutherlands law, modified Eucken and non-interacting sphere models.
- Coupled Eulerian multiphase flow model with a variety of inter-phase transfer models and Lagrangian particle tracking model.
- Free surface modelling includes compressive discretisation, homogenous or inter-phase transfer models and surface tension.
- User-defined of volumetric sources of mass, momentum, energy and species. Also user defined properties through expressions or user FORTRAN subroutines.
- Wide ranges of intrinsic functions are supported including: dynamic evaluation of boundary values and flows, one-dimensional or three-dimensional cloud of point data interpolation.

B.2.7 Main applications

Industrial applications e.g. mixing vessels, settling tanks, chemical reactions in multiphase flows, jet flame impingement, coal-fired combustion etc.

B.2.8 Main users

Diverse.

B.2.9 Programming language

FORTRAN

B.3 Flo++

Flo++ Version 3.08

B.3.1 Supplier

Softflow cc, South Africa

B.3.2 Initial price

The price is R24 200 for commercial purpose including software price and email support. For academic use, it costs approximately 50% of commercial price. A detailed price list and conditions can be found on the website: http://www.softflo.com/Pricing.htm.

B.3.3 Annual license fees

R24 200 for commercial users.

B.3.4 Hardware requirements

Runs under Windows 98/NT platform with minimum 256MB RAM and 65MB hard disk.

B.3.5 Type of code

Finite Volume.

B.3.6 Support

Online support is available using e-mail louis@softflo.com (contact Louis de Grange).

South Africa: Softflo PO Box 19990, Noordbrug, 2522
Tel: (+27) 18 294 3945, Fax: (+27) 18 297 0061
Email: flopp.help@softflo.com
Website: www.softflo.com

B.3.7 Flexibility of program

Allows user-defined subroutines.

B.3.8 Capabilities

Standard features:

- Global and local Cartesian and cylindrical co-ordinate systems, manual or automatic creation of vertices, cells and boundary cells using hexahedral or

prism cells. Multi-dimensional interpolation routines for grid points, unstructured local mesh refinement and embedding to locally enhance the accuracy of solutions, arbitrary mesh coupling, couple any two meshes by simply projecting one surface onto the other. It can also generate moving meshes.

- Incompressible to highly compressible transonic, steady and unsteady flow. Modified versions of the SIMPLE and PISO algorithms are used for steady and unsteady solutions flow.
- Dispersed multi-phase flow model. A general framework is provided for handling different combinations of gas-solid, gas-droplet, and fluid-bubble dispersed phase situations.
- Two-fluid with free surface capability but lacks a proper surface tension model.

B.3.9 Main applications

Viscous compressible flows in complex geometries.

B.3.10 Main users

SASOL, DENEL (South Africa).

B.3.11 Programming language

C++

B.3.12 Expected developments

Fluid-solid interface.

B.4 STAR-CD

The STAR-CD framework includes; STAR-CD Version 3.22, STAR-CD Version 3.2, and STAR-CD Version 3150A.

B.4.1 Supplier

CD Adapco Group, UK.

B.4.2 Hardware requirements

STAR-CD is optimised for all leading workstations, PC platforms and supercomputers. It can run on traditional networked UNIX workstations from vendors such as HP, SGI, IBM

and Sun, as well as Intel Pentium PCs and Athlon / Opteron systems from AMD, either under Linux or in the Windows environment. Detailed information can be found on the website: http://www.cd-adapco.com/products/supported_3.22.htm.

B.4.3 Type of code

Finite Volume.

B.4.4 Support

Online support is available in the website http://www.cd-adapco.com. Information can be found by email: info@uk.cd-adapco.com or info@us.cd-adapco.com.

UK: CD adapco Group
200 Shepherds Bush Road, London, W6 7NY
Tel: +44 (0)20 7471 6200, Fax: +44 (0)20 7471 6201
Email: support@uk.cd-adapco.com, info@uk.cd-adapco.com
Website: www.cd-adapco.com

USA: CD adapco Group

60 Broadhollow Road, Melville, NY 11747
Tel: (+1) 631 549 2300, Fax: (+1) 631 549 2654
Email: info@us.cd-adapco.com
Website: www.cd-adapco.com

South Africa: CSIR
Box 395, Pretoria 0001
Tel: (+27) 12 841 4843, Fax: (+27) 12 349 1156
Email: agent@starcd.za.net
Website: www.csir.co.za

India: CSM (India) P.V.T. Ltd.
11, Niton, Palace Road, Bangalore 560052
Tel: (+91) 80 2200996, Fax: (+91) 80 2200998
Email: akb@csmsoftware.com
Website: www.csmsoftware.com

Australia: Veta Pty Ltd
PO Box 40, Cottesloe, WA, 6011
Tel: (+61) 89284 6500, Fax: (+61) 89284 6095
Email: info@veta.com.au
Website: www.veta.com.au

B.4.5 Capabilities

Standard features:

- Complex unstructured meshes including distorted tetrahedral meshes, for both steady and transient simulations.
- Free surface modelling and cavitation, multiphase and multi physics capabilities, multi-phase Lagrangean flows, two-phase flows, Eulerian approach.
- Steady and transient, laminar Newtonian and non-Newtonian flows, varieties of choice for turbulence model including LES, DES, k-ω, SST and V_{2f}.
- Offers a large variety of boundary conditions, including periodic, non-reflecting, and moving boundaries, Hybrid wall functions removing near-wall Y^+ constraints.

B.4.6 Main applications

Industrial applications, e.g. aerospace, automotive, marine, power generation and turbo machinery.

B.4.7 Main users

Diverse

B.4.8 Programming language

FORTRAN

B.5 FIDAP

The FIDAP framework includes; FIDAF V8.7, FIDAP V8.6 and FIDAP V8.5.

B.5.1 Supplier

Fluent Inc, UK.

B.5.2 Hardware requirements

Windows 2000/NT/XP, Pentium or AMD Athlon Family of Processors, Minimum 256 MB RAM, 85MB free hard disk. UNIX/LINUX, Sun, SGI, IBM, HP, Compaq Alpha, Minimum 256 MB RAM, 140 MB free hard disk. More hardware/software details can be found in website http://www.fluent.com/software/fidap/platform.htm.

B.5.3 Type of code

Finite Element

B.5.4 Support

Online support is available. Email: info@fluent.co.uk
Website: http://www.fluent.com/software/fidap/index.htm

B.5.5 Flexibility of program

The program is highly flexible. The program has option-from simple implementation of propriety property data to complex, coupled physical models through user-defined subroutines.

B.5.6 Capabilities

FIDAP is a general-purpose code. Standard features include:

- It can generate meshes comprised of quadrilaterals or triangles for two-dimensional regions, and hexahedra, pyramids and prisms, tetrahedral, pyramid and prism (available in version 8.7) and wedges for three-dimensional regions with an arbitrarily unstructured arrangement.
- Can model non-Newtonian fluids. The Bingham, Carreau and power-law shear thinning viscosity models are built in. Normal stress effects are incorporated through a generalized second-order fluid model.
- It provides two free surface models. The volume of fluid (VOF) is well suited for large deformation problems such as filling, sloshing, droplet break-up and other discrete processes. Surface tension effects can be included in either method. It can model turbulent flow.
- Shape functions in the linear and quadratic elements give a description of the flow solution not only at the nodal points of the mesh but also at all locations in-between.
- The program has two segregated solver choice depending on solution speed and efficiency. For small to moderate-sized problems, the fully coupled solver offers an unparalleled rate of convergence by solving for all unknowns simultaneously. For larger problems where it is more efficient to solve for each field variable individually (using either direct or iterative methods).
- It can solve transient flow problems using high-order time stepping schemes. The time step size is automatically fine-tuned to limit truncation errors to a level specified by user.

B.5.7 Main applications

Industrial applications

B.5.8 Programming language

C++

B.6 FLOW-3D

B.6.1 Supplier

Flow Science Inc

B.6.2 Initial price

Commercial price is approx. US$44 000.

B.6.3 Annual license fees

A University can acquire a license in one of two ways, by lease for US$4 000 or by purchase for US$11 000. These prices include one FLOW-3D solver and unlimited licenses for pre and post processors, technical support and software upgrades. Additional solvers can be leased for US$500 per year or purchased for US$2 500 each. Two other types of low priced version are available for University use; a one solver token costing US$500 without support or a ten solver token costing US$2 500 without support. To add the support and upgrade rights costs US$2,500 and US$3 500 respectively.

B.6.4 Hardware requirements

Windows 2000/NT/XP, UNIX Pentium or AMD Athlon Family of Processors, UNIX/LINUX, Sun, SGI, IBM, HP, Compaq Alpha, Linux, Minimum 1 GH processor with 512 RAM. More hardware/software requirements information can be found on the website:
http://www.flow3d.com/hardware/index.htm

B.6.5 Type of code

Finite Volume

B.6.6 Support

On line support via website: http://www.flow3d.com/Contact/ContactUs.htm

Flow Science Inc.

683 Harkle Rd Suite A, Santa Fe, NM 87505, USA
Tel: 505-982-0088, Fax: 505-982-5551 fax
Email: cfd@flow3d.com
Website: http://www.flow3d.com

Distributors' addresses may be found at: http://www.flow3d.com/assoc.htm

B.6.7 Flexibility of program

Highly flexible and user-defined variables, subroutines and output

B.6.8 Capabilities

FLOW 3D is a general-purpose code. Standard features include:

- Structured finite difference grid, multi-block gridding with embedded and linked blocks, "free-gridding". FAVOR method can used to define general geometric regions within the rectangular grid. Cartesian or cylindrical coordinates, It can solve time-dependent or steady state three-, two- or one-dimensional problems.
- It has a different solver for hydrodynamic problems i.e., Navier-Stokes and Euler solvers. It can also model two-phase flows.
- Wide choice of turbulence model; Prandtl mixing length, one-equation transport, two-equation k-ε transport, RNG (renormalized group theory), large eddy simulation (LES).
- It can model the free surface of a complex flow field using the volume of fluid **(**VOF) or TruVOF methods.
- Other features include; Shallow-water model, general topography model, wetting and drying, wind shear effects and ground roughness effects.

B.6.9 Main applications

Industry, University, and research.

B.6.10 Main users

Diverse

B.6.11 Programming language

FORTRAN and C++

B.7 PHONICS

The PHONICS framework includes; PHONICS-3.5.0, PHONICS-3.5.1, PHONICS-3.4 and PHONICS-3.3.

B.7.1 Supplier

Cham Corporation, UK

B.7.2 Hardware requirements

It can be supplied for any personal computer using the Windows/95/98/2000/NT or XP operating systems. There is a Digital Visual FORTRAN Compiler for Windows 95/98/NT, and/or Salford FORTRAN Compiler for DOS/DBOS.

B.7.3 Type of code

Finite Volume.

B.7.4 Support

Online and 24 hour answer phone support available on: +44 (208) 879 6872

UK: CHAM, Bakery House, 40 High Street, Wimbledon Village, London SW19 5AU
Tel: +44 (208) 947 7651, Fax: +44 (208) 879 3497
Email: support@cham.co.uk
Website: http://www.cham.co.uk/

B.7.5 Flexibility of program

Highly flexible – permits the user-defined subroutines for work with individual elements, as well as to manipulate whole segments of the array containing variables of a defined class.

B.7.6 Capabilities

The equations solved by the program are those expressing the balances of mass, momentum, energy, chemical (i.e. material species) and other conserved entities (e.g. electrical charge). These equations express the influences of diffusion (including viscous action and heat conduction), convection, variation with time, sources and sinks. The following standard features are available:

- The cells are arranged in an orderly (structured) manner in a grid that may be Cartesian, cylindrical-polar, or so-called "body-fitted" e.g. arbitrarily curvilinear.
- It can simulate flow phenomena that are; laminar or turbulent, compressible or incompressible, steady or unsteady and single- or multi-phase.
- Large choice of turbulence models (16 options) including *k*-ε, RNG-derived *k*-ε, LAM-Bremhorst *k*-ε, TWO-Layer *k*-ε, Chen-Kim modified *k*-ε, RSTM, etc.
- It is equipped with a large variety of higher-order schemes including QUICK, SMART, Van Leer, and others.
- It can model free surface and transient flows.

B.7.7 Main applications

Multipurpose.

B.7.8 Main users

Diverse

B.7.9 Programming language

FORTRAN

Appendix C

Specialised river modelling CFD codes that could be used to solve scour and deposition problems

The information given in Appendix C was obtained by the authors from the relevant suppliers and/or their websites and refers to the situation as at September 2004. Where the information is incomplete it is because it was not readily available.

C.1 Delft3D

The Delft3D framework includes;

- Delft3D-FLOW (Hydrodynamic)
- Delft3D-SED (Sediment transport)
- Delft3D-MOR (Morphology)
- Delft3D-WAVE (Waves)
- Delft3D-WAQ (Water quality)
- Delft3D-PART (Particle tracking)
- Delft3D-CHEM (Chemical)
- Delft3D-ECHO (Ecology).

The common utility program includes;

- Delft3D-GRFGRID (Grid generator)
- Delft3D-QUICKIN (Bathymetry generator)
- Delft3D-GPP (Visualization)
- Delft3D-TRIANA (Tide Analysis)
- Delft3D-TIDE (Tide analysis)
- Delft3D-GIS (ArcGIS)
- Delft3D-MATLAB (MATLAB interface).

C.1.1 Supplier

Delft Hydraulics, Netherlands.

C.1.2 Initial price

An academic license for the typical package including the Delft3D modules FLOW coupled with SED; WAVE and MOR with the pre- and post-processing tools QUICKIN, RGFGRID and GPP interfaces costs Euro 6,500. The full suit of Delft3D costs Euro 13,000. The commercial price is variable and depends on the number modules to be purchased. A typical package is approximately twice the cost of academic prices.

C.1.3 Annual license fees

Annual maintenance and support costs Euro 3,250 for academic use. Support includes online helpdesk, bug fixing and version updates.

C.1.4 Hardware requirements

The platforms supported include Unix (HP, SGI and Sun), and Windows/Intel (Windows 95, 98, 2000 and NT4). Linux is being tested and will be released soon. The minimum and preferred configurations are as follows:

Windows/Intel platform

Configuration Item	Minimal	Preferred
Processor	IA32 500 MHz	IA32 1 GHz or more
Internal memory	128 MB	1024 MB or more
Swap space	2 times internal memory	4 times internal memory
Stack space	32 MB	32 MB
Free disk space	2 GB	10 GB
Display	17 inch color monitor, 800 x 600 pixels, 256 colours	19 inch color monitor, 1280 x 1024 pixels, 16 million colours
Printer	PCL, HPCL	Postscript or compatible
Other	CD-ROM drive	CD-ROM drive, Internet connectivity

UNIX workstation

Workstation	Supported Operating System
SUN	SOLARIS 2.6 or higher
SG RAS 10000	IRIX 6.5 or higher

C.1.5 Type of code

Option of finite difference or finite volume schemes

C.1.6 Support

On-line technical and general supports are available:

Technical: delft3d.sales@wldelft.nl (Contact Rene Brocatus)
General: delft3D.support@wldelft.nl (Contact Heleen Leepel)
Website: http://www.wldelft.nl/soft/d3d/intro/index.html

Apart from the above, there are agents in Australia and the USA:

Australia:

Brisbane office, PO Box 2476, Brookside Centre, QLD 4053
Tel: 07 3855 3809, Fax: 07 3855 1904
Melbourne office, 19 Business Park drive, Notting Hill, VIC 3168
Tel: 03 9558 9231, Fax: 03 9558 9956
Sydney office, PO Box 852, Pymble, NSW 2073
Tel: 02 9983 1267, Fax: 02 9983 1055
General enquiries: info@delftsoftware.com.au
Website: http://www.delftsoftware.com.au

USA:

Mahwah office, 4914 West Genesee Street, Suite 119, Camillus, NY 13031
Tel: 315 484 6220, Fax: 315 484 6221
Boulder office, 900 Valley Lane, Boulder, CO 80302
Tel: 303 49 2409, Fax: 303 449 7794
General enquiries: vpassaro@hydroqual.com
Website: http://www.hydroqual.com

Delft3D documentation is also available on the website:
http://www.wldelft.nl/soft/d3d/support/doc/index.html

There is no local support although the program is used by the CSIR in Stellenbosch.

C.1.7 Flexibility of program

The Delft3D software is delivered as an executable only i.e. it cannot compute any additional variables through user-defined subroutines; however, inclusion of open process library for water quality is in under process.

C.1.8 Capabilities

Only the relevant ones are mentioned here.

a) FLOW module

The FLOW module of Delft3D performs a multi-dimensional hydrodynamic simulation, calculating non-steady flow and transport phenomena resulting from tidal and meteorological forcing on a curvilinear, boundary-fitted grid. In the 3D simulation, this module applies the so-called sigma-coordinate transformation in vertical in order to get smooth representation of the bottom topography. The constant number of vertical layers over whole computational domain results high computing efficiency. One main area of application is that of river flow. The FLOW module is based on the full Navier-Stokes equations with the shallow water approximation applied. The equations are solved with a highly accurate unconditionally stable solution procedure. The release information can be found in website:

http://www.wldelft.nl/soft/d3d/support/releasenotes/pdf/RM_FLOW-FLOW.pdf

Standard features:

- Three coordinate systems, i.e. rectangular, curvilinear and spherical in the horizontal plane and a sigma-coordinate transformation system in the vertical planes. Domain decomposition both in the horizontal and vertical directions, several options to define boundary conditions, such as time series, harmonic and astronomical constituents.

- Advection-diffusion solver included the computing of density gradients with an optional facility to treat very sharp gradients in the vertical. Inclusion of pressure gradient terms in the momentum equations (density driven flows).
- The turbulence model to account for the vertical turbulent viscosity and diffusivity is based on the eddy viscosity concept. Four options *k*-ε, *k*-*L*, algebraic and constant model are provided.
- The shear stresses exerted by the turbulent flow on the bed are based on a quadratic Chezy, Manning or White-colebrook formulation.
- It can model a free surface including the effects of wind. Wind stresses on the water surface are modelled by a quadratic friction law. The program also considers heat flux through a free surface.
- It can enhance of the bottom stresses due to waves. Wave-current interaction, taking into account the distribution over the vertical. It can calculate drogue tracks and coriolis force.

Special features:

- Horizontal turbulent exchange coefficients as the sum of a 3D turbulence model and a 2D sub-grid turbulence model. There is an optional facility to take into account the effect of space varying wind and barometric pressure, including the hydrostatic pressure correction at open boundaries.
- Built in automatic switch converting 2D bottom-stress coefficient to 3D coefficient and anti-creep correction.
- It has optional facility to calculate the intensity of the spiraling motion phenomenon in the flow especially important for sedimentation and erosion studies.
- It has online visualization of model parameters enabling the production of animations.

b) SED module

The SED module of Delft3D can be applied to model the transport of cohesive and non-cohesive sediments e.g. sediment/erosion patterns, spreading of dredged material, water quality and ecology studies where sediment is the dominant factor. This module is generally used to calculate the short- or medium-term (days, weeks, month) modelling of erosion and sedimentation process as the changes of bottom topography and its effect on the flow is neglected. The separate morphological and sediment module, Delft3D-MOR, is used for long-term (years) process, where the flow changes induced by changing bottom topography is significant. In the sedimentation process, there is no correlation between the cohesive and non-cohesive components, i.e. between sand and silt; each is treated independently.

The erosion and deposition rates are modelled with a formula by Partheniades and Krone for fine, cohesive sediment. Critical shear stress for erosion and deposition and settling velocities (as function of concentration) are user-defined parameters. The 3D advection-diffusion equation for various sediment fractions is solved with appropriate boundary conditions based on the Van Rijn formulations. For non-cohesive sediment (sand) transport rate is calculated according to the transport formulae of Engelund-Hansen and Ackers-White. These (semi-)empirical relation describe the total transport (bed load and suspended load) in the situation of local equilibrium. The picking up or settling of sediment from or to the bottom leads to a lowering or accretion of the bed level, which can be multiplied by a scaling factor. This means that during the combined flow and sediment run the bottom is adapted dynamically and effects of the bottom changes on the flow and sediment concentrations are accounted for.

Standard features:

- Sedimentation takes place when the bottom shear stress falls below a certain value. The total shear stress is the linear sum of the total shear stresses caused by water velocities and wind effects. Effects of shipping and fisheries can also be included.
- The effects of hindered settling (i.e. decrease in sedimentation at very high suspended solids concentration) can be included.
- Each of the particle fractions is treated independently. Sedimentation always results in an increase in sediment in the uppermost sediment layer.
- The bottom sediments are homogenous within a layer. Therefore, the composition of the re-suspending sediment is the same as that of the bottom sediment.
- The re-suspension flux is limited based on the available amount of sediment in a sediment layer for the variable layer option. The re-suspension is unlimited if the fixed layer option is used. It is zero if the water depth becomes too small.
- Sediment can be transferred downward or upward from one-sediment layer to an underlying or overlying layer. The process is known as ‘burial’ (downward transfer) and ‘digging’ (upward transfer).

Special features:

- Bed level changes resulting from erosion and deposition fluxes are computed using a given value for the bed concentration which is determined in terms of the porosity.

c) MOR module

The MOR module of Delft3D can integrate the effects of waves, currents and sediment transport on morphological development related to sediment sizes ranging from sand to

gravel. This module is designed to simulate the morphodynamic behavior of rivers, estuaries and coasts on time scales of days to years due to the complex interactions between waves, currents, sediment transport and bathymetry. A steering module allows the user to link model inputs for the model components. The morphological process can be specified as a hierarchical tree structure of processes and sub-processes. Process may be executed a fixed number of times, for a given time span or as long as a certain condition is not satisfied. A variety of options are available to specify the time progress.

The MOR module possess numerous options for bed load and equilibrium suspended load transport formulations, i.e. Engelund-Hansen, Meyer-Peter-Muller, Bijker, Bailard and Van Rijn for sand and a separate formulation for silt transport. Release details can be found in website:
http://www.wldelft.nl/soft/d3d/support/releasenotes/pdf/RN_MOR-MOR.pdf

Standard features:

- Computes the bed load and (the equilibrium) suspended load on the curvilinear model grid as a local function of wave and flow properties and the bed characteristics.
- Considers two transport modes, one is the total transport mode and the other is suspended load mode. In the total transport (equilibrium) mode, bed load and equilibrium suspended load transport are added. In the suspended load mode, the entrainment, deposition, advection and diffusion of the suspended sediment are computed by a transport solver. Here, a quasi-three-dimensional approach is followed where the vertical profiles of sediment concentration and velocity are given by shape functions.
- It can take into account the effects of the bed slope on magnitude and direction of transport, and the effects of non-eroding layers for all formulations.
- It guarantees positive concentrations by applying a Forrester filter. It contains several explicit schemes of the Lax-Wendroff type in the update module.
- Offers options on fixed or automatic time stepping, fixed layers and various boundary conditions.

Special features:

- Allows a positive feedback between the processes which can affect water flow and sediment movement by linking between the MOR module and the FLOW and WAVE modules via dynamic coupling.

d) WAVE module

The Delft3D-WAVE module can be used to simulate the propagation and transformation of random, short-crested, wind generated waves in coastal waters which may extend to estuaries, tidal inlets, barrier islands with tidal flats, channels etc. Applications range

from projects related to coastal development and management to design studies for harbour and offshore installations. Moreover, the module may serve as a wave hind- cast modelling tool. At present two models are available in the WAVE module of Delft3D. They are the second-generation HISWA wave model and its successor, the third-generation SWAN wave model. The HISWA wave model is presently the standard wave model for the WAVE module of Delft3D; the SWAN model is available as an option.

Standard features:

- It can compute wave propagation, wave generation by wind, and non-linear wave-wave interactions and dissipation for given bottom topography, wind field, water level, and current field in waters of deep, intermediate and finite depth.
- Energy dissipation considers wave breaking (Battjes-Janssen type) and/or bottom friction. Current driving process is determined directly through radiation stress gradients or by a formulation based on energy dissipation. Shoaling and refraction over a bottom of variable depth or due to a (spatially varying) current can be accommodated.
- The solution technique applied entails the solution of the equations using a forward marching technique over the grid, beginning at the incident wave boundary where wave characteristics must be imposed. The propagation of energy is simulated using the energy balance equation, which allows for the inclusion of all aforesaid phenomena.

Special features:

- The Graphical User Interface (GUI) ensures the convenient use of HISWA and SWAN models as an integral part of the Delft3D model suite.

C.1.9 Main applications

River flow where the FLOW module is used to simulate the hydrodynamics, the SED module can be used to predict sediment movement, the MOR module can be used for the morphodynamic simulation, the WAVE module can be used to model short wave propagation and the WAQ module can be used to model water quality.

C.1.10 Programming language

Fortran90 and C/C++ (not relevant as the package is only provided as an executable)

C.1.11 Expected developments

Additional turbulence models, unstructured Finite Volumes. New features in the upcoming Delft3D release are:

- Delft3D-Quickplot: new MatLab based postprocessing tool
- Delft3D- GISView: ESRI ArcGIS based visualisation tool
- Delft3D-GIS-RGFGRID: ESRI ArcGIS based gridgenerator tool
- Delft3D-GIS-QUICKIN: ESRI ArcGIS based grid interpolation tool
- Improved Dredge and Dumping functionality as part of the Delft3D-Online Morphology module
- Generalisation of the shallow water equations to spherical curvilinear coordinates
- Domain Decomposition both in vertical and horizontal
- New improved Oil spill modelling option

C.2 MIKE 3

The MIKE 3 framework includes;

- MIKE 3 HD (Hydrodynamic)
- MIKE 3 MT (Sediment transport)
- MIKE 3 PA (Particle)
- MIKE 3 AD (advection-dispersion)
- MIKE 3 WQ (Water quality)
- MIKE 3 EU (Eutrophication)
- MIKE 3 EU SEA (Rooted vegetable)
- MIKE 3 PP (pre and post processor).

C.2.1 Supplier

DHI, Denmark.

C.2.2 Initial price

The price is variable and depends on set of modules to be included in the package. The cost of typical package – the so called MIKE 3 ELP that includes module PP HD and AD is:

Euro 5 900 (for 10 000 maximum number of water points)

Euro 13 900 (for 50 000 maximum number of water points)

Euro 24 900 (for 100 000 maximum number of water points)

The above prices are the same for commercial and academic use and exclude maintenance and updates fees. A full set of documentation, manuals and proven

documentation is included with the package. Combination of related modules is available upon request and costs are:

Module	Single grid Price Euro	Multiple grids Price Euro	Flexible mesh Price Euro
Pre and post processing module (Common for all module), MIKE 3 PP	4 900	4 900	4 900
Hydrodynamics requiring PP MIKE 3 HD	33 200	37 500	41500
Sediment requiring PP and HD MIKE 3 MT MIKE 3 PA	 13 900 13 900	 18 700 18 700	

A discount on the AD module corresponding to 30% of the list price is offered if any of the MIKE 3 WQ, EU or MT modules is purchased. This discount cannot be combined with any other discounts. The software prices include one set of manuals and are exclusive of the operating system.

MIKE 21 users can upgrade the MIKE 21 main and add-on modules to the corresponding MIKE 3 modules at very attractive prices

University Licenses, the use of which is strictly limited to educational and research purposes, are granted with a discount corresponding to 80% of the list price.

C.2.3 Annual license fees

Maintenance for the first year is included in the sales price. Subsequently the annual maintenance price is 10% of the initial price. It covers 'hotline' assistance and an annual update of the software. For licenses at a reduced price such as University License and Dedicated License, maintenance for the first year is not included but is offered at full price.

C.2.4 Hardware requirements

MIKE 3 is based on a fully Windows integrated Graphical User Interface and is compiled with 32-bit application. The program can execute under Windows 98 second edition and Windows NT/2000/XP.

The minimum hardware requirement for MIKE 3 is a Pentium IV 500 MHz (or more) with 256 (or more) MB Ram and 20 (or more) GB hard disk, SVGA Monitor (resolution 1024x768), 16 MB RAM (or more) Graphic card (24 bit true color), 20x speed CD-ROM and NTFS File system. Microsoft Internet Explorer 4.0 (or later) is required for network license management.

C.2.5 Type of code

Finite difference

C.2.6 Support

Technical support is available at the website: http://dhisoftware.com/mike3/support/.

Some support centres are:

Denmark: Agern Allé 5, DK-2970 Hørsholm
Tel: 454 516 9200, Fax: 454 516 9292
Email: software@dhi.dk
Website: www.dhi.dk

Australia: Suite 204, 781 Pacific Highway, Chatswood NSW 2067
Tel: 612 844 05700, Fax: 612 844 05701
Email: rcarr@dhiwae.com
Website: www.dhiwae.com

New Zealand: PO Box 300 705-Albany NZ, Albany
Tel: 649 448 5230, Fax: 649 441 3438
Email: nz@dhiwae.com

UK: 46 Ludlow Road, Church Stretton, Shropshire SY6 6AD
Tel: 44 1694-722795
Email: sm@dhi.dk
Website: www.dhi-uk.com

USA: 301 S State Street, Newtown, PA 18940
Tel: 1 215 504 8497, Fax: 1 215 504 8498
Email: dhi-pa@dhi.us
Website: www.dhi.us

There is no local support for MIKE 3 in South Africa, but DHI have a lot of experience in supporting via e-mail, fax, and telephone. Their software is used by more than 4,000 customers in 75 countries.

C.2.7 Flexibility of program

The MIKE 3 software package can model many phenomena. The program, however, is only delivered as executable code and the user cannot make changes to the code. It is however possible to export results from MIKE 3 to an ASCII file for further post-processing.

C.2.8 Capabilities

a) Hydrodynamic module

The hydrodynamic module (HD) is the core of the MIKE 3 modelling system and provides the hydrodynamic basis for computations performed in other modules. This module solves the time-dependent conservation equations of mass and momentum in three dimensions, the so-called Reynolds-averaged Navier-Stokes equations, where the flow is decomposed into mean quantities and turbulent fluctuations.

Standard features:

- The flow field and pressure variation are computed in response to a variety of forcing functions when provided with the bathymetry, bed resistance, wind field, hydrographic boundary conditions, etc.
- The closure problem is solved in the turbulence module through the Boussinesq eddy viscosity concept relating the Reynolds stresses to the mean velocity field.
- The turbulence module and the transport equation module are integrated components of the hydrodynamic module, and the suite of those three constitutes the HD module.
- The turbulent fluctuations (Reynolds stresses) are modelled employing the Boussinesq eddy viscosity concept. Five options, constant eddy viscosity, Smagorinsky subgrid scale, *k,* *k*-ε*,* and mixed Smagorinsky/*k*-ε models are provided. The last turbulence formulation is a combination of the Smagorinsky model in the two horizontal directions and the *k*-ε model in the vertical direction. This formulation utilises the advantages from both models.
- The hydrodynamic phenomena included in the equations are tidal propagation, effects of stratification, turbulent (shear) diffusion and dispersion, Coriolis forces, barometric pressure gradients, wind stress, variable bathymetry and bed resistance, flooding and drying of inter tidal areas, the hydrodynamic effects of rivers and outfalls, sources and sinks (both mass and momentum) and heat exchange with the atmosphere including evaporation and precipitation

b) MT module

The MT module of MIKE 3 is similar to the MT module of MIKE 21, which describes the erosion, transport, and deposition of mud and sand/mud mixtures under the action of currents and waves.

Standard features:

- Mud transport can be simulated in two modes, i.e., the multi-fraction and multi-layer mode. A discrete settling velocity spectrum is specified in the multi-fraction mode, which is applicable for sand/mud mixture. Depending on the grain size of these individual settling velocities, a non-cohesive sediment

transport based on Van Rijn (1984) or a cohesive sediment transport (default) may be calculated. Erosion of a uniform bed caused by wind and tidal driven currents, deposition of grains with a constant settling velocity and transport are modelled.

- The multi-layer mode differs from the multi-fraction mode by including waves, a more detailed description of the settling process and a layered description of the bed. In the multi-layer mode, the settling velocity varies, according to salinity and concentration to take into account flocculation in the water column.
- Waves may be simulated using, for instance, MIKE 21 NSW.
- Inside the MIKE 21 MT Module, a wave data base is created with the wind speed, direction and water surface elevation as input parameters; the output parameters, i.e. scalar values of wave height, period and direction at each model grid point are used to calculate a bed shear stress together with the current velocities and water depth.
- Hindered settling and consolidation in the fluid mud and under a consolidated bed are included in the model.
- The model is essentially based on the principles in Mehta et al. (1989) with the innovation that the bed shear stresses due to waves are included.
- Bed erosion is not only due to shear forces. It is possible to include liquefaction in areas where breakdown of the bed structure caused by cyclic loading, i.e. waves, is important.
- In areas with deep channels or large water depth variations, the model includes a sliding process, which allows the sediment to move down to deeper areas under the action of gravity and currents. Sliding is modelled through a dispersion equation.
- For the cohesive sediment, a stochastic model for flow and sediment interaction is applied. This approach was first developed by Krone (1962).
- In the multi-fraction mode, the constant settling velocity is used, whereas in the multi-layer mode, following Van Rijn (1989), the settling velocity in saline water (>5 ppt) can be expressed by taking flocculation into account.
- Erosion can be described in two ways depending upon whether the bed is dense, consolidated, and soft or partly consolidated Mehta et al (1989).
- The bed shear stress can be calculated for a pure current or a combined wave-current motion, Fredsøe (1981).
- The advection-dispersion equation is solved using an explicit, third order finite difference scheme known as the ULTIMATE scheme, Leonard (1991). This scheme is based on the well known QUICKEST.

- The solution of the erosion and deposition equations is straightforward and does not require special numerical methods.

MIKE 3 can simulate three-dimensional free-surface flow with unsteady flow condition. MIKE 3 models can run 25% to 40% faster in release 2000 than similar models did in the earlier releases, i.e. version 2.72b or older.

C.2.9 Main applications

MIKE 3 was designed for the simulation of the hydraulics, water quality and sediment transport of rivers.

C.2.10 Main users

Universities, Consultants, public and private organisations.

C.2.11 Programming language

FORTRAN for the "engines" i.e. the solvers, and C++ for the Graphical User Interface.

C.3 TELEMAC

The TELEMAC framework includes;

- TELEMAC-2D (Bi-dimensional flow using Saint-Venant equations)
- TELEMAC-3D (Tri-dimensional flow using Navier-Stokes equations)
- ARTEMIS (Harbour agitation using Mild-slope equations)
- TOMAWAC (Wave climate)
- SUBIEF-2D (2D water quality / 2D suspended sediment transport)
- SUBIEF-3D (3D water quality / 3D suspended sediment transport)
- SISYPHE-2D (bed load sediment transport)
- SEDI-3D-3D (suspended sediment transport included into TELEMAC-3D)
- ESTEL-2D (2D Underground flow)
- ESTEL-3D (3D Underground flow)
- RUBENS-2D (Graphical post-processor)
- MATISSE (Mesh generation)
- STBTEL (Interface between pre-processing and simulation software)
- POSTEL-3D (Extraction of 2D planes in 3D simulation results)

C.3.1 Suppliers

Electricite de France, France
HR Wallingford, UK
SOGREAH Consultants, France

C.3.2 Initial price

Universities may obtain the software for about Euro 1 750, which includes technical support and maintenance. The price excludes tax. A three-day introductory course that would cover the main concepts of the system, and the setting up and running of the flow module in particular is strongly recommended. This costs about Euro 1000 excluding travel and accommodation. A full training course would take about a week.

The commercial price of TELEMAC varies and depends on the number of modules to be purchased. A typical TELEMAC-3D package costs approximately Euro 40,000.

C.3.3 Annual license fees

Free but the license agreement is renewable at the end of each year. At the end of this period the license has to supply to the TELEMAC distributor a report presenting the works performed with TELEMAC. Then the license can be renewed.

C.3.4 Hardware requirements

The software runs under Windows NT4/XP/2000 or UNIX (HP, Sun, SGI etc.). Requires a Visual FORTRAN compiler (Version 6.5 or later) with 128 MB RAM, 2 GHz Pentium IV processor, and 550 MB free hard disk space under Windows.

C.3.5 Type of code

Finite elements on a completely unstructured grid.

C.3.6 Support

Electricite de France – Laboratoire National d'Hydraulique originally developed the program. It is extensively used, marketed and developed by HR Wallingford, UK, in close partnership with EDF-LNH. The program is also distributed by SOGREAH Consultants, France.

The TELEMAC support agreement provides full product maintenance with telephone and e-mail support. Training conducted at HR Wallingford or at client offices is tailored to users specific needs and experience. All users become members of the TELEMAC Users-club that meets regularly with the software authors, EDF-LNH.

UK: HR Wallingford Limited
Howbery Park,Wallingford, Oxon OX10 8BA, UK.
Tel: 0944 1491 835 381 Fax: 0944 1491 832 233
Email: telemac.sales@hrwallingford.co.uk
Website: http://www.hrwallingford.co.uk

France: Departement Laboratoire National d'Hydraulique Electricité de France,
6 Quai Watier, BP49, 78401 Chatou
Tel: +33 (1)3087 7251 Fax: +33 (1)3087 8086
Website: http://www.edf.fr/der/lnh-env

SOGREAH Consultants
6, rue de Lorraine, 38130 Echirolles, BP 172, 38042 Grenoble Cedex 9
Tel: 047 633 4000 Fax: 047 633 4296
E-mail: sogreah@sogreah.fr
Website: http://www.telemacsystem.com

C.3.7 Flexibility of program

The user has access to a range of FORTRAN90 subroutines. One subroutine calculates and outputs new variables in the system. The graphical post-processor RUBENS allows the manipulation of additional variables from those normally output by the model.

C.3.8 Capabilities

TELEMAC 2D and TELEMAC 3D are designed to solve hydrodynamic problems. TELEMAC 2D solves Saint-Venant equations and is capable of solving two-dimensional flow. TELEMAC 3D solves Navier-Stokes equations to model three-dimensional flow.

Standard features:

- Unstructured triangular grids. Areas of interest can be modelled in finer detail.
- It can solve the shallow water equations; either vertically averaged in two dimensions or layered in three dimensions.
- It includes horizontal turbulence options for the simulation of very detailed flow patterns, spherical co-ordinates for very large area models, simulation of wetting and drying within the model domain and solution for transcritical flow. Turbulence models available include k-ε and mixing length.
- Simulates three-dimensional flow affected by stratification (thermal or saline), wind or wave breaking.
- The results from TELEMAC 2D and TELEMAC 3D are often used as input to other modules to study, for example, water quality and sediment transport.
- The SUBIEF module of TELEMAC can model suspended sediment transport. It is mainly used for the transport of cohesive sediments.

The SISYPHE module is used to model the transport of non-cohesive (sand) under the combined action of waves and currents. This module is based on Bijker and Engelund-Hansen formulas with information on the wave and flow conditions derived using TELEMAC and ARTEMIS (or COWADIS).

The ARTEMIS module is based on the mild-slope equation and can determine resonant behaviour or wave disturbance within a port for specified offshore wave conditions. It can represent shoaling, diffraction, refraction and reflections. ARTEMIS includes depth-induced wave breaking and the computation of radiation stresses, which can be coupled with TELEMAC 2D to compute wave-induced currents.

SEDPLUME-3D is a particle-tracking module used mainly for dredging related applications including the dispersion of suspended sediments during dredging and disposal operations.

C.3.9 Main applications

TELEMAC is a modelling system for hydrodynamics, sediment transport and water quality in the natural environment. It can be applied to a wide range of phenomena, from small eddies behind bridge piers to pollutant transport in large coastal areas. It is the main flow model used by HR Wallingford for rivers, estuaries, coastal seas and large ocean areas.

C.3.10 Main users

Civil engineering contractors, national hydraulic labs, research institutions, universities, and water companies.

C.3.11 Programming language

FORTRAN 90

C.4 TABS

The TABS framework includes;

- RMA2 (2D dimensional depth-averaged flow and water levels)
- RMA4 (2D dimensional depth-averaged transport of one to six constituents)
- RMA10 (also known as TABS MDS, Multi-dimensional hydrodynamic)
- RMA11 (water quality)
- RMAGEN (File generator)
- RMAPLT (advance plotting module)
- SED2D (Formerly STUDH, 2D dimensional depth-averaged sediment transport)
- GFGEN (pre-processor)

C.4.1 Supplier

BOSS International, USA

C.4.2 Initial price

Variable – depends on the number of modules. University version costs 50% of the commercial price.

C.4.3 Annual license fees

RMA10 module (hydrodynamic) costs approx. US$3,000 and SED-2D module (sediment transport) costs US$480.

C.4.4 Hardware requirements

Any Pentium class under Windows 98/2000/XP platform; minimum 700 MHz processor and 128 MB RAM recommended.

C.4.5 Type of code

Finite Element

C.4.6 Support

Online support is available.

USA: BOSS International
6300 University Ave., Madison, WI 53562-3486
Tel: 608-258-9910 Fax: 608-258-9943
Email: support@bossintl.com, info@bossintl.com
Website: http://www.bossintl.com

C.4.7 Capabilities

The full non-linear Navier-Stokes and continuity equations for three dimensions are used to describe the flow.

Standard Features:

- It utilizes an unstructured grid with a Galerkin based Finite Element numerical scheme. Elements consist of curved bricks, tetrahedral and other complex shapes. It has the capacity to include one-dimensional, depth-averaged, laterally averaged and three-dimensional elements within a single mesh as appropriate.

- It uses the shallow-water and hydrostatic assumptions with coupling of advection and diffusion of temperature, salinity and sediment to the hydrodynamics. Salinity, temperature and suspended sediment are simulated using the advection diffusion equation coupled to density through an equation of state. An implicit time scheme is used for time dependent systems.
- The turbulence model is the Reynolds stress form. Vertical turbulence quantities are estimated by either a quadratic parameterization of turbulent exchange or a Mellor-Yamada level 2 turbulence sub-model. Partial and full slip conditions can be applied at both lateral boundaries. Also partial or no slip conditions can be applied at the bed.

C.4.8 Main applications

Coastal, river and estuarine flows.

C.4.9 Main users

San Francisco Bay (US), Galveston Bay (US), Sydney coastal waters and Illawarra (Australia) and Hong Kong coastal waters (China).

C.4.10 Programming language

FORTRAN

C.5 SMS

The SMS 8.1 SMS framework includes;

- RMA-2 (Hydrodynamic)
- RMA-4 (Advanced hydrodynamic)
- SED-2D (Two-dimensional sediment transport)
- HIVEL-2D (Graphical interface)
- MESH (Meshing)
- MAP (Mapping)
- Scatterpoint module (interpolation tools)

C.5.1 Supplier

Boss International, USA

C.5.2 Initial price

The academic price is US$2 408. The commercial price is approximately double the academic price. The price includes manuals, online and telephone support and lifetime technical support.

C.5.3 Annual license fees

No annual license fees are required for academic use.

C.5.4 Hardware requirements

Any Pentium class or equivalent computer with Windows/98/2000/XP or ME operating system; 700MHz processor, 128MB or higher RAM, resolution of 1068x762.

C.5.5 Type of code

Finite Difference

C.5.6 Support

Online support is available.

USA: BOSS International
6300 University Ave., Madison, WI 53562-3486
Tel: 608-258-9910, Fax: 608-258-9943
Email: support@bossintl.com, info@bossintl.com
Website: http://www.bossintl.com

C.5.7 Flexibility of program

SMS is extendable using the “Generic Module” interface

C.5.8 Capabilities

The SMS (Surfacewater Modelling System) models the water surface elevation, flow velocity, containment transport and deposition, sediment transport and deposition, subcritical-supercritical flow, and long shore waves for complex two-dimensional (2D) horizontal flow problems.

Standard features:

- It has automatic mesh generator for complex flow domain. It uses staggered cells and a rectilinear grid. The cells can have constant or variable side length.
- Finite Difference numerical approximation of the depth-integrated continuity and momentum equations.

- Time-varying wind drag coefficient, variable spaced bottom-friction coefficient, time-and space-varying wave-stress forcing, flooding and drying calculation.
- Bed scour and sediment transport can be analysed for different soil types (sand and clay) for different layers.
- Output can be transferred to AutoCAD 2000 interface.

C.5.9 Main applications

Coastal and river flows

C.5.10 Main users

US Army Corps of Engineers

C.5.11 Programming language

C++

C.6 SSIIM

SSIIM options include;

- SSIIM Version 1.4
- SSIIM Version 1.3
- SSIIM Version 1.2
- SSIIM Version 1.1

C.6.1 Supplier

Nils R Olsen, Department of Hydraulic and Environmental Engineering, The Norwegian University of Science and Technology.

C.6.2 Initial price

Freeware

C.6.3 Annual license fees

None

C.6.4 Hardware requirements

Windows 2000/XP/NT, PC with a minimum of 128 MB RAM

C.6.5 Type of code

Finite Volume

C.6.6 Support

Limited support may be obtained.

Contact: Nils R Olsen
Department of Hydraulic and Environmental Engineering
The Norwegian University of Science and Technology
Email: Nils.R.Olsen@civil.sintef.no Website: www.ntnu.no/~nilsol/

C.6.7 Flexibility of program

Not Flexible.

C.6.8 Capabilities

SSIIM is an abbreviation for Sediment Simulation In Intakes with Multiblock option. The program solves the Navier-Stokes equations with the k-epsilon model on a three-dimensional almost general non-orthogonal grid. The grid is structured. A control volume method is used for the discretization, together with the power-law scheme or the second order upwind scheme. The SIMPLE method is used for the pressure coupling. The velocity field is used when solving the convection-diffusion equations for concentrations of different sediment sizes. This gives trap efficiency and sediment deposition pattern. The calculations can be time-dependent with an adaptive grid moving vertically to account for changes in water and bed level. An addition to version 1.4 includes a water quality module, which solves the convection-diffusion equation for a number of water quality constituents. The user can specify the source/sink terms for the biochemical reactions.

The model has a user interface with capabilities of presenting graphical plots of velocity vectors, contour plots, particle animations and 2D and 3D OpenGL graphics with colour shading. By using global variables and multi-threading, the graphics can be seen while the numerical calculations are running. The model includes several utilities, which makes it easier to give input data. The most commonly used data can be given in dialog boxes. There is an interactive graphical grid editor with elliptic and transfinite interpolation. The grid and some of the input data can be changed while the numerical calculations are running.

C.6.9 Main applications

River, environmental, hydraulic and sedimentation engineering

C.6.10 Main users

University / Research organisations

C.6.11 Expected developments

Fluid-solid interface.

C.7 CCHE3D

C.7.1 Supplier

National Centre for Computational Hydroscience and Engineering, University of Mississippi

C.7.2 Initial price

The research version costs US$4 000 including technical supports. The commercial price is approximately US$10 000.

C.7.3 Annual license fees

Approximately US$4 000 including technical support

C.7.4 Hardware requirements

UNIX, LINUX and Windows 2000/XP/NT, PC with a minimum of 256 MB RAM

C.7.5 Type of code

Mixed Finite Element and Finite Volume, the so-called Efficient Element Method

C.7.6 Support

Online support is available.

Email: wang@ncche.olemiss.edu (contact Dr. Sam S Y Wang)
jia@ncche.olemiss.edu (contact Yafei Jia)

USA: NCCHE
The University of Mississippi
Carrier Hall, Room 102
University, MS 38677
Website: http://ncche.olemiss.edu/

C.7.7 Flexibility of program

Flexible – user-defined subroutines and modules are possible.

C.7.8 Capabilities

CCHE3D is a three-dimensional hydrodynamic and sediment transport model. The model is a collocation version of the Galerkin approach. The basic element is a cube with twenty-seven nodes. Both hydrostatic and dynamic pressure of the flow can be simulated depending on the nature of the problem. Staggered grid is used for the pressure solution. The velocity correction method is adopted to compute the dynamic pressure and enforce the mass conservation. The kinematics equation for the free surface is solved to determine the location of the free surface. Five eddy viscosity models, parabolic, mixing length, k-ε, RNG k-ε and non-linear k-ε model are available for a variety of applications.

C.7.9 Main applications

River, environmental, hydraulic and sedimentation engineering

C.7.10 Main users

University and Research organisations

C.7.11 Programming language

FORTRAN 90